

# **An overview into advantages and applications of conventional and unconventional hydro(solvo)thermal approaches for novel advanced materials design**

Mary C. M. D. de Conti,<sup>1,2,3</sup> Swayandipta Dey,<sup>4</sup> Walimir E Pottker<sup>3</sup> and Felipe A. La Porta<sup>1,3\*</sup>

<sup>1</sup> Post-Graduation Program in Chemistry, State University of Londrina, Rodovia Celso Garcia Cid, 445, km 380, Londrina, Paraná, 86057-970, Brazil.

<sup>2</sup> Laboratory of Nanotechnology and Computational Chemistry, Federal University of Technology – Paraná, Londrina, Brazil.

<sup>3</sup> Federal University of Technology – Paraná, Nature Sciences Academic, Avenida Alberto Carazzai, 1640 CEP 86300- 000 - Cornélio Procopio - PR, Brazil.

<sup>4</sup> Department of Applied Physics & Institute for Complex Molecular Systems (ICMS), Eindhoven University of Technology, Postbus 513, 5600 MB Eindhoven, The Netherlands

\*Corresponding author:

Email: [felipelaporta@utfpr.edu.br](mailto:felipelaporta@utfpr.edu.br)

## **ABSTRACT**

**The hydro(solvo)thermal approaches due to their simplicity and relatively low cost have attracted great attention to novel advanced materials processing with controlled particle sizes and well-defined morphologies, including the desirable obtaining of diverse metastable phases. Furthermore, in this case, such advanced materials obtained by this strategy generally have a high crystallinity structure as the main characteristic, which is interesting for a wide range of technological applications of high performance. This critical review presents the recent progress and challenges in conventional and unconventional hydro(solvo)thermal synthesis of novel advanced materials with desirable functionality and outstanding physicochemical properties designed using such methods. Finally, in this perspective, we believe that this detailed knowledge of the effect of processing parameters and as they will affect the prepared materials structure-composition-morphology is a key step to providing new chemical insights for the rational advanced materials design.**

**Keywords:** Hydro(solvo)thermal processing; Nucleation and growth stages; Morphologies; Microwave-assisted synthesis; Materials design

## HIGHLIGHTS

- Strategies focused on solution-based synthesis provide precise control of desired physical parameters.
- Chemical reactions in conventional and unconventional hydro(solvo)thermal processes involve the interaction between neutral and ionic species in solution and one or more solid phases.
- When designing advanced materials, controlling aspects such as size, shape, state of agglomeration, solubility, porosity and other characteristics are of great interest.

## INTRODUCTION

It is known that the physicochemical properties of the advanced materials are altered by changes in the physical parameters like particle size, morphology, composition, structure, and imperfections (at short-, medium- and long-range) [1,2,11,3–10]. These parameters are, in turn, strongly dependent on processing conditions, which can lead to obtaining advanced materials with more or less defects depending on its desired application [12–15]. Currently, strategies focused on solution-based synthesis have attracted great attention over everything in processing of a wide variety of advanced materials, since such strategies provide precise control of the desired physical parameters [1,16–22]. Among these solution-based methods, the hydrothermal synthesis stands out for its popularity related simple, effective and low cost preparation of a huge variety of advanced materials (organic, inorganic or hybrid) with controlled particle sizes and well-defined morphologies [2,16,17,23–43]. Such advanced structures, are usually obtained through heterogeneous reactions above 100 °C and 1 bar in aqueous medium, or applying different solvents (in this last case, this process can also be conveniently called solvothermal) [17,37,44–46]. Therefore, in this review, we will apply the term hydro(solvo)thermal more often.

In addition, this hydro(solvo)thermal strategy is, of course, nature-inspired and considered appropriate for producing metastable materials in large quantities [47–49]. Under these hydro(solvo)thermal conditions, the conventional and unconventional chemical reactions involve the interaction between neutral and ionic species in solution and one or more solid phases. Through chemical, mass, and electroneutrality balances,

for all species involved, reaches the equilibrium between solid phases [50–52]. Thus, a hydro(solvo)thermal synthesis occurs through the interplay of minerals solubility in a solution heated under high pressure. In such manner, that the solvent will be heated to the boiling point temperatures, by an increase in autogenous heating pressures (i.e., the pressure generated during autoclave heating) [47,53]. This way, it explores how the parameters of experimental synthesis (e.g., temperature, pressure, solvent, nature of the precursors, reaction time, and so on) affect the formation of crystalline particles leading to highly adjustable properties of a given target material [54–58]. In relation to the materials prepared by this strategy, we highlight the superiority in applications such as superionic conductors [28,59,60], chemical and gas sensors [29,61–65], electronically conductive solids [30,66–68], complex ceramic oxide and fluorides [31,32,69–74], magnetic materials [33,75–78], optoelectronic devices [34,79–82], and so on.

Furthermore, it is known that the kinetics of hydro(solvo)thermal reactions undergo significant changes when associating technologies such as electrochemistry, microwave, sonochemistry, and others [70,81,83–94]. Among these, microwave-assisted hydro(solvo)thermal synthesis is one of the main unconventional methods widely employed to produce advanced materials [16,89,95–113]. Microwave enhanced heating is, of course, based on more efficient dielectric heating of specific solvent, which is responsible to absorb-convert energy into heat [114–118]. The uniqueness of the dielectric heating mechanism causes the specific (thermal) effects of microwaves not being possible to reach by conventional heating. Undoubtedly, the use of microwave-assisted heating contributes to an increase in crystallization kinetics, in orders of magnitude, thereby improving material productivity and favoring the obtainment of more complex structures [86,119–125]. Also, is well established that the use of microwave energy substantially impacts the physicochemical properties of these advanced materials [126–128]. This feature can also offer many benefits by making it cost-effective, and reducing reaction time and energy in processing when microwaves are used, thus making it an interesting strategy to obtain of novel designed advanced materials with unique physicochemical properties [129–141].

### ***Unconventional hydro(solvo)thermal approaches***

For hydro(solvo)thermal process, thermal equilibrium must be reached throughout the reaction [142,143]. In the conventional process, heating is carried out with convection currents, which create a thermal gradient over time [144,145]. A significant contribution is made by conductivity of the reactor material as well [146,147].

Current research has explored the benefits related to the potential use of microwave irradiation for the synthesis of advanced materials with the specific purpose of improving heating efficiency and accelerating processing of such materials [116–118,143–189]. In particular, microwave heating systems generally use frequencies in the range of 900 MHz to 2.45 GHz [143,188,189]. Studies aimed at optimizing the heating process with the use of microwaves began in the 1970s [189]. Later in 1986, Giguere and Majerich reported rapid rates for certain organic reactions conducted in microwave reactors [148], establishing a relationship between the heating process and the dielectric properties [149,150]. In chemistry, this exploitation of microwaves is referred to as microwave-assisted synthesis [116,117,151–169]. Recent studies have been dedicated to understanding the nature of the phenomena surrounding microwaves such as the induced acceleration of the chemical reaction rate [118,170]. This feature has increased the popular utility of other methods among various synthetic methods [171,172].

Heating can occur through conduction and the species (particles or carriers) in the material must be free to move and promote the induction of a current. However, if charged species present a certain resistance to movement, which can occur due to geometric factors, these charges will move until an opposing force counterbalance them. This results in the establishment of a dielectric polarization. Thus, we observe that the effects of microwave heating result in both conduction and dielectric polarization [102,170,173–178,190–192].

We observed that the heating became more uniform and faster, thereby increasing the thermal/kinetic effects in the case of microwave coupling in chemical processes as a heating strategy, when compared to conventional heating. Consequently, this decreases the processing time and provides energy savings [103,183,184,193]. As a result, this strategy based on microwave-assisted synthesis leads to a significant increase in reaction kinetics by at least two orders of magnitude [185]. It should be considered that accelerated microwave heating depends on various physicochemical parameters of the species involved (i.e., liquids and solids) that make up the reaction medium, the nature of electromagnetic radiation, as well as the instrumental design [118,143,186,187,189].

It is well known that the ability of a material to convert the energy contained in microwave radiation into heat depends on its dielectric properties [116,174,184]. Thus, from this perspective, heating will only occur if the dipoles have sufficient time to realign with the oscillating electric field (high frequency) and the speed of realignment (low frequency); otherwise, either no heating occurs or the magnitude of heating will be weak [194–197]. In addition, it is known that an increase in temperature affects the viscosity of water and, consequently, Brownian movement increases the mobility of water molecules [198,199]. This affects the orientation of the dipoles [179–182].

At low frequencies, water dipoles have sufficient time to align with the applied field and the dielectric constant assumes maximum values. At high frequencies (near infrared and visible range), water dipoles do not follow rapid changes in the applied external field, which causes the relaxation and polarization effects to be reduced. However, in the intermediate region (microwave frequencies), the dielectric constant decreases sufficiently to promote orientation/relaxation phenomena [117,145,151,170]. When the critical frequency assumes a small value, the interaction of the parameter is known as tangent loss. This parameter defines the ability of a material (in most cases, a solvent) to convert microwave energy into thermal energy. According to the loss tangent values, solvents or materials can, in principle, be classified as strong ( $\tan \delta > 0.5$ ), moderate ( $\tan \delta \approx 0.1-0.5$ ), and weak ( $\tan \delta < 0.1$ ) absorbents [117]. For practical purposes, achieving efficient microwave heating (2.45 GHz) requires the presence of a solvent or material classified as a strong absorber ( $\tan \delta > 0.5$ ) [117].

Therefore, the nature of microwave heating is related to the characteristics of electromagnetic radiation (input power and frequency), physicochemical properties associated with the reaction medium that contain the species responsible for effectively promoting heating (dielectric permittivity, dielectric constant, electrolyte concentration, temperature, viscosity, relaxation time, penetration depth, etc.), and phenomena related to microwave-matter interaction (absorption, transmission, and reflection) [116–118,143–189,194,198–203].

Therefore, microwave-assisted hydro(solvo)thermal synthesis offers significant advantages compared to traditional methods, including the following: (i) a rapid heating rate for the desired reaction temperature, (ii) uniform distribution of temperature, (iii) improved crystallization kinetics, as well as, (iv) extremely short reaction times

[89,95,96,106,123,162–168,204–206]. In addition, it is widely recognized that rapid microwave heating can suppress the formation of by products [197].

## **NUCLEATION AND GROWTH STAGES**

In the last few decades, an enormous library of nanocrystals has been designed using the colloidal approach, which is essentially a phase separation process primarily associated with nucleation and crystal growth stages [116,153–161,207]. In general, it is well known that colloidal systems are distorted solid structures primarily responsible for the nucleation step [208,209]. From this perspective, nucleation as a solute precursor occurs in systems that present their suspended solid phase with a high degree of dispersion, which contributes to the growth stage of nanoparticles [58,210–213].

To elaborate further on these preliminary stages, La Mer introduced the first approach to a nucleation system in colloidal suspensions [214,215]. According to La Mer, the process occurs in three stages: (i) pre-nucleation, (ii) nucleation, and (iii) crystal growth [216], as shown in Figure 1(a). Pre-nucleation usually occurs because of the absence of precipitates in an unsaturated solution. However, the application of precipitating agents leads to an increase in the concentration of the precursor species. Hence, it is well known that the nucleation rate is sensitive to the concentration of dissolved species and the nucleation process usually has a slower speed than the generation of precursors [217–219]. The nucleation phase then begins spontaneously upon reaching the minimum supersaturation concentration (Figure 1(a)). These precursors further interact among themselves to form clusters and when the cluster growth reaches a critical stage, it results in a thermodynamically irreversible condition leading to crystal formation, the growth, of which can be further controlled with the help of stabilizers [140,220–222]. Further, it is well known that the crystal nucleation can, in principle, be homogeneous or heterogeneous [223]. If the nucleation and growth stages occur simultaneously, the polydispersity (crystal size distribution) of the particle size will increase [224]. Particularly, the classical nucleation theory stipulates the balance existing between the volume and the surface energy in the formation of the nuclei of the new phase, the density fluctuations resulting from the stochastic process are due to random collisions of the dissolved constituents, which is, of course, originated from a particular association of monomers in a stage of pseudo-equilibrium [208,225–228]. Therefore, the

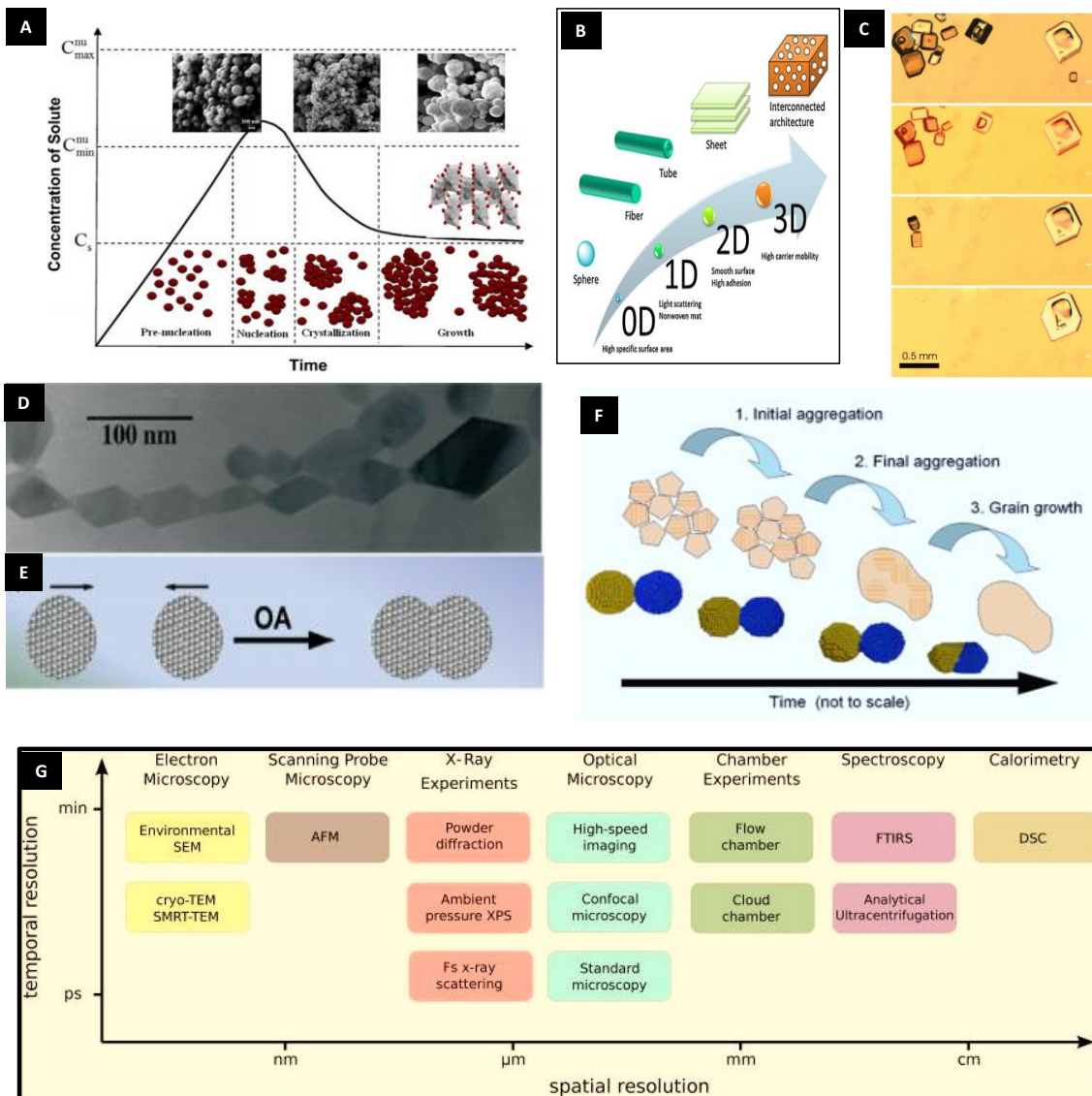
contributions of factors directly related to the interaction between ions on the surface (counter ions, surfactants, and so on) are responsible for minimizing energy in specific crystallographic planes [222,229,230].

During the heterogeneous nucleation process, which is of interest in this review, the variation in Gibbs energy (owing to the critical radius of the crystal) occurs because of the interaction of the nucleus/clusters in the solution acting as monomers during nucleation and crystal growth [139,223,231,232]. Hence, these clusters play a critical role in reaching a specific geometric arrangement, which creates a minimization of the surface energy [233]. In this way, the crystal stability depends on the size of the critical radius; usually, those with smaller dimensions tend to be unstable and therefore are more likely to dissolve in solution and recrystallize about larger nuclei that are relatively more stable. This physical mechanism is known as Ostwald Ripening (OR) [234–237].

In the case of the OR mechanism, the growth of the particles occurs through dissolved ions propagating into regions of lower solute concentration (see Figure 1(c)). This diffusion controls the process of crystal growth, which ends when the solubility value reaches a thermodynamic equilibrium. As a result, this mechanism typically produces nanoparticles with regular shapes and a more homogeneous particle distribution [236–238]. Usually, crystal growth under equilibrium conditions is related to the coarsening process also known as OR, which can be described as diffusion or reaction-rate-limited growth to larger nanoparticles at the expense of smaller ones [222,239–241].

Although, from a kinetic perspective, both the size and morphology of the nanocrystals can be precisely controlled using an optimal and suitable combination of various solvents and stabilizers. The process, by which nanocrystals mutually interact with each other to generate larger structures via particle-particle or particle-solvent interactions is referred to as nanocrystal-based self-assembly. Recent research also suggests the oriented attachment (OA) of monomers mechanism could be a plausible fundamental process that helps to explain the initial growth process after nucleation events that occur when there is a significant concentration of both monomers and clusters [222,242–249]. Another outstanding crystal growth process is the OA mechanism, which involves the spontaneous self-organization and coalescence of adjacent particles by eliminating a common boundary that shares a standard crystallographic orientation with a flat interface (see Figure 1(d and e)) [222]. Hence, the driving force that induces the growth mechanism of OA is not specific, but likely due to a decrease in the free energies

of the surface and grain boundaries [242,248,250]. However, it is known that the reduction in surface energy eliminates some crystalline facets of high energy. In this way, nanocrystals collide and form loosely bound compounds, which can reorganize and form irreversible attachments along preferred crystallographic orientations [155,244,251–254]. By suppressing the growth of the crystal faces with specific addition of an additive (e.g., anions, amines, carboxylic acids, surfactants, etc.), the shape and size of the nanoparticles can be controlled. This effect occurs because of the selectivity of adsorption on a specific face, leading to structures with high symmetry [129,243,255,256]. The localized nature of this OA mechanism, often in the early stages of nucleation, leads to the formation of irregular and anisotropic nanocrystals (e.g., nanorods, nanodumbbells, nanowires) [257,258].





**Figure 1.** (A) LaMer diagram - Separation of the crystal nucleation and growth process. [259]. (B) Schematic illustration of structural dimensionality of materials with expected properties [260]. (C) Polarized light microscopy images of NaClO<sub>3</sub> crystals in equilibrium with a saturated solution showing the OR process [261]. (D) A single crystal in the form of an anatase chain that has grown hydrothermally by the OA mechanism. (E) Scheme of growth of nanocrystals controlled by a guided fixation mechanism [243]; (F) Schematic diagram showing the coalescence mechanisms [262,263]. (G) Main characterization techniques used for the study of crystal nucleation and growth [219]

Grain growth can also occur through the coalescence of crystals with a similar crystallographic orientation. This process is called the coalescence mechanism, where the driving force reduces the surface area or contours (see Figure 1(f)). Among the modes of mass transport observed during coalescence, surface diffusion stands out [264,265]. Thus, the mechanism begins with contact between the particles. This mechanism begins with contact between the particles, which leads to their reorientation. As the system behaves as a single body, the growth rate slows, resulting in an oblong, ovoid, or dumbbell shape [263,265–269]. This naturally enables the formation of complex defects, most likely due to rapid reorientation of the clusters among a significant number of newly formed bonds that block the rotational movement of such particles. One other notable characteristic of disordered structures is that they may also alter the crystal nucleation and growth processes [1,2,11]. Hence, from this perspective, the control of these crystal features is achieved by suppressing the growth of the crystal face by selectively adsorbing an additive to a specific face [255,270–275]. In addition, the suppression of the aggregation of nuclei can also be controlled by adding a dispersant/thickener or by controlling the pH of the solution. During synthesis, the chemical potential of the ions dispersed in a solvent affects the solubility of the precursors [276].

However, it is not only size that is important for nanoscale material properties. The shape, state of agglomeration, solubility, porosity, and other characteristics are of great interest for designing desirable advanced materials [9,12,277–286]. Figure 1(b) shows the different dimensions of the materials obtained from the application of this strategy. In general, it is well known that the zero-dimensional (0D) materials have a large surface area and hence provide high reaction rates [260]. One-dimensional (1D) materials, such as nanotubes, nanowires, and nanobands exhibit a reduction in the

electron-hole recombination rate and a high transfer rate of the interfacial charge carrier [260,287–290]. These characteristic features make such nanomaterials useful for many photocatalytic reactions [260]. Additionally, two-dimensional (2D) materials allow the manufacture of flat surfaces, which results in excellent adhesion to substrates and high smoothness [260]. In contrast, the main characteristic of three-dimensional (3D) materials are interconnections, facilitating charge mobility [260]. By changing parameters such as chemical factors (solvent, pH, reagents, and limiting agents), thermodynamic factors (temperature and pressure), and associated technologies, the synthesis of advanced materials can be controlled [4,291,292].

## **INSIGHTS INTO PROCESS PARAMETERS HYDRO(SOLVO)THERMAL FOR CONTROLLED GROWTH OF ADVANCED MATERIALS**

With growing industrial demand for novel advanced materials, both conventional and unconventional hydro(solvo)thermal approaches have received considerable attention in recent years [47–85,87–141,204]. This is likely because these strategies enable facile scalable preparation of a wide variety of advanced materials with a high level of purity. In particular, materials obtained using hydro(solvo)thermal method may possess a wide particle size distribution; however, it is well known that adjustment of the synthesis conditions can, in principle, lead to the preparation of single crystals with a uniform size distribution [293–306]. Many studies have focused on the optimisation of conventional and unconventional hydro(solvo)thermal processing parameters, particularly because of the low cost as well as flexibility of such synthetic approaches [47–85,87–141,204]. Thus, in this section, we discuss the main effects of changes in the chemical synthesis parameters on the physical characteristics of diverse advanced materials prepared using these strategies.

The first step in preparing a target material using this synthesis strategy is to determine the initial concentrations of the precursors based on the stoichiometric relationship. Knowing the phase diagram of the target system, in principle, it is possible to determine the initial conditions for performing experiments under hydro(solvo)thermal conditions. These chemically intuitive aspects are key to obtaining better results in the use of hydrothermal reactions. In addition, controlling thermodynamic factors (pressure

and temperature) facilitates diffusion by reducing viscosity [307], thereby promoting the solubility of the reagents [308] and affecting the growth of the crystal. After obtaining and confirming the initial results, the chemical parameters of the process are optimized for the synthesis of the target advanced material.

Following the order of synthetic stages, we start our discussion with an analysis of the effects of concentration variation as well as the nature of the precursors and solvents used. Controlling the solubility and interaction conditions of the intermediate compounds formed during the process is extremely important [291,309,310]. Therefore, these parameters play a fundamental role in modulating reaction kinetics because of their interaction with the mobility of suspended particles and the proportion of effective shocks [311]. In the literature, we found studies in which the solvent concentration was tuned to obtain different morphologies of the same compounds [291,312–317]. The objective of such tuning is to change the precipitation equilibrium constant, thus affecting the adsorption of ions on the crystal surface and consequently inducing growth anisotropy [310,318]. It has been shown that the longer the crystal nucleation, the better is the crystallinity [291,310].

Chen et al. [310] demonstrated a change in morphology by replacing ions (chlorine, nitric oxide and bromine) in iron fluoride crystals, which affected the growth rate of the crystal planes. Thus, the properties of the ions used in the synthesis affect the reaction kinetics, making it slower or faster, influencing the control of crystal growth. The same strategy was used in the synthesis of  $\text{CsPbX}_3$  ( $\text{X} = \text{Cl}^-$ ,  $\text{Br}^-$  and  $\text{I}^-$ ) to obtain ultralong nanowires [319]. Both aqueous and non-aqueous solvents can, in principle, be used to synthesise these types of advanced materials with precise control of their physical characteristics [291,312–317]. In addition, the interaction between the solvent and the surface impacts on the interfacial tension. The decrease in tension leads to a transition from a smooth to rough interface and accelerates surface growth [320]. Inhibitory agents, known as adsorbed additives, are used to prevent deposition and inhibit crystal growth on a specific face [321]. Also, the use of mixed solvents provides control over crystal growth, leading to the formation of different morphologies [292]. The adaptation of crystal facets has been widely recognised as an innovative strategy to adjust the chemical and physical properties of advanced materials [143,146,256]. For example, the addition of an additive can control the shape and size of the nano- and microparticles through selective

adsorption on a given face [255], which can also cause a decrease in particle size, from submicrometric to nanometric [322].

When choosing a solvent for the conventional or unconventional hydro(solvo-)thermal synthesis, its pH must be considered because of its impact on the solubility of the precursor and, consequently, on the crystallisation rate [17]. Hence, pH plays an important role in obtaining different morphologies. Different morphologies were obtained under different pH conditions (alkaline or acidic) [323–328]. For instance, in the case of titanium dioxide ( $\text{TiO}_2$ ) in the anatase phase, alkaline conditions lead to the formation of cubic or hexagonal structures. In contrast, under acidic conditions, the crystal morphology is almost exclusively truncated tetragonal bipyramidal [323]. He et al. [326] reported the hydrothermal preparation of boehmite ( $\gamma\text{-AlOOH}$ ) nanocrystals at different pH values in the presence of different anions. According to these authors,  $\gamma\text{-AlOOH}$  nanorods were obtained in the presence of nitrate or chloride under acidic conditions (at pH  $\sim 4.0$ ). In contrast, in the presence of sulfate (at pH  $\sim 4.0$ ),  $\gamma\text{-AlOOH}$  nanowires were formed. At pH  $\sim 10.5$ , the authors observed the growth of  $\gamma\text{-AlOOH}$  nanoplates for all the studied anions. In addition, it has been suggested that, in some cases, the effect of medium pH can be less pronounced with an increase in the temperature of the hydrothermal treatment [324].

It is well known that the chemical potential of ions dispersed in a solvent is inversely proportional to the dielectric constant of the medium [276]. This relationship directly affects the solubility of the precursors or intermediate compounds during chemical synthesis. To improve the solubility of synthetic compounds, mineralising agents are commonly added to the system. These agents form soluble mobile complexes that allow for the presence of ions with the necessary valence for the reaction [129,329],[329]. In turn, the increase in the thermal stability of the reagents affects the mass transfer and solubility. Consequently, it alters the kinetics of the reactions involved and helps stabilise the denser structures [292,330,331].

In this context, the kinetics, solubility, stability, chemical composition, and the state of formal oxidation of transition metals usually change with temperature [332–334]. Hence, diverse advanced materials can be formed over a wide temperature range [292,335,336]. Tuning temperature and time in the hydro(solvo-)thermal process allows improving the solubility of the reagents and thus enables greater control of the size and crystallinity of the obtained material [307,333,337–343]. Hence, these characteristics contribute to obtaining advanced materials with more or fewer defects, directly impacting

their applications of interest [13–15]. In addition, different hydro-(solvo-)thermal techniques can, in principle, be used to modify the chemical reactivity, impacting the reaction kinetics. However, the most important characteristic is the change in water properties (density and dielectric constant), which are directly dependent on temperature and pressure [344–347]. Among these technologies, the most studied one is the use of microwaves, which increases the energy efficiency of the synthesis process [348–351].

After a general explanation of the main parameters that are adjusted during the optimisation of a synthetic protocol based on conventional and unconventional hydro(solvo)thermal methods, we discuss some highly complex structures that can be easily obtained using these approaches. As a general feature, we observed that these complex structures can be obtained using very similar hydro(solvo)thermal strategies. In this review, we highlight the following systems: (i) hollow spheres and porous structures; (ii) one-dimensional (1D) materials (such as tubes, wires, and rods); (iii) two-dimensional (2D) materials; and (iv) heterostructured materials (such as decorated, Janus-like, core–shell, and yolk–shell). The choice of these structures is based on their promising properties for many applications, especially in the catalytic field.

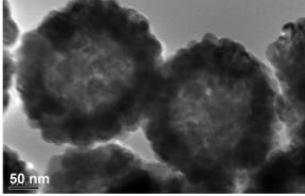
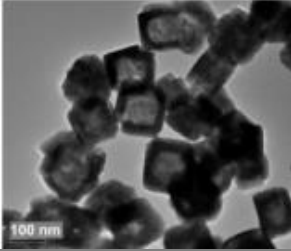
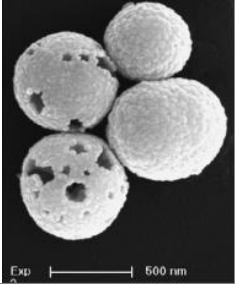
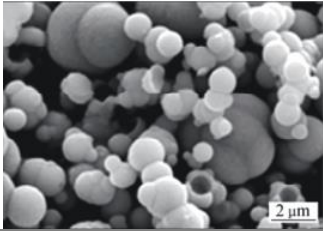
### *Hollow sphere and porous structures*

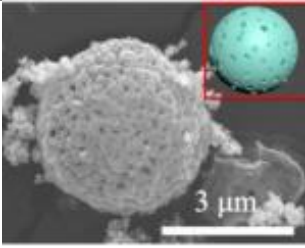
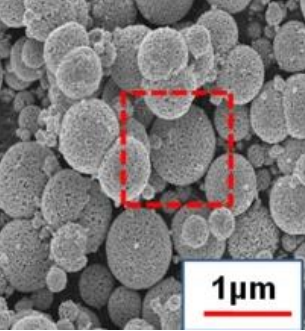
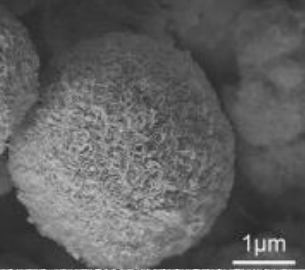
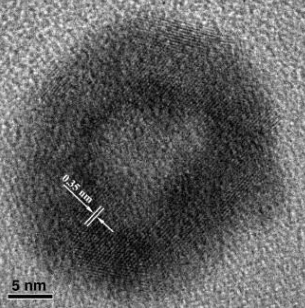
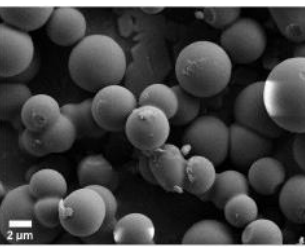
Hollow spheres and porous structures are of great interest for catalysis [352–355]. These complex structures have a crystalline nature with a high surface area and are suitable for the diffusion of electrolytes, as electrochemical catalysts, and in energy storage [356–358]. These structures in the form of composites can also prolong the chemical stability during electrochemical reactions.

Strategies used to obtain hollow structures fall into three categories: hard templating, soft templating, and self-templating [359,360]. Hard templating synthesis is usually based on three successive steps: (i) hard-template preparation in a specific format, (ii) coating/depositing (selective) of the target material on the template, and (iii) selective mould removal to obtain hollow and open structures, usually by calcination, dissolution, or chemical corrosion. At the same time, it is known that soft-template synthesis is thermodynamically metastable with high deformability owing to its liquid/gaseous form. Because of this, in particular, the soft-template strategy strongly depends on the experimental conditions used (e.g., pH, temperature, solvent, ionic strength, etc.). Lastly,

self-templating synthesis generally depends on specific formulations and conditions and is classified into three sub-categories according to the nature of the target material: (i) inorganic and metallic particles, (ii) polymer particles, and (iii) small organic particles [359,360]. Table 1 presents a variety of morphologies obtained from spherical materials and hollow structures prepared by conventional and unconventional hydro(solvo)thermal synthesis.

**Table 1** Spherical morphologies and hollow structures via hydro(solvo)thermal synthesis.

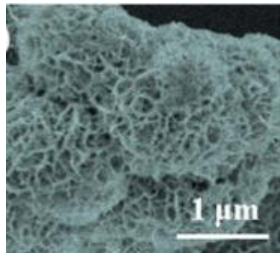
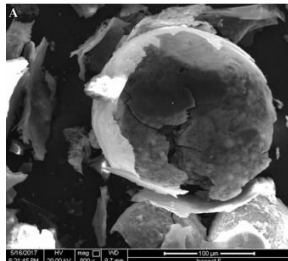
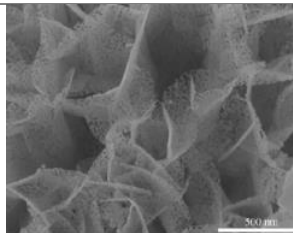
Chemical factors	Thermodynamic factors	Design	Ref.
$\text{Cu}(\text{NO}_3)_2 \cdot 3\text{H}_2\text{O} + \text{N,N-dimethylformamide (DMF)}$	two-step experiment: (i) 140-150 °C for 22-40 h (ii) 180 °C for 8-42 h.		[361]
$[\text{Cu}^{2+}] + \text{DMF} + \text{H}_2\text{O}$	180 °C for 15 h		[362]
$\text{Gd}(\text{NO}_3)_3 + \text{Eu}(\text{NO}_3)_3 + \text{CO}(\text{NH}_2)_2$	120°C for 8 h		[363]
$\text{CdCl}_2 \cdot \text{H}_2\text{O} + \text{deionized water} + \text{solution}$ $\text{Na}_2\text{S}_2\text{O}_3 \cdot 5\text{H}_2\text{O} + \text{EDTA}$	140 °C for 20 min in a microwave hydrothermal synthesis system.		[364]
$\text{NiSO}_4 \cdot 6\text{H}_2\text{O} + \text{CoCl}_2 \cdot 6\text{H}_2\text{O}$ + deionized water + hard and soft template	180° for 20h		[365]

			
$\text{SnCl}_4 \cdot 5\text{H}_2\text{O} + \text{urea} + \text{Eu}_2\text{O}_3 + \text{HNO}_3$	microwave-solvothermal route with the microwave power of 200 W, 400 W and 600 W and post-annealed at 1000°C.		[366]
PEG-6000 surfactant + deionized water + $\text{Ni}(\text{NO}_3)_2 \cdot 6\text{H}_2\text{O} + \text{CO}(\text{NH}_2)_2$	Teflon-lined autoclave and treated at 160 °C for specific 30 min under the temperature-controlled mode in a MDS-8 microwave hydrothermal system		[367]
Praseodymium oxide + nitric acid + NaF + ammonia + deionized water	Placed in a microwave oven (650 W, 2.45 GHz) with a refluxing apparatus. The suspension was heated by microwave irradiation for 20 min at 70% of the maximum power under refluxing.		[368]
$\text{CuSO}_4 \cdot 5\text{H}_2\text{O} + \text{D-glucose} + \text{distilled water} +$	the mixed solution was placed and heated in the microwave hydrothermal oven to 180 °C for 20 min, frequency of 2.45 GHz and can operate at a power level of 300, 600, or 1200 W.		[369]

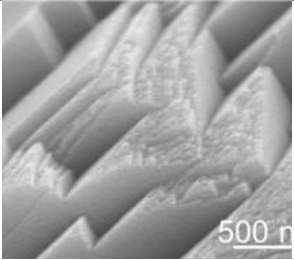
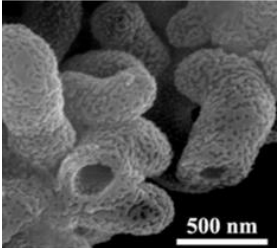
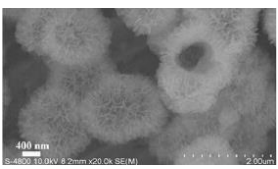
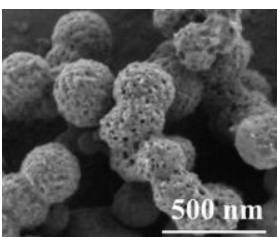
According to their pore size, these materials can be classified into three classes: microporous (<2 nm), mesoporous (2 to 50 nm), and macroporous (>50 nm). Porous materials have high surface area and high chemical and thermal stabilities [370]. Different strategies can be used to obtain porous materials, depending on the properties required by a particular application of the material. In the literature, strategic methods to obtain porous structures follow two main approaches: (i) introducing macroporous templates in the reaction, or (ii) combining supplementary chemical and physical methods [370,371].

For example, one of the strategies, which is considered a basic technology, is to synthesise a compound with the desired precursor using surfactants/porous substrates. The second step can be calcination/heating or washing with acidic/basic reagents to remove some of the compounds, thereby generating a porous structure. In this context, hydro(solvo)thermal strategies enable the direct (single-step) synthesis of diverse porous materials, which is attractive in terms of cost. This method targets the chemistry of the metal alkoxides and alkyls to generate a porous hierarchy without the use of external templates [371]. Table 2 summarises some strategies based on conventional and unconventional hydro(solvo)thermal methods to obtain diverse porous materials.

**Table 2.** Examples of the formation of porous structures using the hydrothermal method followed or not by complementary steps.

Chemical factors	Thermodynamic factors	Complementary Steps	Design	Ref.
$\text{Na}_2\text{WO}_4 \cdot 2\text{H}_2\text{O}$ + deionized water + acetic acid + HCl	120 °C for different time (4 h, 8 h, and 12 h).	Dried in vacuum at 70 °C for 6 h	 (4 h)	[372]
pluronic P127 + distilled water + HCl + 1-butanol + TEOS	100°C for 24 h	Calcined at 550°C for 5 h in air to remove polymer surfactant templates.		[373]
$\text{Ni}(\text{NO}_3)_2 \cdot 6\text{H}_2\text{O}$ + urea + absolute ethanol	180 °C for 12 h	Calcined at 500 °C for 2 h	 Flower-shaped microspheres morphology	[374]
$\text{Zn}(\text{CH}_3\text{COO})_2 \cdot 2\text{H}_2\text{O}$ + $\text{Co}(\text{CH}_3\text{COO})_2 \cdot 4\text{H}_2\text{O}$ +	180 °C for 10 h	Thermal annealing treatment at 350 °C for 4 h in air.		[375]



urea + distilled water + glycerin				
SnCl <sub>4</sub> + D-(+) glucose + distilled water	<p>Microwave-assisted hydrothermal reaction (CEM Discover S-Glass). The setting temperature, pressure limit, and reaction time are preset to 150°C, 180 psi, and 30 min, respectively.</p>	<p>Annealed in a furnace at 500 °C (rate of 2 °C min<sup>-1</sup>) at air conditions for 1 h.</p>		[376]
KAl(SO <sub>4</sub> ) <sub>2</sub> ·12H <sub>2</sub> O + CO(NH <sub>2</sub> ) <sub>2</sub> + distilled water	<p>Teflon lined autoclave and was microwave-treated at 180 °C for 40 min or hydrothermally treated at 180 °C for 3h, 300W.</p>	<p>calcining in air at 600 °C for 2 h</p>		[377]
mPEG-PLA + Na <sub>2</sub> ATP + deionized water + anhydrous CaCl <sub>2</sub> + NaOH	<p>sealed and heated in a microwave oven to a temperature of 120, 140, 160 or 180 °C and maintained at this temperature for 30 min.</p>	<p>Dried by freeze drying.</p>		[378]

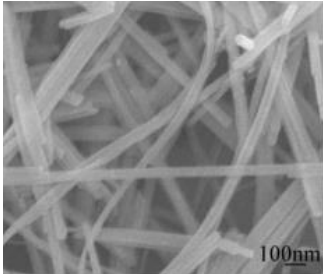
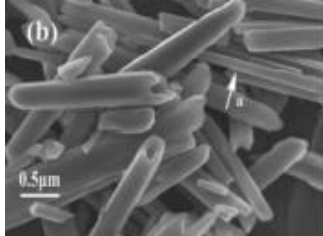
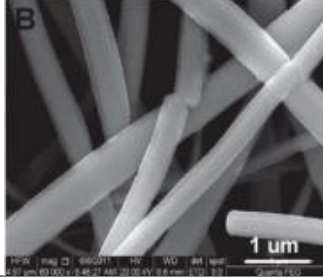

### *One-dimensional (1D) materials*

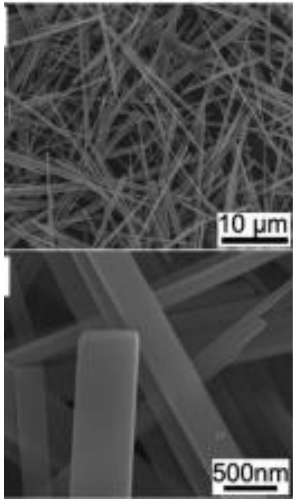
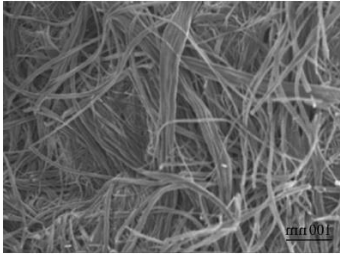
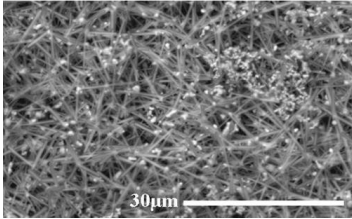
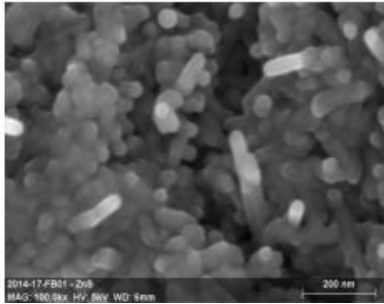
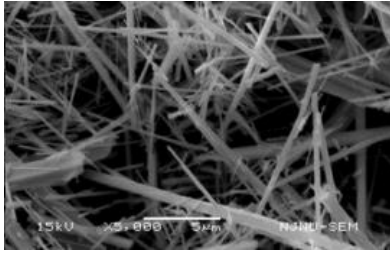
Wires, rods, tubes, and other related 1D structures show great technological potential as (bio)sensors, catalysts, optoelectronics, etc [379–382]. This can be explained by the preferential exposure of low-energy crystal facets, long segments of flat crystal planes, and fewer defects [380,383,384]. In addition, these 1D materials have anisotropic structure, which them with a quantum confinement effect, efficient electron transport, and optical excitations [385].

The formation of 1D nanostructures is strongly related to the crystallisation process. Thus, the aggregation of nuclei through homogeneous nucleation initiates the formation of building blocks that can serve as seeds for the growth and formation of 1D structures. Materials with polar surfaces preferentially grow to 1D structures [12,101,193,386]. Synthetic strategies for obtaining 1D nanostructures can be classified

by the form of growth. Symmetry can be controlled in several ways, such as the introduction of a liquid–solid interface and the addition of models with 1D morphology to induce growth. In this sense, controlling the amount of reagent or even the addition of a coating causes the growth rates of the facets to be kinetically controlled, and finally we can also mention the self-assembly of 0D structures [387]. Thus, wet synthesis has intrinsic advantages, such as the use of a wide range of solvents, precursors, stabilising agents, and anionic/cationic surfactants [388–390]. Examples of hydro(solvo)thermal growth for diverse 1D materials are summarised in Table 3.

**Table 3.** Examples of morphologies in tubes, wires, and rods via thermal hydro (solvo) synthesis.

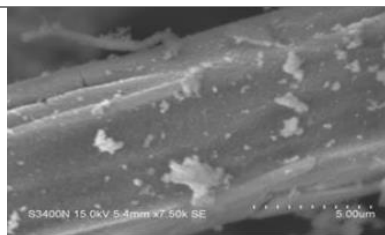
Chemical factors	Thermodynamic factor	Design	Ref.
$\text{KMnO}_4 + \text{NH}_4\text{Cl} +$ distilled water	140 °C for 24 h	 Scanning electron micrograph (SEM) showing a dense network of thin, randomly oriented nanowires. A scale bar in the bottom right corner indicates 100 nm.	[391]
$\text{MnSO}_4 \cdot \text{H}_2\text{O} +$ distilled water + PVP + $\text{NaClO}_3$	160 °C for 10 h	 Scanning electron micrograph (SEM) showing a collection of rod-like structures. A scale bar in the bottom left corner indicates 0.5 μm. The label '(b)' is in the top left corner.	[392]
$\text{TiO}_2$ NFs + glucose + deionized water	180 °C for 4 h	 Scanning electron micrograph (SEM) showing a network of nanofibers. A scale bar in the bottom right corner indicates 1 μm. The label 'B' is in the top left corner.	[393]
$\text{V}_2\text{O}_5 +$ distilled water + polyethylene glycol	220 °C and 260 °C for different times	 Scanning electron micrograph (SEM) showing a network of nanowires. A scale bar in the bottom right corner indicates 1 μm. Technical data at the bottom of the image includes: HV: 20.0 kV, X-Magnification: 10000x, Working Distance: 10.0 mm, X-Y-Z Size: 10.0 μm x 10.0 μm x 10.0 μm, Date: 2011-08-27, Time: 10:10:10, Operator: J. Liu, Model: S4800.	[394]

			
		220 °C and 3 days	
TiO <sub>2</sub> + KOH	heated in a microwave oven with a maximum power of 1200 W, at a pressure of 22 bars for 15 min.		[395]
poly(ethylene glycol) + AgNO <sub>3</sub> + HAuCl <sub>4</sub>	MW synthesis system maintaining a temperature of 100 °C for 1 h with a maximum pressure of 280 psi.		[396]
Zn(NO <sub>3</sub> ) <sub>2</sub> ·6H <sub>2</sub> O + (CH <sub>3</sub> OO) <sub>2</sub> Mn·4H <sub>2</sub> O, CS(NH <sub>2</sub> ) <sub>2</sub> + ethylenediamine	Stirred for 10 min, transferred into a teflon container and placed into the microwave reactor. Time: 15 – 20 min Pressure: 15 – 25 bar Temperature: 220 – 240°C		[397]
Na(SbO)C <sub>4</sub> H <sub>4</sub> O <sub>6</sub> + Se + ethylene glycol	Microwave oven equipped with a condenser to carry out the reaction under refluxing. The microwave frequency was 2.45 GHz and the power was set at 280 W. The microwave irradiation time was 3 h.		[398]

---

ZnO + NaOH  
TiO<sub>2</sub> + ethanol

Microwave-oven for 5  
minutes.  
Annealed at different  
temperatures such as  
500°C, 600°C, 700°C  
and 800°C



[399]

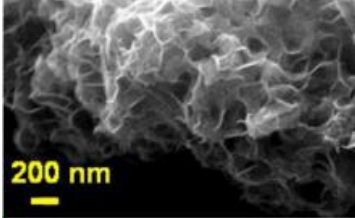
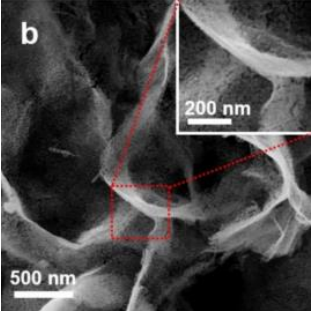
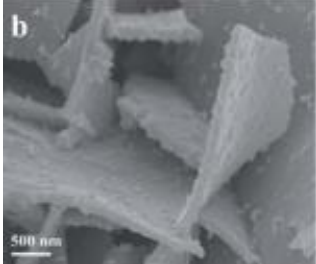
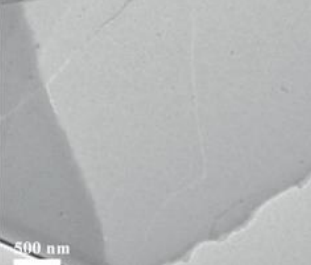
---


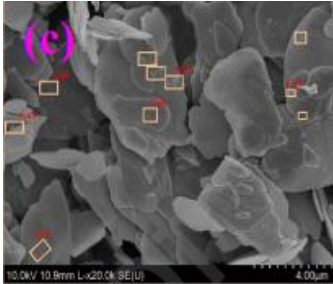
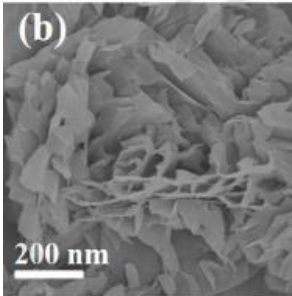
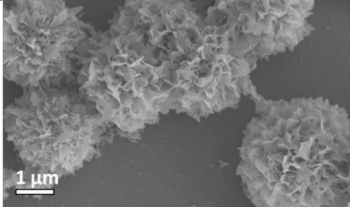
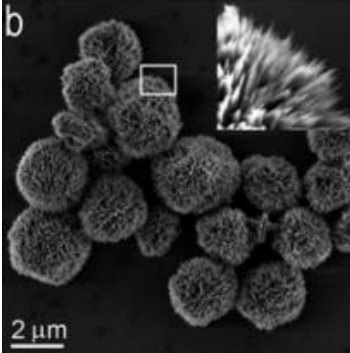
### *Two-dimensional (2D) materials*

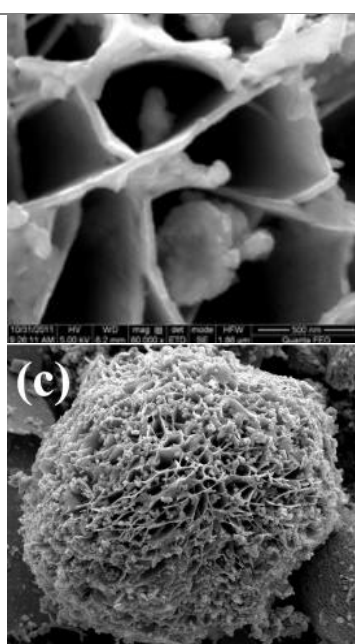
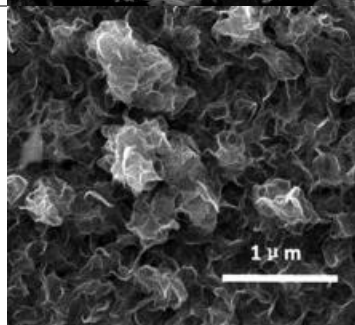
2D materials are currently the most studied systems, owing to their superior mechanical, electrical, magnetic, and optical properties [400–405]. In addition, these materials have an almost flat structure and are organised in extremely thin layers. The growth of a few or single 2D layered materials, called van der Waals layered crystals, can occur through three types of hybrid nanostructures obtained using (i) controlled growth of other 2D models [406–409], (ii) assembly of 2D nanomaterials in 1D and 3D [410–416], or (iii) formation of heterostructures by stacking different types of 2D materials [417–421].

For instance, Feng et al. [422] reported the large-scale preparation of Co<sub>3</sub>O<sub>4</sub> nanosheets with a thickness of sub-3 nm in the cubic Fd-3m space group using a non-surfactant and substrate-free hydrothermal method. These authors explored the effect of hydrothermal growth temperature on reaction yield and morphology. In 2015, Dunne et al. [423] implemented the first continuous hydrothermal flow synthesis of MoS<sub>2</sub> nanosheets. In addition, the number of MoS<sub>2</sub> layers nanosheets could be controlled under hydrothermal conditions from the varying the reaction time as well as the used organic reducing agent [424]. Ongoing efforts have been focused in scalable production of a huge variety of 2D layered materials for high-quality materials growth with well-controlled nanoscale properties [13]. In this scenario, we believe that the conventional and unconventional hydro(solvo)thermal strategies may play a more prominent role in relation to preparing novel 2D materials. From the examples presented in Table 4, we can see the conditions for obtaining these systems. Based on these conditions, we can see that the hydro(solvo)thermal growth of 2D layered materials is usually performed at low relatively temperature.

**Table 4.** Summary of the formation of 2D layered structures using the conventional and unconventional hydro(solvo)thermal strategies.

Chemical factors	Thermodynamic factor	Design	Ref.
Indium nitrate + thiourea + isopropyl alcohol + deionized water + nickel foam sheet	180 °C for 24 h		[425]
Cobalt chloride hexahydrate + urea + deionized water + ethylene glycol	150 °C for 5 min		[426]
Precursor: Ammonium molybdate tetrahydrate + absolute ethanol	180 °C for 20 h.		[427]
Ethylenediamine +red phosphorus	165 °C for 24 h		[428]

$\text{Bi}(\text{NO}_3)_3 \cdot 5\text{H}_2\text{O}$ + acetic acid + KBr + deionized water	120°C for 24h		[429]
$\text{BiOBr}$ + ethanol + $\text{Co}(\text{OAc})_2 \cdot 4\text{H}_2\text{O}$ + thiourea	180 °C for 12h		[430]
Iron chloride hexahydrate + 2- amino terephthalic acid + DMF/ethanol/water (v:v:v = 14:1:1)	125 °C for 12 h		[431]
Poly(allylamine hydrochloride) + $\text{CaCl}_2$ + $\text{Na}_2\text{HPO}_4$	Microwave– hydrothermal reactor maintained at 180 °C for 0.5 h.		[207]
$\text{CuO}$ + $\text{CuCl}_2 \cdot 2\text{H}_2\text{O}$ + deionized water + $\text{NH}_4\text{OH}$	Microwave- hydrothermal system (2.45 GHz/800 W) and kept at 100 °C for 30 seconds and for 15min under autogenous pressure.		[431]

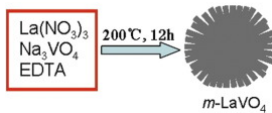
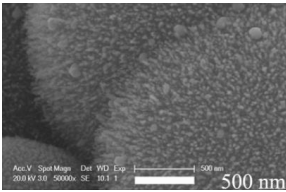
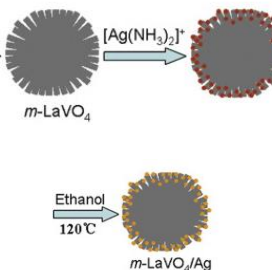
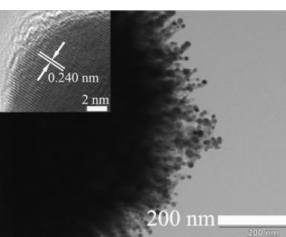
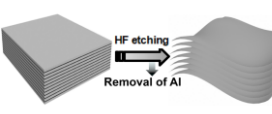
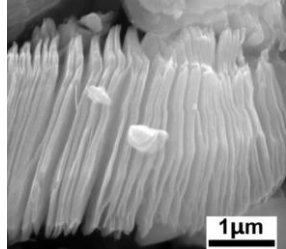
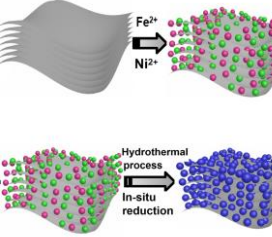
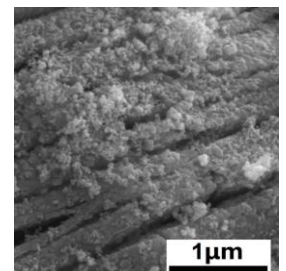
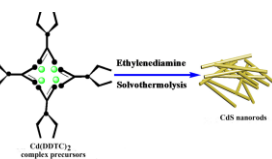
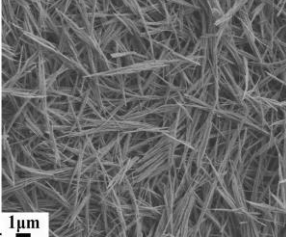

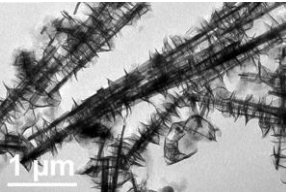
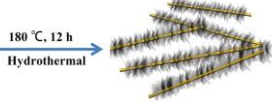
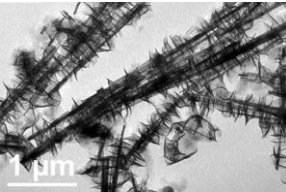
<p>SnCl<sub>2</sub>·2H<sub>2</sub>O + distilled water + citric acid +</p> <p>Microwave Accelerated Reaction System at 90°C, 120°C and 160°C for 30 min, and at 120°C for 10 and 60 min, respectively.</p> <p>Annealed at 700°C in air for 2h</p>		<p>[432]</p>
<p>ITO substrate + L-Cysteine + NaWO<sub>4</sub>·2H<sub>2</sub>O + (NH<sub>4</sub>)<sub>6</sub>Mo<sub>7</sub>O<sub>24</sub>·4H<sub>2</sub>O</p> <p>heated up to 220°C for 1.5 h in a microwave reaction system</p>		<p>[433]</p>

*Heterostructured materials: decorated, Janus like, core-shell, and yolk-shell*

Current research has been moving towards the new configuration development of heterostructured materials with increasingly complex structures to maximize their properties. Thus, the heterostructured materials by definition are usually based on the combination of two or more components to form composite structures, which can also be classified into decorated (or open-shell), core-shell, yolk-shell and Janus-like structures according to their configurations exhibit superior physical properties [434–448].

The purpose of obtaining advanced materials into new configurations led to the development of strategies to surface decorated is to give unique functionality to this novel material. In general, these decorated materials have an open-shell structure, which can be understood as an intermediary for obtaining a core-shell structures. In this way, a chemical group capable of undergoing successive reactions is added to the surface, leading to a heterostructure. Examples of the conventional and unconventional hydro(solvo)thermal growth of decorated materials are summarised in Table 5.

**Table 5.** Summary of the formation of decorated structures using the hydro(solvo)thermal.

Synthesis		Scheme	Design	Ref.
Chemical factors	Thermodynamic factor			
<p>Urchin-like <math>m\text{-LaVO}_4</math> microspheres</p> <p><math>\text{La}(\text{NO}_3)_3 + \text{Na}_3\text{VO}_4 + \text{EDTA} + \text{distilled water}</math></p>	200 °C for 12 h			[449]
<p>Deposition of Ag nanoparticles on urchin-like <math>m\text{-LaVO}_4</math> microspheres</p> <p><math>\text{AgNO}_3 + \text{ammonia solution} + \text{ethanol} + \text{urchin-like } m\text{-LaVO}_4 \text{ powder}</math></p>	110 °C for 1 h			
<p><math>\text{Ti}_3\text{C}_2\text{T}_x</math> MXene</p> <p>Removing the Al atomic layer from <math>\text{Ti}_3\text{AlC}_2</math> MAX in the HF solution, resulting black <math>\text{Ti}_3\text{C}_2\text{T}_x</math> MXene powders.</p>				
<p>FeNi/<math>\text{Ti}_3\text{C}_2\text{T}_x</math> MXene composites</p> <p><math>\text{Ti}_3\text{C}_2\text{T}_x \text{ MXene} + \text{deionized water} + \text{FeSO}_4 \cdot 7\text{H}_2\text{O} + \text{NiCl}_2 \cdot 6\text{H}_2\text{O} + \text{NaOH} + \text{N}_2\text{H}_4 \cdot \text{H}_2\text{O}</math></p>	60 °C for 4 h			[450]
<p>CdS nanorods</p> <p><math>\text{Cd}(\text{DDTC})_2 + \text{ethanediamine}</math></p>	180 °C for 12 h			[451]
<p>Pure <math>\text{ZnIn}_2\text{S}_4</math> microspheres</p> <p>zinc acetate dehydrate + indium nitrate hydrate + L-cysteine + distilled water</p>	180 °C for 12 h			
<p>1D <math>\text{CdS}@\text{ZnIn}_2\text{S}_4</math> helical architecture</p> <p>zinc acetate dehydrate + indium nitrate hydrate + L-</p>	180 °C for 12 h			



cysteine + CdS NRs +  
distilled water

The graphene oxide (GO) was prepared from natural graphite powder by a two-step oxidation reaction of pre-oxidation followed by modified Hummer's oxidation to reach complete oxidation of graphite.

$\text{BiVO}_4$  and W-doped  $\text{BiVO}_4$  nanoparticles

Pure and W-doped  $\text{BiVO}_4$  nanoparticles were synthesized by the modified metal organic decomposition method

W- $\text{BiVO}_4$ /rGO  
nanocomposite

6W- $\text{BiVO}_4$  + deionized  
water + GO powder

$\text{MoS}_2$

$\text{Na}_2\text{MoO}_4 \cdot 2\text{H}_2\text{O}$  +  
thioacetamide + deionized  
water + oxalic acid

$\text{Pd-SnO}_2/\text{MoS}_2$  in two steps

To obtain  $\text{SnO}_2$ :  
 $\text{SnCl}_4 \cdot 5\text{H}_2\text{O}$  +  $\text{NaOH}$  +  
deionized water

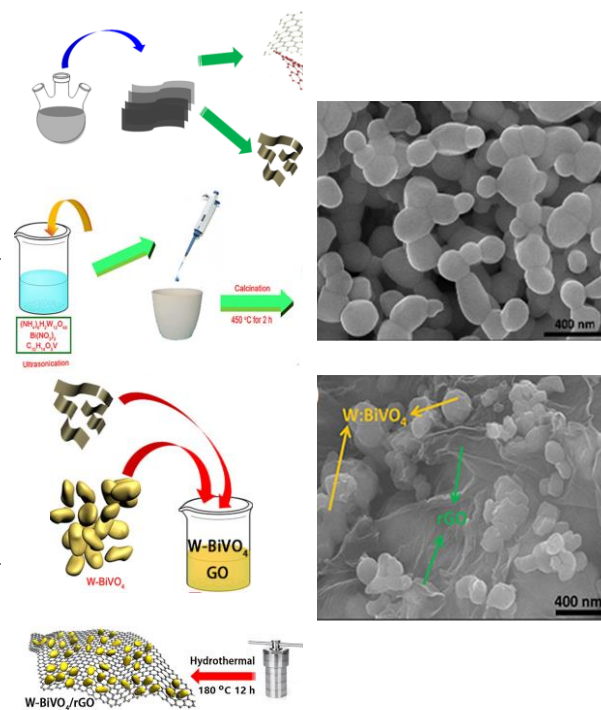
$\text{SnO}_2$  + hydrazine hydrate +  
 $\text{PdCl}_2$  +  $\text{MoS}_2$

180 °C for 12 h

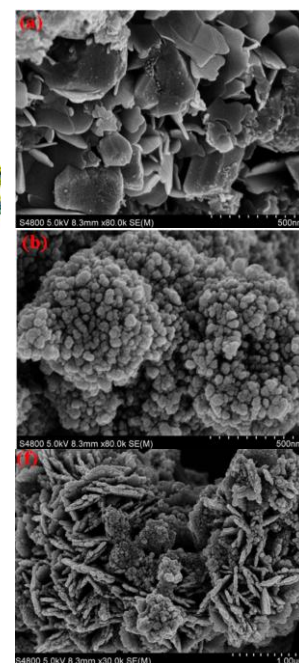
200 °C for 24 h

120° C for 12 h

180 °C for 16 h



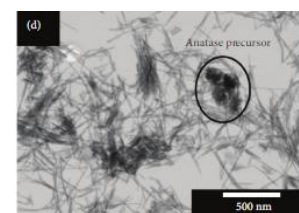
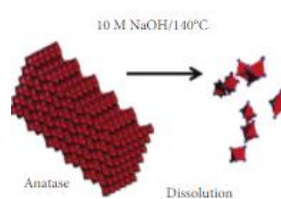
[452]



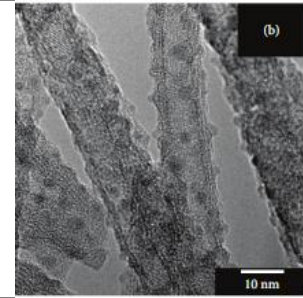
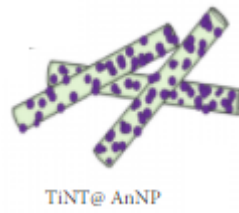
[453]

$\text{TiO}_2$  +  $\text{NaOH}$

microwave  
irradiation  
(domestic micro-  
oven, 2.45 MHz,  
maximum power  
of 700 W) at 140  
°C for 3 h



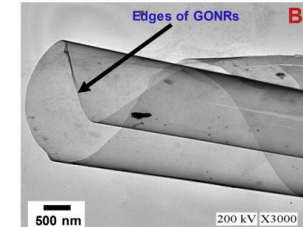
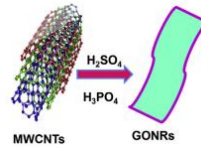
[454]



GONRs

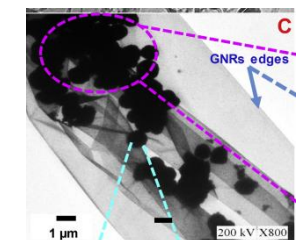
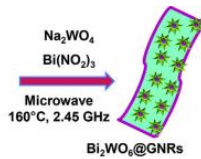
Multiwalled carbon nanotubes +  $H_2SO_4$  +  $H_3PO_4$

70 °C for 2 h



GONRs +  $Na_2WO_4 \cdot 2H_2O$  +  $Bi(NO_3)_3 \cdot 5H_2O$

microwave irradiation (2.45 GHz) at 160 °C for 30 min



Calcinated at 400 °C in air for 3 h

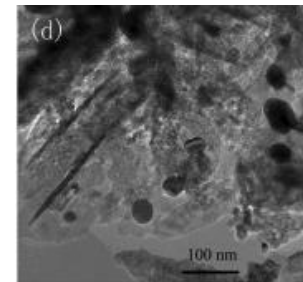
[455]

$Zn(Ac)_2 \cdot 2H_2O$  +  $Na_2O_2$  + deionizer water

400 W for 5 min



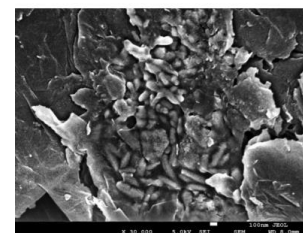
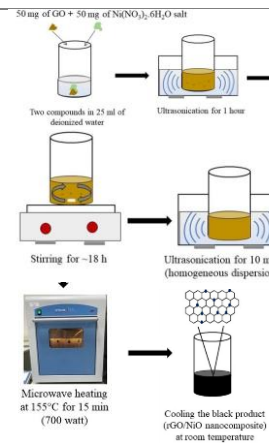
Ethylene glycol +  $AgNO_3$



[456]

$Ni(NO_3)_2 \cdot 6H_2O$  + pristine GO + deionized water

Microwave irradiation, the temperature was heated up to 155 °C in 10 min, and then the reaction was completed in 15 min (700 W).

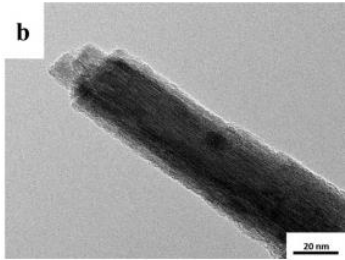


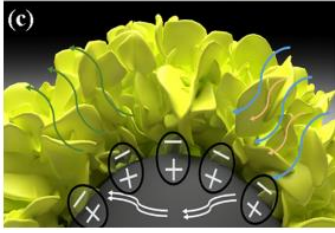
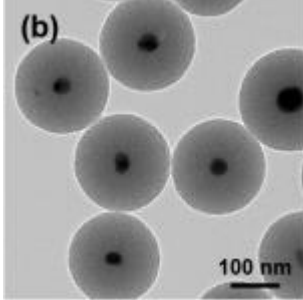
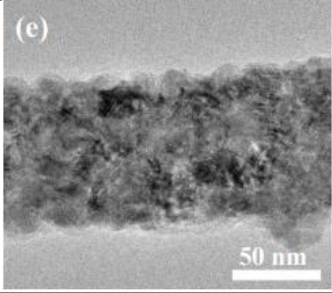
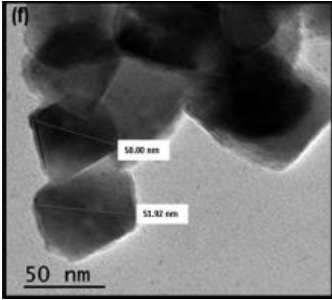
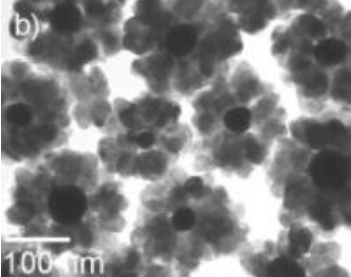
[457]

Core-shell structures have been intensively studied in the last decades, mainly due to its great technological potential [344,458,459]. Particularly, the first studies involving this core-shell system date back to the early 1990s. However, currently this field of research is highly diverse leading to obtained the different configurations, including multi-shells, yolk/shell and among others [460–463]. In this case, it is well known that the formation of the core is due to the precursor, prioritizing the function of the target nanoparticle. Hence, this process starts mainly with the formation of the core and later the shell layer [464,465]. Thus, the most commonly strategy used for the preparation of these materials with core-shell structure is based on a two or more step procedure [466,467]. However, continuous hydro(solvo)thermal synthesis eliminates the need for multi-stage processes and has been widely used for the growth of core-shell structures [468–473].

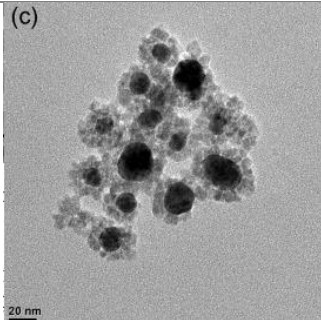
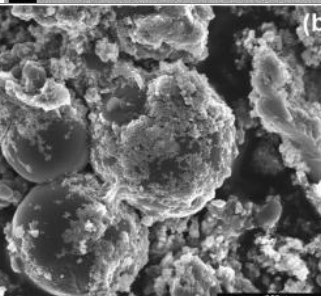
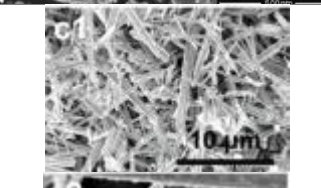
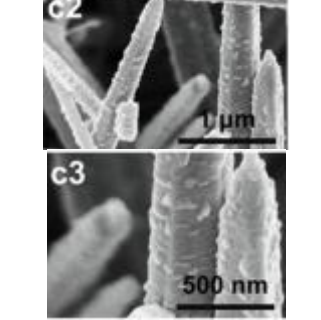
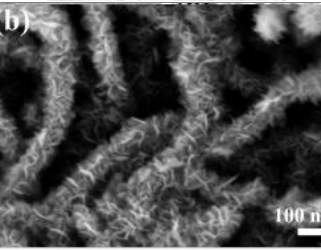
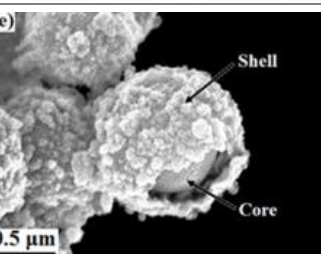
In this way, we can obtain several morphologies of crystals with core-shell structure, such as spherical, nanowires, nanotubes, nanobonds, nanowires and nanostars [474–477]. Its application occurs in several areas, such as catalysis, electronics, photonics, energy capture, drug administration, cell therapy, cancer treatment, biotechnology and environmental applications [478–484], depending on the chosen technique is possible to obtain different structural dimension. Examples of the conventional and unconventional hydro(solvo)thermal growth of decorated materials are summarised in Table 6.

**Table 6.** Summary of the formation of core-shell structures using the hydro(solvo)thermal.

Steps	Chemical factors	Thermodynamic factor	Design	Ref.
Preparation of h-WNRAs	$\text{Na}_2\text{WO}_4 \cdot 2\text{H}_2\text{O}$ + deionized water + HCl solution + $\text{H}_2\text{CO}_4$ + $\text{Rb}_2\text{SO}_4$	180 ° C for 5 h		[485]
Preparation of core/shell WTNRAs	$\text{TiO}_2$ + hydrochloric acid + deionized water + ethanol + tetrabutyl titanate + acetylacetone	Annealed at 550 °C for 30 min		

Synthesis of $\text{Fe}_3\text{O}_4$ nanoparticles	$\text{FeCl}_3 \cdot 6\text{H}_2\text{O}$ + ethylene glycol + NaAc	200 °C for 16 h		[486].
Production of flower-like core@shell structure $\text{Fe}_3\text{O}_4$ @ $\text{MoS}_2$ NCs	$(\text{NH}_4)_6\text{Mo}_7\text{O}_{24} \cdot 4\text{H}_2\text{O}$ + $\text{CH}_4\text{N}_2\text{S}$ + distilled water + $\text{Fe}_3\text{O}_4$ nanoparticles	different temperatures (170, 180 and 200 °C) for 12 h		
Synthesis of Ag NPs	Ammonia + $\text{AgNO}_3$ + deionized water + cetyltrimethyl ammonium bromide + glucose	120 °C for 8 h		[487]
Synthesis of Ag@ $\text{MSiO}_2$ NPs	Ag NPs + water + ethanol + cetyltrimethyl ammonium bromide + ammonia + TEOS			
Synthesis of $\text{ZnCo}_2\text{O}_4$ nanowires	$\text{Zn}(\text{NO}_3)_2 \cdot 6\text{H}_2\text{O}$ + $\text{Co}(\text{NO}_3)_2 \cdot 6\text{H}_2\text{O}$ + urea + $\text{NH}_4\text{F}$ + deionized water	100 °C for 8 h		[488]
Synthesis of $\text{ZnCo}_2\text{O}_4$ @ $\text{CoMoO}_4$ core-shell structures	Ammonium molybdate + $\text{Co}(\text{NO}_3)_2 \cdot 6\text{H}_2\text{O}$ + deionized water + precursor solution with $\text{ZnCo}_2\text{O}_4$	120 °C for 6 h. annealed at 350 °C for 2 h		
Synthesis of magnetite nanoparticles ( $\text{Fe}_3\text{O}_4$ ).	$\text{Fe}(\text{NO}_3)_3 \cdot 9\text{H}_2\text{O}$ + urea ( $\text{CON}_2\text{H}_4$ ) + sodium citrate ( $\text{C}_6\text{H}_5\text{O}_7\text{Na}_3 \cdot 2\text{H}_2\text{O}$ ) + distilled water + polyacrylamide (PAM)	200 °C for 12 h		[489]
Synthesis of core-shell hybrid nanoparticles of $\text{Fe}_3\text{O}_4$ @M (M = Ag or Au).	$\text{Fe}_3\text{O}_4$ @M core-shell nanoparticles + $\text{AgNO}_3$ or $\text{HAuCl}_4 \cdot 3\text{H}_2\text{O}$ , for the synthesis of $\text{Fe}_3\text{O}_4$ @Ag or $\text{Fe}_3\text{O}_4$ @Au	200 °C for 12 h		
Au@ $\text{TiO}_2$ core-shell	$\text{HAuCl}_4$ + sodium citrate + ascorbic acid + $\text{TiF}_4$ + deionized water	microwave oven for 10 min, and maintained at 180 °C with rapid stirring for 1h		[490]

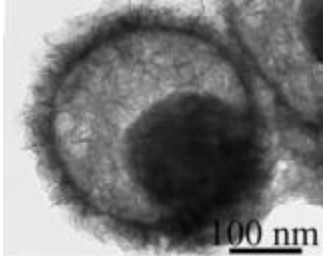
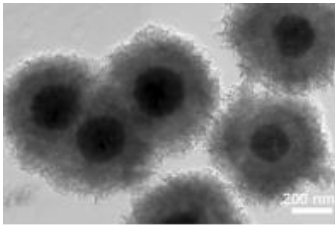
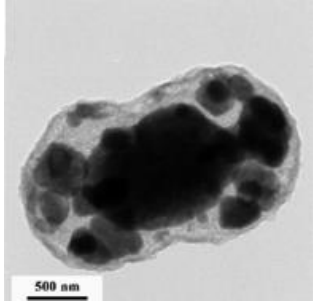


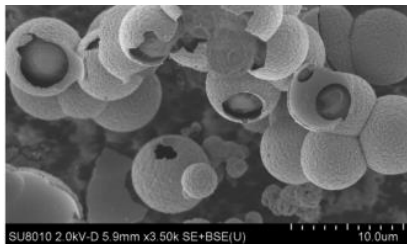
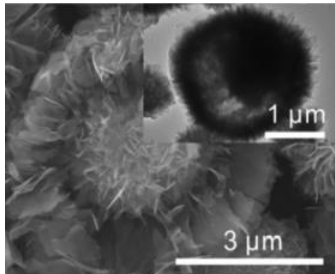
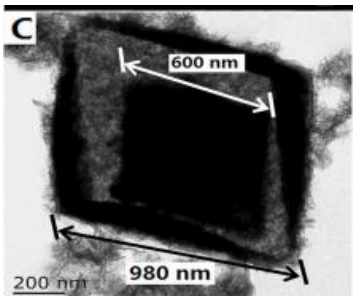
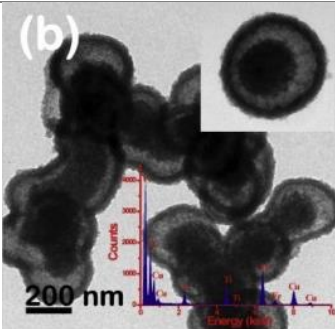
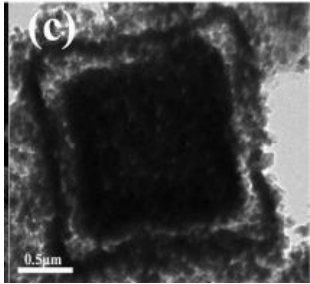
Au/SnO <sub>2</sub> core-shell NPs	HAuCl <sub>4</sub> + tri-sodium citrate + sodium hydroxide + sodium stannate	microwave oven heated to 180°C for 5 min, and maintained with rapid stirring at the temperature for 1 h		[491]
Microwave-assisted hydrothermal acid treatment	p-toluenesulfonic acid + GO@TiO <sub>2</sub> core-shell solid spheres +	transferred to a microwave oven (for 4 h at 160°C)		[492]
Synthesis of ZnO microrods/microflowers	Zn(NO <sub>3</sub> ) <sub>2</sub> ·6H <sub>2</sub> O + CO(NH <sub>2</sub> ) <sub>2</sub> + water	microwave digestion system and heated at 150 °C for 40 min.		[493]
Preparation of ZnO/ZnFe <sub>2</sub> O <sub>4</sub> /Fe core-shell composites		synthesized by chemical vapor decomposition (CVD)		[493]
CNT@NiMn <sub>2</sub> O <sub>4</sub> nanocomposite	KMnO <sub>4</sub> + Ni(NO <sub>3</sub> ) <sub>2</sub> ·6H <sub>2</sub> O + CO(NH <sub>2</sub> ) <sub>2</sub> + NH <sub>4</sub> F + deionized water	heated at 160 °C for 1 h at power of 800 W		[494]
SnO <sub>2</sub> core-shell microspheres	SnCl <sub>2</sub> ·2H <sub>2</sub> O + carbon spheres (template)	Microwave oven at a power of 400 W for 90 min. The hydrothermal temperatures were 120, 150 and 180 °C		[495]

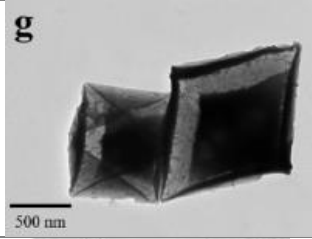
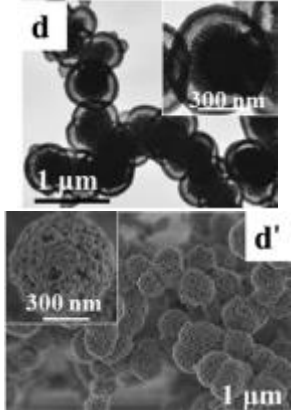
Yolk shell structures have a movable core within a hollow cavity covered by a porous outer layer [496]. It has characteristics such as low density, large surface area and

excellent load capacity. These structures are applied in several areas, such as catalysis [497–500] nanoreactors [501,502], energy storage [503–507] and biomedicine [440,508–513]. It is possible to obtain this structure through three methods. (i) Hard-templating that consists of coating the gem with a rigid material. (ii) Soft-templating, where the gem wall is formed by the self-assembly of the amphiphilic molecules. (iii) Self-modeling that does not use additional models. This method besides creating the empty cavity also involves the composition of the nanoparticle [440]. Notable examples of yolk shell structures prepared by hydro(solvo)thermal are presented in the Table 7.

**Table 7.** Summary of the formation of yolk shell structures using the hydrothermal.

Steps	Chemical factors	Thermodynamic factors	Design	Ref.
MoO <sub>2</sub>	MoCl <sub>5</sub> + Ethanol	180° C for 20 h		[514]
YS-MoS <sub>2</sub>	MoO <sub>2</sub> + n-hexanol + L-cystein	180 °C for 14 h		
Fe <sub>3</sub> O <sub>4</sub>	FeCl <sub>3</sub> + ethylene glycol + sodium acetate + trisodium citrate	200 °C for 8h		[515]
Fe <sub>3</sub> O <sub>4</sub> @SiO <sub>2</sub> core-shell	Fe <sub>3</sub> O <sub>4</sub> + ethanol + water + ammonia + TEOS	8 h under stirring		
Fe <sub>3</sub> O <sub>4</sub> @TiO <sub>2</sub> yolk-shell	Fe <sub>3</sub> O <sub>4</sub> @SiO <sub>2</sub> coated by TiO <sub>2</sub>	200 °C for 24h		
MnCO <sub>3</sub> particles	MnCl <sub>2</sub> + urea + C <sub>6</sub> H <sub>5</sub> Na <sub>3</sub> O <sub>7</sub> ·2H <sub>2</sub> O + PAA + deionized water	190 °C for 6h		[516]
MnO/C microsphere	MnCO <sub>3</sub> + ethanol/water (2:1) + resorcinol + formaldehyde + ammonia	mechanical stirring and calcined under vacuum at 600 °C for 9 h		

CeVO <sub>4</sub>	Ce(NO <sub>3</sub> ) <sub>3</sub> ·6H <sub>2</sub> O + NH <sub>4</sub> VO <sub>3</sub> + citric acid + distilled water	150 °C for 9h		[517]
α-Fe <sub>2</sub> O <sub>3</sub>	Fe(NO <sub>3</sub> ) <sub>3</sub> ·9H <sub>2</sub> O + CH <sub>3</sub> COONa + CO(NH <sub>2</sub> ) <sub>2</sub> + ethylene glycol	200 °C for 10 h annealed at 400 °C for 3 h		[518]
octahedron-shaped ZnFe <sub>2</sub> O <sub>4</sub> /SiO <sub>2</sub> with yolk-shell structure	Zn(NO <sub>3</sub> ) <sub>2</sub> ·6H <sub>2</sub> O + Fe(NO <sub>3</sub> ) <sub>3</sub> ·9H <sub>2</sub> O + urea + ethylene glycol + SiO <sub>2</sub> spheres with mesoporous shells.	200 °C for 24 h		[519]
Synthesis of FeTi yolk-shell adsorbents	Ti(OC <sub>4</sub> H <sub>9</sub> ) <sub>4</sub> + FeSO <sub>4</sub> ·7H <sub>2</sub> O + HOCH <sub>2</sub> CH <sub>2</sub> OH	microwave (MCR-3, 500 W) heated at 160 °C for 30 min		[520]
Synthesis of yolk-shell CdS microcubes	Cd-Fe PBA microcubes + water + Na <sub>2</sub> S	150 °C for 120 min under microwave-irradiation with continuous magnetic stirring in a single mode microwave reactor		[521]

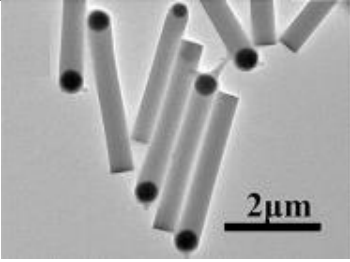
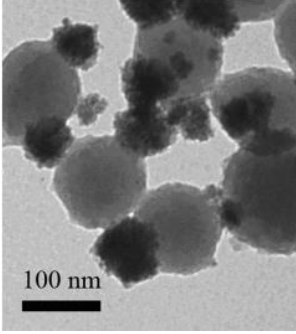
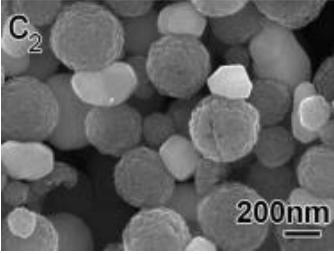
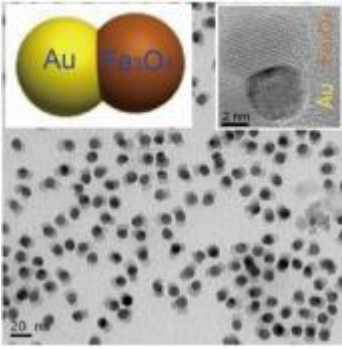
Synthesis of MIL-53(Fe) Nanocrystal	$\text{FeCl}_3 \cdot 6\text{H}_2\text{O} + \text{H}_2\text{BDC} + \text{DMF}$	150 °C for 2 h in a single-mode microwave reactor		[522]
Synthesis of yolk-shell porous microspheres of calcium phosphate	Calcium l-lactate pentahydrate + deionized water + Adenosine 5'-triphosphate disodium salt (ATP) + NaOH	Microwave oven to a temperature of 120, 140, or 160 °C and maintained at that temperature for 5, 15, 30, 60, or 90 min		[523]

Janus-like structures are particles that have different functionalities on their opposite sides. It can be composed of three distinct groups, (i) hard (inorganic), (ii) soft (organic or polymeric) and (iii) hybrids (organic/inorganic) [441]. These Janus-like nanoparticles have several shapes, from traditional conventional spheres to more elaborate structures, such as dumbbells [524–527], snowman [528–535], nameplate [536–538], rod [539,540] or tadpole shapes [541]. Due to its peculiarity, the control and manipulation of these particles is achieved by manipulating various external factors (temperature, light, pH or ionic strength). The mass transport at the interface between the two phases of the particle controls the particle size, edge geometry and material porosity [441]. Some examples are shown in Table 7.

**Table 7.** Summary of the formation of *Janus* structures using the hydro(solvo)thermal.

Steps	Chemical factors	Thermodynamic factors	Design	Ref.
Hydrophilic $\text{Fe}_3\text{O}_4$	$\text{FeCl}_3 \cdot 6\text{H}_2\text{O} + \text{ethylene glycol} + \text{NaAc} + \text{polyethylene glycol}$	200 °C for 8–72 h		[540]



The matchstick shaped Janus rods	PVP + n-pentanol + $\text{Fe}_3\text{O}_4$ + ethanol + water + sodium citrate dihydrate + ammonia hydroxide + TEOS	a simple wet-chemical method		
Synthesis of P(methylmethacrylate - acrylic acid - Divinylbenzene) nanoparticles	methylmethacrylate + acrylic acid + Divinylbenzene + Potassium peroxy sulfate + deionized water	soapfree emulsion polymerization  heated from ambient temperature to 100 °C		[542]
Synthesis of P(methylmethacrylate - acrylic acid - Divinylbenzene)/ $\text{Fe}_3\text{O}_4$ magnetic Janus nanoparticles	P(MMA-AA-DVB) nanoparticles + $\text{FeCl}_3 \cdot 6\text{H}_2\text{O}$ + Trisodium citrate + Sodium acetate	200 °C for 10 h.		
$\text{Fe}_3\text{O}_4$ particles	Hexahydrated ferric chloride + sodium acetate + sodium polyacrylate + ethylene glycol	220°C for 6 h		[543]
$\text{Fe}_3\text{O}_4$ -Ag Janus composite particles	sodium oleate + oleic acid + ethanol + silver nitrate + $\text{Fe}_3\text{O}_4$ particles	200 C for 1 h, 6 h, 10 h, and 20 h		
Synthesis of Janus Au- $\text{Fe}_3\text{O}_4$ Nanoparticles	Hexane + Au nanoparticles + Iron(III) acetylacetonate + oleylamine + oleic acid	Prestirred for 2 min and then heated to 155 °C (for 15 min) by 400 W of microwave radiation with stirring. The mixture was further heated to 235 °C by 120 W with stirring and aged at 235 °C for another 8 min.		[544]

To prevent functional modification of the particles, it must immobilize. Therefore, an interface can be used. In order to obtain this immobilization, a monolayer of symmetrical particles is usually adsorbed onto a flat solid surface and, subsequently, its outer upper part is modified [545–547]. In this way, Janus particles come from

symmetrical particles. For desymmetrization, chemical or physicochemical processes are used. Among these processes, we can highlight (i) top-selective modification, (ii) self-assembly by templates, (iii) controlled phase separation phenomena and (iv) controlled surface nucleation. Among the various synthesis strategies, self-assembly, masking and phase separation stand out [545–547].

Obtaining Janus nanoparticles by self-assembly, as the name implies, is based on the self-assembly of block copolymers or the competitive adsorption of binders [280]. This method aims at the thermodynamic process of polymer mixtures. As is well-known, parameters like pH, temperature, and ionic strength (polyelectrolytes) are important for process control [545–547].

The masking process among the techniques is the most flexible as it is capable of modifying the nanocrystal's surfaces with a huge variety of functional groups. As such, the mechanism of this technique can be described as the trapping of nanoparticles at the interface between two fluid phases, or depositing or adsorbing them on a solid surface [545–547]. Obtaining Janus-like nanoparticles through phase separation is normally used for inorganic materials, being recently applied to polymeric materials as well as to hybrid organic/inorganic materials. This technique stands out for the possibility of obtaining complex structures with advanced functionality [545–547].

## **Summary and Outlook**

This critical review provides an overview of the main advantages related to conventional and unconventional hydro(solvo)thermal approaches for novel advanced materials design. This versatile synthetic strategy has been industrially used since the nineteenth century, making it possible to obtain several crystals with a high level of purity that in turn cannot be achieved by other synthetic methods [548]. We can highlight that, although there are a lot of unknowns on the anisotropic crystal growth, the conventional and unconventional hydro(solvo)thermal approaches are relatively simple and low-costs and have displayed a prominent role in the development and discovery of new advanced materials with entirely new physical/chemical properties and unique multi-functionalities for many technological applications. In this direction, the continuous advances in this research field, in particular, have more recently led to the integration of machine-learning

algorithms to predict hydro(solvo)thermal reaction outcomes leading to a success rate of about 89 percent [549]. Thus, we anticipate that these advances will contribute so that in the future we can select the better materials for a particular technology application of interest, as well as we will have the ability to predict the experimental conditions to obtain their desired structure-composition-morphology. Furthermore, we can also conclude that diverse highly complex structures can be directly synthesized from such strategies, which provide a feasible approach for creating a huge variety of advanced materials, as summarized in this review.

### **Author contributions**

MCMDC wrote the original draft with help from SD and WEP. FAL conceived the project, supervised students, and contributed to the revised manuscript.

### **Declaration of Competing Interest**

The authors declare that they have no known competing financial interests or personal relationships that could have appeared to influence the work reported in this paper.

### **Acknowledgements**

The authors are grateful for the support provided by the Brazilian agencies Conselho Nacional de Desenvolvimento Científico e Tecnológico (CNPq), Fundação Araucária, and Coordenação de Aperfeiçoamento de Pessoal de Nível Superior (CAPES).

### **References**

- [1] U. Naresh, R.J. Kumar, K.C.B. Naidu, Hydrothermal synthesis of barium copper ferrite nanoparticles: Nanofiber formation, optical, and magnetic properties, *Mater. Chem. Phys.* 236 (2019) 121807. <https://doi.org/10.1016/j.matchemphys.2019.121807>.
- [2] M. Baghbanzadeh, L. Carbone, P.D. Cozzoli, C.O. Kappe, Microwave-Assisted Synthesis of Colloidal Inorganic Nanocrystals, *Angew. Chemie Int. Ed.* 50 (2011) 11312–11359. <https://doi.org/10.1002/anie.201101274>.
- [3] C. Nan, J. Lu, C. Chen, Q. Peng, Y. Li, Solvothermal synthesis of lithium iron phosphate nanoplates, *J. Mater. Chem.* 21 (2011) 9994. <https://doi.org/10.1039/c0jm04126b>.
- [4] S.W. Kim, N.T. Khoa, J.W. Yun, D. Van Thuan, E.J. Kim, S.H. Hahn,

- Hierarchical ZnO nanosheets/nanodisks hydrothermally grown on microrod backbones, *Mater. Chem. Phys.* 171 (2016) 252–259.  
<https://doi.org/10.1016/j.matchemphys.2016.01.015>.
- [5] T. Yu, J. Joo, Y. Il Park, T. Hyeon, Large-scale nonhydrolytic sol-gel synthesis of uniform-sized ceria nanocrystals with spherical, wire, and tadpole shapes, *Angew. Chemie - Int. Ed.* 44 (2005) 7411–7414.  
<https://doi.org/10.1002/anie.200500992>.
- [6] Q. Fu, X. Tang, B. Huang, T. Hu, L. Tan, L. Chen, Y. Chen, Q. Fu, X. Tang, B. Huang, T. Hu, L. Tan, L. Chen, Y. Chen, Recent Progress on the Long-Term Stability of Perovskite Solar Cells, *Adv. Sci.* 5 (2018) 1700387.  
<https://doi.org/10.1002/ADVS.201700387>.
- [7] M.M. Nakata, T.M. Mazzo, G.P. Casali, F.A. La Porta, E. Longo, A large red-shift in the photoluminescence emission of  $\text{Mg}_{1-x}\text{Sr}_x\text{TiO}_3$ , *Chem. Phys. Lett.* 622 (2015) 9–14. <https://doi.org/10.1016/j.cplett.2015.01.011>.
- [8] I. Khan, K. Saeed, I. Khan, Nanoparticles: Properties, applications and toxicities, *Arab. J. Chem.* 12 (2019) 908–931. <https://doi.org/10.1016/j.arabjc.2017.05.011>.
- [9] W.E. Pottker, R. Ono, M.A. Cobos, A. Hernando, J.F.D.F. Araujo, A.C.O. Bruno, S.A. Lourenço, E. Longo, F.A. La Porta, Influence of order-disorder effects on the magnetic and optical properties of  $\text{NiFe}_2\text{O}_4$  nanoparticles, *Ceram. Int.* 44 (2018) 17290–17297. <https://doi.org/10.1016/j.ceramint.2018.06.190>.
- [10] F.M. Pinto, V.Y. Suzuki, R.C. Silva, F.A. La Porta, Oxygen Defects and Surface Chemistry of Reducible Oxides, *Front. Mater.* 6 (2019).  
<https://doi.org/10.3389/fmats.2019.00260>.
- [11] M. Krasovska, V. Gerbreder, V. Paskevics, A. Ogurcovs, I. Mihailova, Obtaining a Well-Aligned ZnO Nanotube Array Using the Hydrothermal Growth Method, *Latv. J. Phys. Tech. Sci.* 52 (2015) 28–40. <https://doi.org/10.1515/lpts-2015-0026>.
- [12] J.P.A. de Jesus, A.C.L. Santos, F.M. Pinto, C.A. Taft, F.A. La Porta, Review: theoretical and experimental investigation of the intrinsic properties of  $\text{Zn}_2\text{GeO}_4$  nanocrystals, *J. Mater. Sci.* 56 (2021) 4552–4568.  
<https://doi.org/10.1007/s10853-020-05549-8>.
- [13] F. de A. La Porta, C.A. Taft, *Functional Properties of Advanced Engineering Materials and Biomolecules*, 1st ed., Springer International Publishing, Cham, Switzerland, 2021. <https://doi.org/10.1007/978-3-030-62226-8>.
- [14] F. de A. La Porta, C.A. Taft, *Emerging Research in Science and Engineering Based on Advanced Experimental and Computational Strategies*, 1st ed., Springer International Publishing, Cham, Switzerland, 2020.  
<https://doi.org/10.1007/978-3-030-31403-3>.
- [15] E. Longo, F. de A. La Porta, *Recent Advances in Complex Functional Materials*, 1st ed., Springer International Publishing, Cham, Switzerland, 2017.  
<https://doi.org/10.1007/978-3-319-53898-3>.
- [16] C.S. Riccardi, R.C. Lima, M.L. dos Santos, P.R. Bueno, J.A. Varela, E. Longo, Preparation of  $\text{CeO}_2$  by a simple microwave–hydrothermal method, *Solid State*

- Ionics. 180 (2009) 288–291. <https://doi.org/10.1016/j.ssi.2008.11.016>.
- [17] G. Canu, V. Buscaglia, Hydrothermal synthesis of strontium titanate: thermodynamic considerations, morphology control and crystallisation mechanisms, *CrystEngComm*. 19 (2017) 3867–3891. <https://doi.org/10.1039/C7CE00834A>.
- [18] L. Wang, J. Zhou, G. Liu, S. Ouyang, H. Liu, Structure and properties of microwave sintering ZnO ceramics, *Ferroelectrics*. 356 (2007) 185–188. <https://doi.org/10.1080/00150190701512235>.
- [19] Z. Zhu, D. Liu, H. Liu, J. Du, H. Yu, J. Deng, Fabrication and luminescent properties of Al<sub>2</sub>O<sub>3</sub>:Cr<sup>3+</sup> microspheres via a microwave solvothermal route followed by heat treatment, *Opt. Commun.* 285 (2012) 3140–3142. <https://doi.org/10.1016/j.optcom.2012.02.084>.
- [20] O.D. Jayakumar, H.G. Salunke, R.M. Kadam, M. Mohapatra, G. Yaswant, S.K. Kulshreshtha, Magnetism in Mn-doped ZnO nanoparticles prepared by a co-precipitation method, *Nanotechnology*. 17 (2006) 1278–1285. <https://doi.org/10.1088/0957-4484/17/5/020>.
- [21] W.J. Li, E.W. Shi, Y.Q. Zheng, Z.W. Yin, Hydrothermal preparation of nanometer ZnO powders, *J. Mater. Sci. Lett.* 20 (2001) 1381–1383. <https://doi.org/10.1023/A:1011679124219>.
- [22] H. Zhang, D. Yang, X. Ma, Y. Ji, J. Xu, D. Que, Synthesis of flower-like ZnO nanostructures by an organic-free hydrothermal process, *Nanotechnology*. 15 (2004) 622–626. <https://doi.org/10.1088/0957-4484/15/5/037>.
- [23] D.R. Modeshia, R.I. Walton, Solvothermal synthesis of perovskites and pyrochlores: crystallisation of functional oxides under mild conditions, *Chem. Soc. Rev.* 39 (2010) 4303. <https://doi.org/10.1039/b904702f>.
- [24] K. Byrappa, T. Adschiri, Hydrothermal technology for nanotechnology, *Prog. Cryst. Growth Charact. Mater.* 53 (2007) 117–166. <https://doi.org/10.1016/j.pcrysgrow.2007.04.001>.
- [25] W. Shi, S. Song, H. Zhang, Hydrothermal synthetic strategies of inorganic semiconducting nanostructures, *Chem. Soc. Rev.* 42 (2013) 5714. <https://doi.org/10.1039/c3cs60012b>.
- [26] L. Liang, X. Kang, Y. Sang, H. Liu, One-Dimensional Ferroelectric Nanostructures: Synthesis, Properties, and Applications, *Adv. Sci.* 3 (2016) 1500358. <https://doi.org/10.1002/advs.201500358>.
- [27] A.K. Cheetham, G. Férey, T. Loiseau, Open-Framework Inorganic Materials, *Angew. Chemie Int. Ed.* 38 (1999) 3268–3292. [https://doi.org/10.1002/\(SICI\)1521-3773\(19991115\)38:22<3268::AID-ANIE3268>3.0.CO;2-U](https://doi.org/10.1002/(SICI)1521-3773(19991115)38:22<3268::AID-ANIE3268>3.0.CO;2-U).
- [28] G. Li, L. Li, S. Feng, M. Wang, L. Zhang, X. Yao, An Effective Synthetic Route for a Novel Electrolyte: Nanocrystalline Solid Solutions of (CeO<sub>2</sub>)<sub>1-x</sub>(BiO<sub>1.5</sub>)<sub>x</sub>, *Adv. Mater.* 11 (1999) 146–149. [https://doi.org/10.1002/\(SICI\)1521-4095\(199902\)11:2<146::AID-ADMA146>3.0.CO;2-7](https://doi.org/10.1002/(SICI)1521-4095(199902)11:2<146::AID-ADMA146>3.0.CO;2-7).
- [29] S. Feng, M. Greenblatt, Galvanic cell type humidity sensor with NASICON-

- based material operative at high temperature, *Chem. Mater.* 4 (1992) 1257–1262. <https://doi.org/10.1021/cm00024a027>.
- [30] Q.W. Chen, Y.T. Qian, Z.Y. Chen, K.B. Tang, G.E. Zhou, Y.H. Zhang, Preparation of a Tl-based superconductor by a hydrothermal method, *Phys. C Supercond.* 224 (1994) 228–230. [https://doi.org/10.1016/0921-4534\(94\)90258-5](https://doi.org/10.1016/0921-4534(94)90258-5).
- [31] Y. Mao, G. Li, W. Xu, S. Feng, Hydrothermal synthesis and characterization of nanocrystalline pyrochlore oxides  $M_2Sn_2O_7$  ( $M = La, Bi, Gd$  or  $Y$ ), *J. Mater. Chem.* 10 (2000) 479–482. <https://doi.org/10.1039/a906979h>.
- [32] C. Zhao, S. Feng, Z. Chao, C. Shi, R. Xu, J. Ni, Hydrothermal synthesis of the complex fluorides  $LiBaF_3$  and  $KMgF_3$  with perovskite structures under mild conditions, *Chem. Commun.* (1996) 1641. <https://doi.org/10.1039/cc9960001641>.
- [33] D. Wang, R. Yu, S. Feng, W. Zheng, R. Xu, Y. Matsumura, M. Takano, An Effective Preparation Route to A Giant Magnetoresistance Material: Hydrothermal Synthesis and Characterization of  $La_{0.5}Sr_{0.5}MnO_3$ , *Chem. Lett.* 32 (2003) 74–75. <https://doi.org/10.1246/cl.2003.74>.
- [34] C. Zhao, S. Feng, R. Xu, C. Shi, J. Ni, Hydrothermal synthesis and lanthanide doping of complex fluorides,  $LiYF_4$ ,  $KYF_4$  and  $BaBeF_4$  under mild conditions, *Chem. Commun.* (1997) 945–946. <https://doi.org/10.1039/a607066c>.
- [35] J.W. Gong, X.F. Wan, Hydrothermal synthesis of different nanostructure  $MoO_3$  sensing materials: application for transformer fault diagnosis, *Mater. Technol.* 30 (2015) 332–337. <https://doi.org/10.1179/1753555715Y.0000000008>.
- [36] W. Chen, H. Gan, W. Zhang, Z. Mao, Hydrothermal Synthesis and Hydrogen Sensing Properties of Nanostructured  $SnO_2$  with Different Morphologies, *J. Nanomater.* 2014 (2014) 1–7. <https://doi.org/10.1155/2014/291273>.
- [37] S.-H. Feng, G.-H. Li, Hydrothermal and Solvothermal Syntheses, in: R. Xu, Y. Xu (Eds.), *Mod. Inorg. Synth. Chem.*, Second Edi, Elsevier, Amsterdam, 2017: pp. 73–104. <https://doi.org/10.1016/B978-0-444-63591-4.00004-5>.
- [38] G.I. Dzhardimalieva, I.E. Uflyand, Design and synthesis of coordination polymers with chelated units and their application in nanomaterials science, *RSC Adv.* 7 (2017) 42242–42288. <https://doi.org/10.1039/C7RA05302A>.
- [39] S.H. Mir, L.A. Nagahara, T. Thundat, P. Mokarian-Tabari, H. Furukawa, A. Khosla, Review—Organic-Inorganic Hybrid Functional Materials: An Integrated Platform for Applied Technologies, *J. Electrochem. Soc.* 165 (2018) B3137–B3156. <https://doi.org/10.1149/2.0191808jes>.
- [40] M. Shellaiiah, K.W. Sun, Inorganic-Diverse Nanostructured Materials for Volatile Organic Compound Sensing, *Sensors.* 21 (2021) 633. <https://doi.org/10.3390/s21020633>.
- [41] J. Hwang, A. Ejsmont, R. Freund, J. Goscianska, B.V.K.J. Schmidt, S. Wuttke, Controlling the morphology of metal–organic frameworks and porous carbon materials: metal oxides as primary architecture-directing agents, *Chem. Soc. Rev.* 49 (2020) 3348–3422. <https://doi.org/10.1039/C9CS00871C>.
- [42] M.J.C. De Oliveira, M.R. Quirino, L.S. Neiva, L. Gama, J.B. Oliveira, Síntese de

óxido de cério (  $\text{CeO}_2$  ) com alta área superficial por meio do método hidrotérmico assistido por microondas, *Rev. Eletrônica Mater. e Process.* 6 (2011) 170–174.

- [43] P. Benito, M. Herrero, F.M. Labajos, V. Rives, Effect of post-synthesis microwave–hydrothermal treatment on the properties of layered double hydroxides and related materials, *Appl. Clay Sci.* 48 (2010) 218–227. <https://doi.org/10.1016/j.clay.2009.11.051>.
- [44] R.I. Walton, Perovskite Oxides Prepared by Hydrothermal and Solvothermal Synthesis: A Review of Crystallisation, Chemistry, and Compositions, *Chem. – A Eur. J.* 26 (2020) 9041–9069. <https://doi.org/10.1002/chem.202000707>.
- [45] B.J. Rani, S. Swathi, R. Yuvakkumar, G. Ravi, P. Kumar, E.S. Babu, S. Alfarraj, S.A. Alharbi, D. Velauthapillai, Solvothermal synthesis of  $\text{CoMoO}_4$  nanostructures for electrochemical applications, *J. Mater. Sci. Mater. Electron.* 32 (2021) 5989–6000. <https://doi.org/10.1007/s10854-021-05319-5>.
- [46] Q.-T. Xu, J.-C. Li, H.-G. Xue, S.-P. Guo, Binary iron sulfides as anode materials for rechargeable batteries: Crystal structures, syntheses, and electrochemical performance, *J. Power Sources.* 379 (2018) 41–52. <https://doi.org/10.1016/j.jpowsour.2018.01.022>.
- [47] G.H. Sonawane, S.P. Patil, S.H. Sonawane, Nanocomposites and Its Applications, in: S.M. Bhagyaraj, O.S. Oluwafemi, N. Kalarikkal, S. Thomas (Eds.), *Appl. Nanomater.*, First Edit, Elsevier, San Diego, CA, USA, 2018: pp. 1–22. <https://doi.org/10.1016/B978-0-08-101971-9.00001-6>.
- [48] M. Yoshimura, K. Byrappa, Hydrothermal processing of materials: past, present and future, *J. Mater. Sci.* 43 (2008) 2085–2103. <https://doi.org/10.1007/s10853-007-1853-x>.
- [49] S. Reghunath, D. Pinheiro, S.D. KR, A review of hierarchical nanostructures of  $\text{TiO}_2$ : Advances and applications, *Appl. Surf. Sci. Adv.* 3 (2021) 100063. <https://doi.org/10.1016/j.apsadv.2021.100063>.
- [50] M.M. Lencka, R.E. Riman, Thermodynamic modeling of hydrothermal synthesis of ceramic powders, *Chem. Mater.* 5 (1993) 61–70. <https://doi.org/10.1021/cm00025a014>.
- [51] Y.-J. Zhu, F. Chen, Microwave-Assisted Preparation of Inorganic Nanostructures in Liquid Phase, *Chem. Rev.* 114 (2014) 6462–6555. <https://doi.org/10.1021/cr400366s>.
- [52] R.E. Morris, Ionothermal synthesis—ionic liquids as functional solvents in the preparation of crystalline materials, *Chem. Commun.* (2009) 2990. <https://doi.org/10.1039/b902611h>.
- [53] P. Palanisamy, M. Chavali, E.M. Kumar, K.C. Etika, Hybrid nanocomposites and their potential applications in the field of nanosensors/gas and biosensors, in: K. Pal, F. Gomes (Eds.), *Nanofabrication Smart Nanosensor Appl.*, Elsevier, 2020: pp. 253–280. <https://doi.org/10.1016/B978-0-12-820702-4.00011-8>.
- [54] G. Yang, S.-J. Park, Facile hydrothermal synthesis of  $\text{NiCo}_2\text{O}_4$ - decorated filter carbon as electrodes for high performance asymmetric supercapacitors,

- Electrochim. Acta. 285 (2018) 405–414.  
<https://doi.org/10.1016/j.electacta.2018.08.013>.
- [55] G. Yang, S.J. Park, MnO<sub>2</sub> and biomass-derived 3D porous carbon composites electrodes for high performance supercapacitor applications, *J. Alloys Compd.* 741 (2018) 360–367. <https://doi.org/10.1016/j.jallcom.2018.01.108>.
- [56] K. Kappis, C. Papadopoulos, J. Papavasiliou, J. Vakros, Y. Georgiou, Y. Deligiannakis, G. Avgouropoulos, Tuning the catalytic properties of copper-promoted nanoceria via a hydrothermal method, *Catalysts*. 9 (2019).  
<https://doi.org/10.3390/catal9020138>.
- [57] A. Boudiba, C. Zhang, C. Bittencourt, P. Umek, M.G. Olivier, R. Snyders, M. Debliquy, Hydrothermal synthesis of two dimensional WO<sub>3</sub> nanostructures for NO<sub>2</sub> detection in the ppb-level, *Procedia Eng.* 47 (2012) 228–231.  
<https://doi.org/10.1016/j.proeng.2012.09.125>.
- [58] C. Burda, X. Chen, R. Narayanan, M.A. El-Sayed, Chemistry and Properties of Nanocrystals of Different Shapes, 2005. <https://doi.org/10.1002/chin.200527215>.
- [59] L. Zhu, H. Wang, D. Sun, Y. Tang, H. Wang, A comprehensive review on the fabrication, modification and applications of Na<sub>3</sub>V<sub>2</sub>(PO<sub>4</sub>)<sub>2</sub>F<sub>3</sub> cathodes, *J. Mater. Chem. A*. 8 (2020) 21387–21407. <https://doi.org/10.1039/D0TA07872G>.
- [60] Y.B. Rao, K.K. Bharathi, L.N. Patro, Review on the synthesis and doping strategies in enhancing the Na ion conductivity of Na<sub>3</sub>Zr<sub>2</sub>Si<sub>2</sub>PO<sub>12</sub> (NASICON) based solid electrolytes, *Solid State Ionics*. 366–367 (2021) 115671.  
<https://doi.org/10.1016/j.ssi.2021.115671>.
- [61] L.S.R. Rocha, R.A.C. Amoresi, H. Moreno, M.A. Ramirez, M.A. Ponce, C.R. Foschini, E. Longo, A.Z. Simões, Novel Approaches of Nanoceria with Magnetic, Photoluminescent, and Gas-Sensing Properties, *ACS Omega*. 5 (2020) 14879–14889. <https://doi.org/10.1021/acsomega.9b04250>.
- [62] L.F. da Silva, A.C. Catto, S. Bernardini, T. Fiorido, J.V.N. de Palma, W. Avansi, K. Aguir, M. Bendahan, BTEX gas sensor based on hematite microrhombuses, *Sensors Actuators B Chem.* 326 (2021) 128817.  
<https://doi.org/10.1016/j.snb.2020.128817>.
- [63] L.F. da Silva, A.C. Catto, W. Avansi, L.S. Cavalcante, V.R. Mastelaro, J. Andrés, K. Aguir, E. Longo, Acetone gas sensor based on  $\alpha$ -Ag<sub>2</sub>WO<sub>4</sub> nanorods obtained via a microwave-assisted hydrothermal route, *J. Alloys Compd.* 683 (2016) 186–190. <https://doi.org/10.1016/j.jallcom.2016.05.078>.
- [64] F.C. Romeiro, M.A. Rodrigues, L.A.J. Silva, A.C. Catto, L.F. da Silva, E. Longo, E. Nossol, R.C. Lima, rGO-ZnO nanocomposites for high electrocatalytic effect on water oxidation obtained by microwave-hydrothermal method, *Appl. Surf. Sci.* 423 (2017) 743–751. <https://doi.org/10.1016/j.apsusc.2017.06.221>.
- [65] S. Mani, V. Vedyappan, S.-M. Chen, R. Madhu, V. Pitchaimani, J.-Y. Chang, S.-B. Liu, Hydrothermal synthesis of NiWO<sub>4</sub> crystals for high performance non-enzymatic glucose biosensors, *Sci. Rep.* 6 (2016) 24128.  
<https://doi.org/10.1038/srep24128>.
- [66] Z. Li, J. Yang, T. Guang, B. Fan, K. Zhu, X. Wang, Controlled



- Hydrothermal/Solvothermal Synthesis of High-Performance LiFePO<sub>4</sub> for Li-Ion Batteries, *Small Methods*. 5 (2021) 2100193.  
<https://doi.org/10.1002/smtd.202100193>.
- [67] X. Liu, G. Li, P. Qian, D. Zhang, J. Wu, K. Li, L. Li, Carbon coated Li<sub>3</sub>VO<sub>4</sub> microsphere: Ultrafast solvothermal synthesis and excellent performance as lithium-ion battery anode, *J. Power Sources*. 493 (2021) 229680.  
<https://doi.org/10.1016/j.jpowsour.2021.229680>.
- [68] X. Mu, W. Wang, C. Sun, J. Wang, C. Wang, M. Knez, Recent Progress on Conductive Metal-Organic Framework Films, *Adv. Mater. Interfaces*. 8 (2021) 2002151. <https://doi.org/10.1002/admi.202002151>.
- [69] R.A. Roca, E.R. Leite, Size and Shape Tailoring of Titania Nanoparticles Synthesized by Solvothermal Route in Different Solvents, *J. Am. Ceram. Soc.* 96 (2013) 96–102. <https://doi.org/10.1111/jace.12078>.
- [70] R.C. d. S. Júnior, A.E. Nogueira, A.S. Giroto, J.A. Torres, C. Ribeiro, K.P.F. Siqueira, Microwave-assisted synthesis of Ca<sub>1-x</sub>Mn<sub>x</sub>MoO<sub>4</sub> (x = 0, 0.2, 0.7, and 1) and its application in artificial photosynthesis, *Ceram. Int.* 47 (2021) 5388–5398. <https://doi.org/10.1016/j.ceramint.2020.10.119>.
- [71] G.B. Ayer, V. V. Klepov, K.A. Pace, H.-C. zur Loye, Quaternary cerium (IV) containing fluorides exhibiting Ce<sub>3</sub>F<sub>16</sub> sheets and Ce<sub>6</sub>F<sub>30</sub> frameworks, *Dalt. Trans.* 49 (2020) 5898–5905. <https://doi.org/10.1039/D0DT00616E>.
- [72] L.S. Ribeiro, I.M. Pinatti, J.A. Torres, A.S. Giroto, F. Lesse, E. Longo, C. Ribeiro, A.E. Nogueira, Rapid microwave-assisted hydrothermal synthesis of CuBi<sub>2</sub>O<sub>4</sub> and its application for the artificial photosynthesis, *Mater. Lett.* 275 (2020) 128165. <https://doi.org/10.1016/j.matlet.2020.128165>.
- [73] V. V. Klepov, K.A. Pace, A.A. Berseneva, J.B. Felder, S. Calder, G. Morrison, Q. Zhang, M.J. Kirkham, D.S. Parker, H.-C. zur Loye, Chloride Reduction of Mn<sup>3+</sup> in Mild Hydrothermal Synthesis of a Charge Ordered Defect Pyrochlore, CsMn<sup>2+</sup>Mn<sup>3+</sup>F<sub>6</sub>, a Canted Antiferromagnet with a Hard Ferromagnetic Component, *J. Am. Chem. Soc.* 143 (2021) 11554–11567.  
<https://doi.org/10.1021/jacs.1c04245>.
- [74] X. Xia, A. Pant, X. Zhou, E.A. Dobretsova, A.B. Bard, M.B. Lim, J.Y.D. Roh, D.R. Gamelin, P.J. Pauzauskie, Hydrothermal Synthesis and Solid-State Laser Refrigeration of Ytterbium-Doped Potassium-Lutetium-Fluoride (KLF) Microcrystals, *Chem. Mater.* 33 (2021) 4417–4424.  
<https://doi.org/10.1021/acs.chemmater.1c00420>.
- [75] F. Majid, J. Rauf, S. Ata, I. Bibi, A. Malik, S.M. Ibrahim, A. Ali, M. Iqbal, Synthesis and characterization of NiFe<sub>2</sub>O<sub>4</sub> ferrite: Sol–gel and hydrothermal synthesis routes effect on magnetic, structural and dielectric characteristics, *Mater. Chem. Phys.* 258 (2021) 123888.  
<https://doi.org/10.1016/j.matchemphys.2020.123888>.
- [76] R. Cristina de Oliveira, R.A. Pontes Ribeiro, G.H. Cruvinel, R.A. Ciola Amoresi, M.H. Carvalho, A.J. Aparecido de Oliveira, M. Carvalho de Oliveira, S. Ricardo de Lazaro, L. Fernando da Silva, A.C. Catto, A.Z. Simões, J.R. Sambrano, E. Longo, Role of Surfaces in the Magnetic and Ozone Gas-Sensing Properties of

- ZnFe<sub>2</sub>O<sub>4</sub> Nanoparticles: Theoretical and Experimental Insights, *ACS Appl. Mater. Interfaces*. 13 (2021) 4605–4617. <https://doi.org/10.1021/acsami.0c15681>.
- [77] S.M. Yin, W.Q. Li, R.S. Cheng, Y.F. Yuan, S.Y. Guo, Z.H. Ren, Hydrothermal Synthesis, Photocatalytic and Magnetic Properties of Pure-Phase Bi<sub>2</sub>Fe<sub>4</sub>O<sub>9</sub> Microstructures, *J. Electron. Mater.* 50 (2021) 954–959. <https://doi.org/10.1007/s11664-020-08583-z>.
- [78] B. Hangai, E. Borsari, E.C. Aguiar, F.G. Garcia, E. Longo, A.Z. Simões, Superparamagnetic behaviour of zinc ferrite obtained by the microwave assisted method, *J. Mater. Sci. Mater. Electron.* 28 (2017) 10772–10779. <https://doi.org/10.1007/s10854-017-6854-1>.
- [79] F.A. La Porta, S. Masi, Solvent-Mediated Structural Evolution Mechanism from Cs<sub>4</sub>PbBr<sub>6</sub> to CsPbBr<sub>3</sub> Crystals, *Nanomanufacturing*. 1 (2021) 67–74. <https://doi.org/10.3390/nanomanufacturing1020007>.
- [80] M. Rui, X. Li, L. Gan, T. Zhai, H. Zeng, Ternary Oxide Nanocrystals: Universal Laser-Hydrothermal Synthesis, Optoelectronic and Electrochemical Applications, *Adv. Funct. Mater.* 26 (2016) 5051–5060. <https://doi.org/10.1002/adfm.201600785>.
- [81] R.C. de Oliveira, R.A.C. Amoresi, N.L. Marana, M.A. Zaghete, M. Ponce, A.J. Chiquito, J.R. Sambrano, E. Longo, A.Z. Simões, Influence of Synthesis Time on the Morphology and Properties of CeO<sub>2</sub> Nanoparticles: An Experimental–Theoretical Study, *Cryst. Growth Des.* 20 (2020) 5031–5042. <https://doi.org/10.1021/acs.cgd.0c00165>.
- [82] W. da S. Pereira, C.B. Gozzo, E. Longo, E.R. Leite, J.C. Sczancoski, Morphological aspects and optical properties of Ag<sub>4</sub>P<sub>2</sub>O<sub>7</sub>, *Mater. Lett.* 248 (2019) 193–196. <https://doi.org/10.1016/j.matlet.2019.04.038>.
- [83] Y. Wang, Y.-J. Hu, X. Hao, P. Peng, J.-Y. Shi, F. Peng, R.-C. Sun, Hydrothermal synthesis and applications of advanced carbonaceous materials from biomass: a review, *Adv. Compos. Hybrid Mater.* 3 (2020) 267–284. <https://doi.org/10.1007/s42114-020-00158-0>.
- [84] J.A. Darr, J. Zhang, N.M. Makwana, X. Weng, Continuous Hydrothermal Synthesis of Inorganic Nanoparticles: Applications and Future Directions, *Chem. Rev.* 117 (2017) 11125–11238. <https://doi.org/10.1021/acs.chemrev.6b00417>.
- [85] M. Shandilya, R. Rai, J. Singh, Review: hydrothermal technology for smart materials, *Adv. Appl. Ceram.* 115 (2016) 354–376. <https://doi.org/10.1080/17436753.2016.1157131>.
- [86] L.F. Gorup, L.H. Amorin, E.R. Camargo, T. Sequinel, F.H. Cincotto, G. Biasotto, N. Ramesar, F. de A. La Porta, Methods for design and fabrication of nanosensors: the case of ZnO-based nanosensor, in: *Nanosensors for Smart Cities*, Elsevier, 2020: pp. 9–30. <https://doi.org/10.1016/B978-0-12-819870-4.00002-5>.
- [87] J.C. Sczancoski, L.S. Cavalcante, M.R. Joya, J.A. Varela, P.S. Pizani, E. Longo, SrMoO<sub>4</sub> powders processed in microwave-hydrothermal: Synthesis, characterization and optical properties, *Chem. Eng. J.* 140 (2008) 632–637. <https://doi.org/10.1016/j.cej.2008.01.015>.

- [88] L.S. Cavalcante, V.M. Longo, J.C. Sczancoski, M.A.P. Almeida, A.A. Batista, J.A. Varela, M.O. Orlandi, E. Longo, M.S. Li, Electronic structure, growth mechanism and photoluminescence of CaWO<sub>4</sub> crystals, *CrystEngComm*. 14 (2012) 853–868. <https://doi.org/10.1039/C1CE05977G>.
- [89] E. Silva Junior, F.A. La Porta, M.S. Liu, J. Andrés, J.A. Varela, E. Longo, A relationship between structural and electronic order–disorder effects and optical properties in crystalline TiO<sub>2</sub> nanomaterials, *Dalt. Trans.* 44 (2015) 3159–3175. <https://doi.org/10.1039/C4DT03254C>.
- [90] L.A. Gusmão, D.A. Peixoto, J.Z. Marinho, F.C. Romeiro, R.F. Gonçalves, E. Longo, C.A. de Oliveira, R.C. Lima, Alkali influence on ZnO and Ag-doped ZnO nanostructures formation using the microwave-assisted hydrothermal method for fungicidal inhibition, *J. Phys. Chem. Solids*. 158 (2021) 110234. <https://doi.org/10.1016/j.jpcs.2021.110234>.
- [91] M. Jamshidi, M. Ghaedi, K. Dashtian, S. Hajati, A.A. Bazrafshan, Sonochemical assisted hydrothermal synthesis of ZnO: Cr nanoparticles loaded activated carbon for simultaneous ultrasound-assisted adsorption of ternary toxic organic dye: Derivative spectrophotometric, optimization, kinetic and isotherm study, *Ultrason. Sonochem.* 32 (2016) 119–131. <https://doi.org/10.1016/j.ultsonch.2016.03.004>.
- [92] J.M. Ramos, J.A. Wang, S.O. Flores, L. Chen, U. Arellano, L.E. Noreña, J. González, J. Navarrete, Ultrasound-assisted hydrothermal synthesis of v2o5/zr-sba-15 catalysts for production of ultralow sulfur fuel, *Catalysts*. 11 (2021) 408. <https://doi.org/10.3390/catal11040408>.
- [93] I. Khan, S. Ali, M. Mansha, A. Qurashi, Sonochemical Assisted Hydrothermal Synthesis of Pseudo Flower-Shaped, *Ultrason. - Sonochemistry*. 36 (2016) 386–392. <https://doi.org/10.1016/j.ultsonch.2016.12.014>.
- [94] H. ullah, I. Khan, Z.H. Yamani, A. Qurashi, Sonochemical-driven ultrafast facile synthesis of SnO<sub>2</sub> nanoparticles: Growth mechanism structural electrical and hydrogen gas sensing properties, *Ultrason. Sonochem.* 34 (2017) 484–490. <https://doi.org/10.1016/j.ultsonch.2016.06.025>.
- [95] L.-Y. Meng, B. Wang, M.-G. Ma, K.-L. Lin, The progress of microwave-assisted hydrothermal method in the synthesis of functional nanomaterials, *Mater. Today Chem.* 1–2 (2016) 63–83. <https://doi.org/10.1016/j.mtchem.2016.11.003>.
- [96] G. Yang, S.-J. Park, Conventional and Microwave Hydrothermal Synthesis and Application of Functional Materials: A Review, *Materials (Basel)*. 12 (2019) 1177. <https://doi.org/10.3390/ma12071177>.
- [97] V.K. Ivanov, O.S. Polezhaeva, D.O. Gil', G.P. Kopitsa, Y.D. Tret'yakov, Hydrothermal microwave synthesis of nanocrystalline cerium dioxide, *Dokl. Chem.* 426 (2009) 131–133. <https://doi.org/10.1134/S0012500809060056>.
- [98] S.K. Sahoo, M. Mohapatra, A.K. Singh, S. Anand, Hydrothermal Synthesis of Single Crystalline Nano CeO<sub>2</sub> and Its Structural, Optical, and Electronic Characterization, *Mater. Manuf. Process.* 25 (2010) 982–989. <https://doi.org/10.1080/10426914.2010.480995>.
- [99] M.L. Dos Santos, R.C. Lima, C.S. Riccardi, R.L. Tranquilin, P.R. Bueno, J.A.

- Varela, E. Longo, Preparation and characterization of ceria nanospheres by microwave-hydrothermal method, *Mater. Lett.* 62 (2008) 4509–4511. <https://doi.org/10.1016/j.matlet.2008.08.011>.
- [100] F.-K. Liu, C.-J. Ker, Y.-C. Chang, F.-H. Ko, T.-C. Chu, B.-T. Dai, Microwave Heating for the Preparation of Nanometer Gold Particles, *Jpn. J. Appl. Phys.* 42 (2003) 4152–4158. <https://doi.org/10.1143/JJAP.42.4152>.
- [101] V.Y. Suzuki, L.H.C. Amorin, N.M. Lima, E.G. Machado, P.E. Carvalho, S.B.R. Castro, C.C.S. Alves, A.P. Carli, M.S. Li, E. Longo, F.A. La Porta, Characterization of the structural, optical, photocatalytic and in vitro and in vivo anti-inflammatory properties of Mn<sup>2+</sup> doped Zn<sub>2</sub>GeO<sub>4</sub> nanorods, *J. Mater. Chem. C* 7 (2019) 8216–8225. <https://doi.org/10.1039/C9TC01189G>.
- [102] F.A. La Porta, M.M. Ferrer, Y.V.B. de Santana, C.W. Raubach, V.M. Longo, J.R. Sambrano, E. Longo, J. Andrés, M.S. Li, J.A. Varela, Synthesis of wurtzite ZnS nanoparticles using the microwave assisted solvothermal method, *J. Alloys Compd.* 556 (2013) 153–159. <https://doi.org/10.1016/j.jallcom.2012.12.081>.
- [103] Y.V.B. de Santana, C.W. Raubach, M.M. Ferrer, F. La Porta, J.R. Sambrano, V.M. Longo, E.R. Leite, E. Longo, Experimental and theoretical studies on the enhanced photoluminescence activity of zinc sulfide with a capping agent, *J. Appl. Phys.* 110 (2011) 123507. <https://doi.org/10.1063/1.3666070>.
- [104] F.A. La Porta, J. Andrés, M.V.G. Vismara, C.F.O. Graeff, J.R. Sambrano, M.S. Li, J.A. Varela, E. Longo, Correlation between structural and electronic order–disorder effects and optical properties in ZnO nanocrystals, *J. Mater. Chem. C* 2 (2014) 10164–10174. <https://doi.org/10.1039/C4TC01248H>.
- [105] W.P. Hsu, L. Ronnquist, E. Matijevic, Preparation and properties of monodispersed colloidal particles of lanthanide compounds. 2. Cerium(IV), *Langmuir* 4 (1988) 31–37. <https://doi.org/10.1021/la00079a005>.
- [106] M.M. Ferrer, Y.V.B. de Santana, C.W. Raubach, F.A. La Porta, A.F. Gouveia, E. Longo, J.R. Sambrano, Europium doped zinc sulfide: a correlation between experimental and theoretical calculations, *J. Mol. Model.* 20 (2014) 2375. <https://doi.org/10.1007/s00894-014-2375-5>.
- [107] X. Chu, W. Chung, L.D. Schmidt, Sintering of Sol-Gel-Prepared Submicrometer Particles Studied by Transmission Electron Microscopy, *J. Am. Ceram. Soc.* 76 (1993) 2115–2118. <https://doi.org/10.1111/j.1151-2916.1993.tb08344.x>.
- [108] T.J. Kirk, J. Winnick, A Hydrogen Sulfide Solid-Oxide Fuel Cell Using Ceria-Based Electrolytes, *J. Electrochem. Soc.* 140 (1993) 3494–3496. <https://doi.org/10.1149/1.2221117>.
- [109] A.I.Y. Tok, F.Y.C. Boey, Z. Dong, X.L. Sun, Hydrothermal synthesis of CeO<sub>2</sub> nano-particles, *J. Mater. Process. Technol.* 190 (2007) 217–222. <https://doi.org/10.1016/j.jmatprotec.2007.02.042>.
- [110] Y.C. Zhou, M.N. Rahaman, Hydrothermal synthesis and sintering of ultrafine CeO<sub>2</sub> powders, *J. Mater. Res.* 8 (1993) 1680–1686. <https://doi.org/10.1557/JMR.1993.1680>.
- [111] R. Guo, J. Wang, S. An, J. Zhang, G. Zhou, L. Guo, Effect of cerium oxide

- prepared under different hydrothermal time on electrocatalytic performance of Pt-based anode catalysts, *J. Rare Earths*. 38 (2020) 384–394. <https://doi.org/10.1016/j.jre.2019.05.010>.
- [112] H. Chen, Z. Jiang, X. Li, X. Lei, Effect of cerium nitrate concentration on morphologies, structure and photocatalytic activities of CeO<sub>2</sub> nanoparticles synthesized by microwave interface method, *Mater. Lett.* 257 (2019) 126666. <https://doi.org/10.1016/j.matlet.2019.126666>.
- [113] F. Matei-Rutkowska, G. Postole, C.G. Rotaru, M. Florea, V.I. Pârvulescu, P. Gelin, Synthesis of ceria nanopowders by microwave-assisted hydrothermal method for dry reforming of methane, *Int. J. Hydrogen Energy*. 41 (2016) 2512–2525. <https://doi.org/10.1016/j.ijhydene.2015.12.097>.
- [114] Y. Luo, A simple microwave-based route for size-controlled preparation of colloidal Pt nanoparticles, *Mater. Lett.* 61 (2007) 1873–1875. <https://doi.org/10.1016/j.matlet.2006.07.166>.
- [115] S. Kundu, L. Peng, H. Liang, A New Route to Obtain High-Yield Multiple-Shaped Gold Nanoparticles in Aqueous Solution using Microwave Irradiation, *Inorg. Chem.* 47 (2008) 6344–6352. <https://doi.org/10.1021/ic8004135>.
- [116] M.L. Moreira, V.M. Longo, W. Avansi, M.M. Ferrer, J. Andrés, V.R. Mastelaro, J.A. Varela, É. Longo, Quantum Mechanics Insight into the Microwave Nucleation of SrTiO<sub>3</sub> Nanospheres, *J. Phys. Chem. C*. 116 (2012) 24792–24808. <https://doi.org/10.1021/jp306638r>.
- [117] C.O. Kappe, Controlled Microwave Heating in Modern Organic Synthesis, *Angew. Chemie Int. Ed.* 43 (2004) 6250–6284. <https://doi.org/10.1002/anie.200400655>.
- [118] G.B. Dudley, R. Richert, A.E. Stiegman, On the existence of and mechanism for microwave-specific reaction rate enhancement, *Chem. Sci.* 6 (2015) 2144–2152. <https://doi.org/10.1039/C4SC03372H>.
- [119] B. Hu, S.-B. Wang, K. Wang, M. Zhang, S.-H. Yu, Microwave-Assisted Rapid Facile “Green” Synthesis of Uniform Silver Nanoparticles: Self-Assembly into Multilayered Films and Their Optical Properties, *J. Phys. Chem. C*. 112 (2008) 11169–11174. <https://doi.org/10.1021/jp801267j>.
- [120] A. Bonamartini Corradi, F. Bondioli, A.M. Ferrari, T. Manfredini, Synthesis and characterization of nanosized ceria powders by microwave–hydrothermal method, *Mater. Res. Bull.* 41 (2006) 38–44. <https://doi.org/10.1016/j.materresbull.2005.07.044>.
- [121] R. Prasad, A.K. Jha, K. Prasad, I. Editors (School of Environmental Science and Engineering, Sun Yat-Sen University, Guangzhou, China Amity Institute of Microbial Technology, Amity University, Noida, Uttar Pradesh, Exploring the Realms of Nature for Nanosynthesis, Springer International Publishing, Cham, 2018. <https://doi.org/10.1007/978-3-319-99570-0>.
- [122] M. Tak, V. Gupta, M. Tomar, Flower-like ZnO nanostructure based electrochemical DNA biosensor for bacterial meningitis detection, *Biosens. Bioelectron.* 59 (2014) 200–207. <https://doi.org/10.1016/j.bios.2014.03.036>.

- [123] M.S. de Almeida, M.A.B. dos Santos, R. de F. Gonçalves, M.R. de C. Santos, A.P. de A. Marques, E. Longo, F. de A. La Porta, I.M. Pinatti, M.D.P. Silva, M.J. Godinho, Novel Gd(OH)<sub>3</sub>, GdOOH and Gd<sub>2</sub>O<sub>3</sub> Nanorods: Microwave-Assisted Hydrothermal Synthesis and Optical Properties, *Mater. Res.* 19 (2016) 1155–1161. <https://doi.org/10.1590/1980-5373-MR-2016-0252>.
- [124] K.C.M. Borges, R.F. Gonçalves, A.A. Correa, F.A. La Porta, M.R.C. Santos, M.J. Godinho, A Comparative Study of Conventional and Microwave Sintering of BaCe<sub>1-x</sub>Gd<sub>x</sub>O<sub>3-δ</sub> Ceramic, *J. Inorg. Organomet. Polym. Mater.* 28 (2018) 130–136. <https://doi.org/10.1007/s10904-017-0708-4>.
- [125] A.P. de Moura, L.H. de Oliveira, I.L. V. Rosa, C.S. Xavier, P.N. Lisboa-Filho, M.S. Li, F.A. La Porta, E. Longo, J.A. Varela, Structural, Optical, and Magnetic Properties of NiMoO<sub>4</sub> Nanorods Prepared by Microwave Sintering, *Sci. World J.* 2015 (2015) 1–8. <https://doi.org/10.1155/2015/315084>.
- [126] S. Das, K. Dutta, A. Pramanik, Morphology control of ZnO with citrate: a time and concentration dependent mechanistic insight, *CrystEngComm.* 15 (2013) 6349. <https://doi.org/10.1039/c3ce40822a>.
- [127] S. Zhu, X. Chen, F. Zuo, M. Jiang, Z. Zhou, D. Hui, Controllable synthesis of ZnO nanograss with different morphologies and enhanced performance in dye-sensitized solar cells, *J. Solid State Chem.* 197 (2013) 69–74. <https://doi.org/10.1016/j.jssc.2012.09.001>.
- [128] E. Vorndran, C. Moseke, U. Gbureck, 3D printing of ceramic implants, *MRS Bull.* 40 (2015) 127–136. <https://doi.org/10.1557/mrs.2015.326>.
- [129] K. Byrappa, M. Yoshimura, *Handbook of Hydrothermal Technology*, 2nd ed., William Andrew Publishing, LLC, Norwich, NY, U.S.A., 2012.
- [130] G.A. Tompsett, W.C. Conner, K.S. Yngvesson, Microwave Synthesis of Nanoporous Materials, *ChemPhysChem.* 7 (2006) 296–319. <https://doi.org/10.1002/cphc.200500449>.
- [131] V. Perumal, U. Hashim, S.C.B. Gopinath, R. Haarindraprasad, K.L. Foo, S.R. Balakrishnan, P. Poopalan, ‘Spotted Nanoflowers’: Gold-seeded Zinc Oxide Nanohybrid for Selective Bio-capture, *Sci. Rep.* 5 (2015) 12231. <https://doi.org/10.1038/srep12231>.
- [132] D. Li, S. Komarneni, Microwave-Assisted Polyol Process for Synthesis of Ni Nanoparticles, *J. Am. Ceram. Soc.* 89 (2006) 1510–1517. <https://doi.org/10.1111/j.1551-2916.2006.00925.x>.
- [133] L. Gou, M. Chipara, J.M. Zaleski, Convenient, Rapid Synthesis of Ag Nanowires, *Chem. Mater.* 19 (2007) 1755–1760. <https://doi.org/10.1021/cm070160a>.
- [134] C. LEONELLI, W. LOJKOWSK, Main development directions in the application of microwave irradiation to the synthesis of nanopowders, *Chim. Oggi.* 25 (2007) 34–38.
- [135] V. Polshettiwar, M.N. Nadagouda, R.S. Varma, Microwave-Assisted Chemistry: a Rapid and Sustainable Route to Synthesis of Organics and Nanomaterials, *Aust. J. Chem.* 62 (2009) 16. <https://doi.org/10.1071/CH08404>.

- [136] J. Prado-Gonjal, E. Morán, Síntesis asistida por microondas de sólidos inorgánicos Investigación Química Introducción, An. Quím. 107 (2011) 129–136. [www.rseq.org](http://www.rseq.org).
- [137] S. Balaji, D. Mutharasu, N. Sankara Subramanian, K. Ramanathan, A review on microwave synthesis of electrode materials for lithium-ion batteries, Ionics (Kiel). 15 (2009) 765–777. <https://doi.org/10.1007/s11581-009-0350-4>.
- [138] D. Obermayer, B. Gutmann, C.O. Kappe, Microwave chemistry in silicon carbide reaction vials: separating thermal from nonthermal effects., Angew. Chem. Int. Ed. Engl. 48 (2009) 8321–4. <https://doi.org/10.1002/anie.200904185>.
- [139] I. Bilecka, M. Niederberger, Microwave chemistry for inorganic nanomaterials synthesis, Nanoscale. 2 (2010) 1358. <https://doi.org/10.1039/b9nr00377k>.
- [140] H. Yuan, S. Tan, W. Du, S. Ding, C. Guo, Heterogeneous bubble nucleation model on heated surface based on free energy analysis, Int. J. Heat Mass Transf. 122 (2018) 1198–1209. <https://doi.org/10.1016/j.ijheatmasstransfer.2018.02.062>.
- [141] G. Cao, Y. Wang, Nanostructures and Nanomaterials: Synthesis, Properties, and Applications, 2nd Revise, World Scientific Publishing Company, Incorporated, 2011.
- [142] J.P. Cheng, D.K. Agrawal, S. Komarneni, M. Mathis, R. Roy, Microwave processing of WC-Co composites and ferroic titanates, Mater. Res. Innov. 1 (1997) 44–52. <https://doi.org/10.1007/s100190050017>.
- [143] C. Gabriel, S. Gabriel, E. H. Grant, E. H. Grant, B. S. J. Halstead, D. Michael P. Mingos, Dielectric parameters relevant to microwave dielectric heating, Chem. Soc. Rev. 27 (1998) 213. <https://doi.org/10.1039/a827213z>.
- [144] J.-S. Schanche, Microwave synthesis solutions from personal chemistry, Mol. Divers. 7 (2003) 291–298. <https://doi.org/10.1023/B:MODI.0000006866.38392.f7>.
- [145] D.E. Clark, W.H. Sutton, Microwave Processing of Materials, Annu. Rev. Mater. Sci. 26 (1996) 299–331. <https://doi.org/10.1146/annurev.ms.26.080196.001503>.
- [146] C.O. Kappe, The Use of Microwave Irradiation in Organic Synthesis. From Laboratory Curiosity to Standard Practice in Twenty Years, Chim. Int. J. Chem. 60 (2006) 308–312. <https://doi.org/10.2533/000942906777836273>.
- [147] B. Ondruschka, W. Bonrath, Microwave-Assisted Chemistry – A Stock Taking, Chim. Int. J. Chem. 60 (2006) 326–329. <https://doi.org/10.2533/000942906777836246>.
- [148] R. Gedye, F. Smith, K. Westaway, H. Ali, L. Baldisera, L. Laberge, J. Rousell, The use of microwave ovens for rapid organic synthesis, Tetrahedron Lett. 27 (1986) 279–282. [https://doi.org/10.1016/S0040-4039\(00\)83996-9](https://doi.org/10.1016/S0040-4039(00)83996-9).
- [149] R.N. Gedye, W. Rank, K.C. Westaway, The rapid synthesis of organic compounds in microwave ovens. II, Can. J. Chem. 69 (1991) 706–711. <https://doi.org/10.1139/v91-106>.
- [150] G. Majetich, R. Hicks, The Use of Microwave Heating To Promote Organic Reactions, J. Microw. Power Electromagn. Energy. 30 (1995) 27–45.

<https://doi.org/10.1080/08327823.1995.11688258>.

- [151] A.R. von Hippel, *Dielectric Materials and Applications*, The Technology Press of M.I.T. and John Wiley & Sons, New York, N. Y., 1954.
- [152] A.B. Corradi, F. Bondioli, B. Focher, A.M. Ferrari, C. Grippo, E. Mariani, C. Villa, Conventional and Microwave-Hydrothermal Synthesis of TiO<sub>2</sub> Nanopowders, *J. Am. Ceram. Soc.* 88 (2005) 2639–2641. <https://doi.org/10.1111/j.1551-2916.2005.00474.x>.
- [153] N.T.K. Thanh, N. Maclean, S. Mahiddine, Mechanisms of Nucleation and Growth of Nanoparticles in Solution, *Chem. Rev.* 114 (2014) 7610–7630. <https://doi.org/10.1021/cr400544s>.
- [154] V.M. Longo, L.S. Cavalcante, E.C. Paris, J.C. Sczancoski, P.S. Pizani, M.S. Li, J. Andrés, E. Longo, J.A. Varela, Hierarchical assembly of CaMoO<sub>4</sub> nano-octahedrons and their photoluminescence properties, *J. Phys. Chem. C.* 115 (2011) 5207–5219. <https://doi.org/10.1021/jp1082328>.
- [155] R.L. Penn, J.F. Banfield, Morphology development and crystal growth in nanocrystalline aggregates under hydrothermal conditions: insights from titania, *Geochim. Cosmochim. Acta.* 63 (1999) 1549–1557. [https://doi.org/10.1016/S0016-7037\(99\)00037-X](https://doi.org/10.1016/S0016-7037(99)00037-X).
- [156] M.-M. Titirici, M. Antonietti, Chemistry and materials options of sustainable carbon materials made by hydrothermal carbonization, *Chem. Soc. Rev.* 39 (2010) 103–116. <https://doi.org/10.1039/B819318P>.
- [157] F. Maxim, P. Ferreira, P.M. Vilarinho, I. Reaney, Hydrothermal Synthesis and Crystal Growth Studies of BaTiO<sub>3</sub> Using Ti Nanotube Precursors, *Cryst. Growth Des.* 8 (2008) 3309–3315. <https://doi.org/10.1021/cg800215r>.
- [158] J.C. Sczancoski, L.S. Cavalcante, M.R. Joya, J.W.M. Espinosa, P.S. Pizani, J.A. Varela, E. Longo, Synthesis, growth process and photoluminescence properties of SrWO<sub>4</sub> powders, *J. Colloid Interface Sci.* 330 (2009) 227–236. <https://doi.org/10.1016/j.jcis.2008.10.034>.
- [159] A. Wolff, W. Hetaba, M. Wißbrock, S. Löffler, N. Mill, K. Eckstädt, A. Dreyer, I. Ennen, N. Sewald, P. Schattschneider, A. Hütten, Oriented attachment explains cobalt ferrite nanoparticle growth in bioinspired syntheses, *Beilstein J. Nanotechnol.* 5 (2014) 210–218. <https://doi.org/10.3762/bjnano.5.23>.
- [160] C. Kongmark, R. Coulter, S. Cristol, A. Rubbens, C. Pirovano, A. Löfberg, G. Sankar, W. van Beek, E. Bordes-Richard, R.-N. Vannier, A Comprehensive Scenario of the Crystal Growth of  $\gamma$ -Bi<sub>2</sub>MoO<sub>6</sub> Catalyst during Hydrothermal Synthesis, *Cryst. Growth Des.* 12 (2012) 5994–6003. <https://doi.org/10.1021/cg301070e>.
- [161] F.J.O. Rosal, A.F. Gouveia, J.C. Sczancoski, P.S. Lemos, E. Longo, B. Zhang, L.S. Cavalcante, Electronic structure, growth mechanism, and sonophotocatalytic properties of sphere-like self-assembled NiWO<sub>4</sub> nanocrystals, *Inorg. Chem. Commun.* 98 (2018) 34–40. <https://doi.org/10.1016/j.inoche.2018.10.001>.
- [162] J.D.C. Carregosa, J.P.F. Grilo, G.S. Godoi, D.A. Macedo, R.M. Nascimento, R.M.P.B. Oliveira, Microwave-assisted hydrothermal synthesis of ceria (CeO<sub>2</sub>):



- Microstructure, sinterability and electrical properties, *Ceram. Int.* 46 (2020) 23271–23275. <https://doi.org/10.1016/j.ceramint.2020.06.021>.
- [163] P. Prielcel, J.A. Lopez-Sanchez, Advantages and Limitations of Microwave Reactors: From Chemical Synthesis to the Catalytic Valorization of Biobased Chemicals, *ACS Sustain. Chem. Eng.* 7 (2019) 3–21. <https://doi.org/10.1021/acssuschemeng.8b03286>.
- [164] C. Liu, J. Yang, H. Ma, P. Zhang, Microwave-assisted and conventional hydrothermal synthesis of potassium merlinoite from K-feldspar, *Adv. Powder Technol.* 27 (2016) 2121–2127. <https://doi.org/10.1016/j.apt.2016.07.025>.
- [165] S. Ifrah, A. Kaddouri, P. Gelin, D. Leonard, Conventional hydrothermal process versus microwave-assisted hydrothermal synthesis of  $\text{La}_{1-x}\text{Ag}_x\text{MnO}_{3+\delta}$  ( $x = 0, 0.2$ ) perovskites used in methane combustion, *Comptes Rendus Chim.* 10 (2007) 1216–1226. <https://doi.org/10.1016/j.crci.2007.08.002>.
- [166] S. Tränkle, D. Jahn, T. Neumann, L. Nicoleau, N. Hüsing, D. Volkmer, Conventional and microwave assisted hydrothermal syntheses of 11 Å tobermorite, *J. Mater. Chem. A* 1 (2013) 10318–10326. <https://doi.org/10.1039/c3ta11036b>.
- [167] G. Solomon, R. Mazzaro, V. Morandi, I. Concina, A. Vomiero, Microwave-Assisted vs. Conventional Hydrothermal Synthesis of MoS<sub>2</sub> Nanosheets: Application towards Hydrogen Evolution Reaction, *Crystals*. 10 (2020) 1040. <https://doi.org/10.3390/cryst10111040>.
- [168] V.K. Ivanov, A.S. Shaporev, F.Y. Sharikov, A.Y. Baranchikov, Hydrothermal and microwave-assisted synthesis of nanocrystalline ZnO photocatalysts, *Superlattices Microstruct.* 42 (2007) 421–424. <https://doi.org/10.1016/j.spmi.2007.04.046>.
- [169] Y. Fu, W. Fu, Y. Liu, G. Zhang, Y. Liu, H. Yu, Comparison of ZnO nanorod array coatings on wood and their UV prevention effects obtained by microwave-assisted hydrothermal and conventional hydrothermal synthesis, *Holzforschung*. 69 (2015) 1009–1014. <https://doi.org/10.1515/hf-2014-0156>.
- [170] J. Sun, W. Wang, Q. Yue, Review on Microwave-Matter Interaction Fundamentals and Efficient Microwave-Associated Heating Strategies, *Materials (Basel)*. 9 (2016) 231. <https://doi.org/10.3390/ma9040231>.
- [171] D. Adam, Out of the kitchen, *Nature*. 421 (2003) 571–572. <https://doi.org/10.1038/421571a>.
- [172] M.B. Gawande, S.N. Shelke, R. Zboril, R.S. Varma, Microwave-Assisted Chemistry: Synthetic Applications for Rapid Assembly of Nanomaterials and Organics, *Acc. Chem. Res.* 47 (2014) 1338–1348. <https://doi.org/10.1021/ar400309b>.
- [173] D.A.C. Stuerger, P. Gaillard, Microwave Athermal Effects in Chemistry: A Myth's Autopsy: Part II: Orienting effects and thermodynamic consequences of electric field., *J. Microw. Power Electromagn. Energy*. 31 (1996) 101–113. <https://doi.org/10.1080/08327823.1996.11688300>.
- [174] D. Stuerger, Microwave-Material Interactions and Dielectric Properties, Key

Ingredients for Mastery of Chemical Microwave Processes, in: *Microwaves Org. Synth.*, Wiley-VCH Verlag GmbH, Weinheim, Germany, 2008: pp. 1–61.  
<https://doi.org/10.1002/9783527619559.ch1>.

- [175] G. Lubec, C. Wolf, B. Bartosch, AMINOACID ISOMERISATION AND MICROWAVE EXPOSURE, *Lancet*. 334 (1989) 1392–1393.  
[https://doi.org/10.1016/S0140-6736\(89\)91996-X](https://doi.org/10.1016/S0140-6736(89)91996-X).
- [176] F. Adánek, M. Hájek, Microwave-Assisted Catalytic Addition of Halocompounds to Alkenes, *Tetrahedron Lett.* 33 (1992) 2039–2042.  
<https://doi.org/10.1021/ac00249a776>.
- [177] M. Pagnotta, C.L.F. Pooley, B. Gurland, M. Choi, Microwave activation of the mutarotation of  $\alpha$ -D-glucose: An example of an interinsic microwave effect, *J. Phys. Org. Chem.* 6 (1993) 407–411. <https://doi.org/10.1002/poc.610060705>.
- [178] S. Zijlstra, T.J. De Groot, L.P. Kok, G.M. Visser, W. Vaalburg, Behavior of reaction mixtures under microwave conditions: use of sodium salts in microwave-induced N-[ $^{18}\text{F}$ ]fluoroalkylations of aporphine and tetralin derivatives, *J. Org. Chem.* 58 (1993) 1643–1645.  
<https://doi.org/10.1021/jo00059a002>.
- [179] F. Chemat, D.C. Esveld, M. Poux, J.L. Di-Martino, The Role of Selective Heating in the Microwave Activation of Heterogeneous Catalytic Reactions Using a Continuous Microwave Reactor, *J. Microw. Power Electromagn. Energy*. 33 (1998) 88–94. <https://doi.org/10.1080/08327823.1998.11688364>.
- [180] D.L. Marchisio, F. Omegna, A.A. Barresi, P. Bowen, Effect of Mixing and Other Operating Parameters in Sol–Gel Processes, *Ind. Eng. Chem. Res.* 47 (2008) 7202–7210. <https://doi.org/10.1021/ie800217b>.
- [181] X. Zhang, D.O. Hayward, Applications of microwave dielectric heating in environment-related heterogeneous gas-phase catalytic systems, *Inorganica Chim. Acta*. 359 (2006) 3421–3433. <https://doi.org/10.1016/j.ica.2006.01.037>.
- [182] C. Oliver Kappe, Microwave dielectric heating in synthetic organic chemistry, *Chem. Soc. Rev.* 37 (2008) 1127. <https://doi.org/10.1039/b803001b>.
- [183] M.D. Turner, R.L. Laurence, K.S. Yngvesson, W. Curtis Conner, The effect of microwave energy on three-way automotive catalysts poisoned by  $\text{SO}_2$ , *Catal. Letters*. 71 (2001) 133–138.  
<https://doi.org/10.1023/A:1009063406893>.
- [184] H.J. Kitchen, S.R. Vallance, J.L. Kennedy, N. Tapia-Ruiz, L. Carassiti, A. Harrison, A.G. Whittaker, T.D. Drysdale, S.W. Kingman, D.H. Gregory, Modern Microwave Methods in Solid-State Inorganic Materials Chemistry: From Fundamentals to Manufacturing, *Chem. Rev.* 114 (2014) 1170–1206.  
<https://doi.org/10.1021/cr4002353>.
- [185] S. Komarneni, R. Roy, Q.H. Li, Microwave-hydrothermal synthesis of ceramic powders, *Mater. Res. Bull.* 27 (1992) 1393–1405. [https://doi.org/10.1016/0025-5408\(92\)90004-J](https://doi.org/10.1016/0025-5408(92)90004-J).
- [186] J. Robinson, S. Kingman, D. Irvine, P. Licence, A. Smith, G. Dimitrakis, D. Obermayer, C.O. Kappe, Electromagnetic simulations of microwave heating

- experiments using reaction vessels made out of silicon carbide, *Phys. Chem. Chem. Phys.* 12 (2010) 10793. <https://doi.org/10.1039/c0cp00080a>.
- [187] T. V. de Medeiros, J. Manioudakis, F. Noun, J.-R. Macairan, F. Victoria, R. Naccache, Microwave-assisted synthesis of carbon dots and their applications, *J. Mater. Chem. C* 7 (2019) 7175–7195. <https://doi.org/10.1039/C9TC01640F>.
- [188] S.A. Galema, Microwave chemistry, *Chem. Soc. Rev.* 26 (1997) 233. <https://doi.org/10.1039/cs9972600233>.
- [189] D.M.P. Mingos, D.R. Baghurst, Tilden Lecture. Applications of microwave dielectric heating effects to synthetic problems in chemistry, *Chem. Soc. Rev.* 20 (1991) 1. <https://doi.org/10.1039/cs9912000001>.
- [190] M.N. Nadagouda, T.F. Speth, R.S. Varma, Microwave-Assisted Green Synthesis of Silver Nanostructures, *Acc. Chem. Res.* 44 (2011) 469–478. <https://doi.org/10.1021/ar1001457>.
- [191] J. Anwar, U. Shafique, Waheed-uz-Zaman, R. Rehman, M. Salman, A. Dar, J.M. Anzano, U. Ashraf, S. Ashraf, Microwave chemistry: Effect of ions on dielectric heating in microwave ovens, *Arab. J. Chem.* 8 (2015) 100–104. <https://doi.org/10.1016/j.arabjc.2011.01.014>.
- [192] E.K. Nyutu, C.-H. Chen, S. Sithambaram, V.M.B. Crisostomo, S.L. Suib, Systematic Control of Particle Size in Rapid Open-Vessel Microwave Synthesis of K-OMS-2 Nanofibers, *J. Phys. Chem. C* 112 (2008) 6786–6793. <https://doi.org/10.1021/jp800672m>.
- [193] V.Y. Suzuki, L.H.C. Amorin, N.H. de Paula, A.R. Albuquerque, M.S. Li, J.R. Sambrano, E. Longo, F.A. La Porta, New insights into the nature of the bandgap of CuGeO<sub>3</sub> nanofibers: Synthesis, electronic structure, and optical and photocatalytic properties, *Mater. Today Commun.* 26 (2021) 101701. <https://doi.org/10.1016/j.mtcomm.2020.101701>.
- [194] P. Lidström, J. Tierney, B. Wathey, J. Westman, Microwave assisted organic synthesis—a review, *Tetrahedron* 57 (2001) 9225–9283. [https://doi.org/10.1016/S0040-4020\(01\)00906-1](https://doi.org/10.1016/S0040-4020(01)00906-1).
- [195] C.O. Kappe, D. Dallinger, Controlled microwave heating in modern organic synthesis: highlights from the 2004–2008 literature, *Mol. Divers.* 13 (2009) 71–193. <https://doi.org/10.1007/s11030-009-9138-8>.
- [196] Practical Microwave Synthesis for Organic Chemists: Strategies, Instruments, and Protocols, *J. Am. Chem. Soc.* 131 (2009) 7204–7204. <https://doi.org/10.1021/ja902635q>.
- [197] C. Oliver Kappe, A. Stadler, D. Dallinger, *Microwaves in Organic and Medicinal Chemistry*, 2nd ed., Wiley-VCH, Weinheim, 2012.
- [198] J. Tang, F. Hao, M. Lau, *Microwave Heating in Food Processing*, World Scientific Publisher, New Jersey, 2002.
- [199] A. Angela, M. D'Amore, Relevance of Dielectric Properties in Microwave Assisted Processes, in: *Microw. Mater. Charact., InTech*, 2012. <https://doi.org/10.5772/51098>.

- [200] K. Ando, J.T. Hynes, HF acid ionization in water: the first step, *Faraday Discuss.* 102 (1995) 435. <https://doi.org/10.1039/fd9950200435>.
- [201] S. Imberti, A. Botti, F. Bruni, G. Cappa, M.A. Ricci, A.K. Soper, Ions in water: The microscopic structure of concentrated hydroxide solutions, *J. Chem. Phys.* 122 (2005) 194509. <https://doi.org/10.1063/1.1899147>.
- [202] A.K. Lyashchenko, V.S. Dnyashev, Complementary Organization of the Structure of Water, *J. Struct. Chem.* 44 (2003) 836–845. <https://doi.org/10.1023/B:JORY.0000029822.94836.67>.
- [203] G. Sutmann, R. Vallauri, Dynamics of the hydrogen bond network in liquid water, *J. Mol. Liq.* 98–99 (2002) 215–226. [https://doi.org/10.1016/S0167-7322\(01\)00320-8](https://doi.org/10.1016/S0167-7322(01)00320-8).
- [204] T.A. Mulinari, F.A. La Porta, J. Andrés, M. Cilense, J.A. Varela, E. Longo, Microwave-hydrothermal synthesis of single-crystalline Co<sub>3</sub>O<sub>4</sub> spinel nanocubes, *CrystEngComm.* 15 (2013) 7443. <https://doi.org/10.1039/c3ce41215f>.
- [205] F.A. La Porta, A.E. Nogueira, L. Gracia, W.S. Pereira, G. Botelho, T.A. Mulinari, J. Andrés, E. Longo, An experimental and theoretical investigation on the optical and photocatalytic properties of ZnS nanoparticles, *J. Phys. Chem. Solids.* 103 (2017) 179–189. <https://doi.org/10.1016/j.jpcs.2016.12.025>.
- [206] W. da S. Pereira, M.M. Ferrer, G. Botelho, L. Gracia, I.C. Nogueira, I.M. Pinatti, I.L.V. Rosa, F. de A. La Porta, J. Andrés, E. Longo, Effects of chemical substitution on the structural and optical properties of  $\alpha$ -Ag<sub>2-2x</sub>Ni<sub>x</sub>WO<sub>4</sub> ( $0 \leq x \leq 0.08$ ) solid solutions, *Phys. Chem. Chem. Phys.* 18 (2016) 21966–21975. <https://doi.org/10.1039/C6CP00575F>.
- [207] D.P. Volanti, M.O. Orlandi, J. Andrés, E. Longo, Efficient microwave-assisted hydrothermal synthesis of CuO sea urchin-like architectures via a mesoscale self-assembly, *CrystEngComm.* 12 (2010) 1696. <https://doi.org/10.1039/b922978g>.
- [208] D. Gebauer, M. Kellermeier, J.D. Gale, L. Bergström, H. Cölfen, Pre-nucleation clusters as solute precursors in crystallisation, *Chem. Soc. Rev.* 43 (2014) 2348–2371. <https://doi.org/10.1039/C3CS60451A>.
- [209] M. Li, Z. Yue, Y. Chen, H. Tong, H. Tanaka, P. Tan, Revealing thermally-activated nucleation pathways of diffusionless solid-to-solid transition, *Nat. Commun.* 12 (2021) 4042. <https://doi.org/10.1038/s41467-021-24256-9>.
- [210] J. McGinty, N. Yazdanpanah, C. Price, J.H. ter Horst, J. Sefcik, Nucleation and Crystal Growth in Continuous Crystallization, in: *Handb. Contin. Cryst.*, Royal Society of Chemistry, Cambridge, 2020: pp. 1–50. <https://doi.org/10.1039/9781788013581-00001>.
- [211] D. Kashchiev, G.M. van Rosmalen, Review: Nucleation in solutions revisited, *Cryst. Res. Technol.* 38 (2003) 555–574. <https://doi.org/10.1002/crat.200310070>.
- [212] S.A. Kulkarni, S.S. Kadam, H. Meekes, A.I. Stankiewicz, J.H. ter Horst, Crystal Nucleation Kinetics from Induction Times and Metastable Zone Widths, *Cryst. Growth Des.* 13 (2013) 2435–2440. <https://doi.org/10.1021/cg400139t>.
- [213] C.B. Murray, C.R. Kagan, M.G. Bawendi, Synthesis and Characterization of Monodisperse Nanocrystals and Close-Packed Nanocrystal Assemblies, *Annu.*

- Rev. Mater. Sci. 30 (2000) 545–610.  
<https://doi.org/10.1146/annurev.matsci.30.1.545>.
- [214] V.K. LaMer, R.H. Dinegar, Theory, Production and Mechanism of Formation of Monodispersed Hydrosols, *J. Am. Chem. Soc.* 72 (1950) 4847–4854.  
<https://doi.org/10.1021/ja01167a001>.
- [215] C.B. Whitehead, S. Özkar, R.G. Finke, LaMer's 1950 Model for Particle Formation of Instantaneous Nucleation and Diffusion-Controlled Growth: A Historical Look at the Model's Origins, Assumptions, Equations, and Underlying Sulfur Sol Formation Kinetics Data, *Chem. Mater.* 31 (2019) 7116–7132.  
<https://doi.org/10.1021/acs.chemmater.9b01273>.
- [216] R.A. Laudise, Hydrothermal Synthesis of Single Crystals, in: F.A. Cotton (Ed.), *Prog. Inorg. Chem.*, 2007: pp. 1–47. <https://doi.org/10.1002/9780470166048.ch1>.
- [217] L. Ke, S. Luo, X. Ren, Y. Yuan, Factors influencing the nucleation and crystal growth of solution-processed organic lead halide perovskites: a review, *J. Phys. D. Appl. Phys.* 54 (2021) 163001. <https://doi.org/10.1088/1361-6463/abd728>.
- [218] P. Cubillas, M.W. Anderson, Synthesis Mechanism: Crystal Growth and Nucleation, in: *Zeolites Catal.*, Wiley-VCH Verlag GmbH & Co. KGaA, Weinheim, Germany, 2010: pp. 1–55.  
<https://doi.org/10.1002/9783527630295.ch1>.
- [219] G.C. Sosso, J. Chen, S.J. Cox, M. Fitzner, P. Pedevilla, A. Zen, A. Michaelides, Crystal Nucleation in Liquids: Open Questions and Future Challenges in Molecular Dynamics Simulations, *Chem. Rev.* 116 (2016) 7078–7116.  
<https://doi.org/10.1021/acs.chemrev.5b00744>.
- [220] H. Clfen, M. Antonietti, *Mesocrystals and Nonclassical Crystallization*, 1st ed., John Wiley & Sons, Ltd, Chichester, UK, 2008.  
<https://doi.org/10.1002/9780470994603>.
- [221] F. Wang, G. Xu, Z. Zhang, S. Song, S. Dong, A systematic morphosynthesis of barium sulfate in the presence of phosphonate inhibitor, *J. Colloid Interface Sci.* 293 (2006) 394–400. <https://doi.org/10.1016/j.jcis.2005.06.060>.
- [222] E.R. Leite, C. Ribeiro, *Crystallization and Growth of Colloidal Nanocrystals*, Springer New York, New York, NY, 2012. <https://doi.org/10.1007/978-1-4614-1308-0>.
- [223] G. Amin, M.H. Asif, A. Zainelabdin, S. Zaman, O. Nur, M. Willander, Influence of pH, Precursor Concentration, Growth Time, and Temperature on the Morphology of ZnO Nanostructures Grown by the Hydrothermal Method, *J. Nanomater.* 2011 (2011) 1–9. <https://doi.org/10.1155/2011/269692>.
- [224] J. Park, J. Joo, S.G. Kwon, Y. Jang, T. Hyeon, Synthesis of Monodisperse Spherical Nanocrystals, *Angew. Chemie Int. Ed.* 46 (2007) 4630–4660.  
<https://doi.org/10.1002/anie.200603148>.
- [225] T.A.C.M. van der Put, A new theory of nucleation, *Phase Transitions.* 84 (2011) 999–1014. <https://doi.org/10.1080/01411594.2011.565187>.
- [226] J. Frenkel, A General Theory of Heterophase Fluctuations and Pretransition Phenomena, *J. Chem. Phys.* 7 (1939) 538–547.

<https://doi.org/10.1063/1.1750484>.

- [227] L. Farkas, Keimbildungsgeschwindigkeit in übersättigten Dämpfen, *Zeitschrift Für Phys. Chemie.* 125U (1927) 236–242. <https://doi.org/10.1515/zpch-1927-12513>.
- [228] R. Becker, W. Döring, Kinetische Behandlung der Keimbildung in übersättigten Dämpfen, *Ann. Phys.* 416 (1935) 719–752. <https://doi.org/10.1002/andp.19354160806>.
- [229] C. Ribeiro, C.M. Barrado, E.R. de Camargo, E. Longo, E.R. Leite, Phase transformation in titania nanocrystals by the oriented attachment mechanism: The role of the pH value, *Chem. - A Eur. J.* 15 (2009) 2217–2222. <https://doi.org/10.1002/chem.200801019>.
- [230] B. Ramasubramanian, M. V Reddy, K. Zaghbi, M. Armand, S. Ramakrishna, Growth Mechanism of Micro/Nano Metal Dendrites and Cumulative Strategies for Countering Its Impacts in Metal Ion Batteries: A Review, *Nanomaterials.* 11 (2021) 2476. <https://doi.org/10.3390/nano11102476>.
- [231] P.G. Vekilov, Nucleation, *Cryst. Growth Des.* 10 (2010) 5007–5019. <https://doi.org/10.1021/cg1011633>.
- [232] D. Kashchiev, On the relation between nucleation work, nucleus size, and nucleation rate, *J. Chem. Phys.* 76 (1982) 5098–5102. <https://doi.org/10.1063/1.442808>.
- [233] J.J. De Yoreo, P.G. Vekilov, Principles of Crystal Nucleation and Growth, *Rev. Mineral. Geochemistry.* 54 (2003) 57–93. <https://doi.org/10.2113/0540057>.
- [234] H. Furedi-Milhofer, SPONTANEOUS PRECIPITATION FROM ELECTROLYTIC SOLUTIONS, *Pure Appl.Chem.*, 53 (1981) 2041–2055. <https://doi.org/doi.org/10.1351/pac198153112041>.
- [235] B.L. Cushing, V.L. Kolesnichenko, C.J. O'Connor, Recent Advances in the Liquid-Phase Syntheses of Inorganic Nanoparticles, *Chem. Rev.* 104 (2004) 3893–3946. <https://doi.org/10.1021/cr030027b>.
- [236] W.D.K. Yet-Ming Chiang, Dunbar P. Birnie, *Physical Ceramics: Principles for Ceramic Science and Engineering*, John Wiley & Sons, Inc., 1996. <https://bcs.wiley.com/he-bcs/Books?action=index&bcsId=3573&itemId=0471598739>.
- [237] H. Chun Zeng, Ostwald Ripening: A Synthetic Approach for Hollow Nanomaterials, *Curr. Nanosci.* 3 (2007) 177–181. <https://doi.org/10.2174/157341307780619279>.
- [238] W. Zhou, Reversed Crystal Growth: Implications for Crystal Engineering, *Adv. Mater.* 22 (2010) 3086–3092. <https://doi.org/10.1002/adma.200904320>.
- [239] A.. Brailsford, P. Wynblatt, The dependence of ostwald ripening kinetics on particle volume fraction, *Acta Metall.* 27 (1979) 489–497. [https://doi.org/10.1016/0001-6160\(79\)90041-5](https://doi.org/10.1016/0001-6160(79)90041-5).
- [240] A. Baldan, Progress in Ostwald ripening theories and their applications to the  $\gamma'$ -precipitates in nickel-base superalloys Part II: Nickel-base superalloys, *J. Mater.*

- Sci. 37 (2002) 2171–2202. <https://doi.org/10.1023/a:1015388912729>.
- [241] J.A. Marqusee, J. Ross, Theory of Ostwald ripening: Competitive growth and its dependence on volume fraction, *J. Chem. Phys.* 80 (1984) 536–543. <https://doi.org/10.1063/1.446427>.
- [242] J.F. Banfield, Aggregation-Based Crystal Growth and Microstructure Development in Natural Iron Oxyhydroxide Biomineralization Products, *Science* (80-. ). 289 (2000) 751–754. <https://doi.org/10.1126/science.289.5480.751>.
- [243] X. Xue, R.L. Penn, E.R. Leite, F. Huang, Z. Lin, Crystal growth by oriented attachment: kinetic models and control factors, *CrystEngComm*. 16 (2014) 1419. <https://doi.org/10.1039/c3ce42129e>.
- [244] C.J. Dalmaschio, C. Ribeiro, E.R. Leite, Impact of the colloidal state on the oriented attachment growth mechanism, *Nanoscale*. 2 (2010) 2336. <https://doi.org/10.1039/c0nr00338g>.
- [245] Y. Liu, H. Geng, X. Qin, Y. Yang, Z. Zeng, S. Chen, Y. Lin, H. Xin, C. Song, X. Zhu, D. Li, J. Zhang, L. Song, Z. Dai, Y. Kawazoe, Oriented Attachment Revisited: Does a Chemical Reaction Occur?, *Matter*. 1 (2019) 690–704. <https://doi.org/10.1016/j.matt.2019.05.001>.
- [246] B.B. V. Salzmänn, M.M. van der Sluijs, G. Soligno, D. Vanmaekelbergh, Oriented Attachment: From Natural Crystal Growth to a Materials Engineering Tool, *Acc. Chem. Res.* 54 (2021) 787–797. <https://doi.org/10.1021/acs.accounts.0c00739>.
- [247] J.C. daSilva, M.A. Smeaton, T.A. Dunbar, Y. Xu, D.M. Balazs, L.F. Kourkoutis, T. Hanrath, Mechanistic Insights into Superlattice Transformation at a Single Nanocrystal Level Using Nanobeam Electron Diffraction, *Nano Lett.* 20 (2020) 5267–5274. <https://doi.org/10.1021/acs.nanolett.0c01579>.
- [248] M. Niederberger, H. Cölfen, Oriented attachment and mesocrystals: Non-classical crystallization mechanisms based on nanoparticle assembly, *Phys. Chem. Chem. Phys.* 8 (2006) 3271–3287. <https://doi.org/10.1039/b604589h>.
- [249] J.J. De Yoreo, P.U.P.A. Gilbert, N.A.J.M. Sommerdijk, R.L. Penn, S. Whitelam, D. Joester, H. Zhang, J.D. Rimer, A. Navrotsky, J.F. Banfield, A.F. Wallace, F.M. Michel, F.C. Meldrum, H. Colfen, P.M. Dove, Crystallization by particle attachment in synthetic, biogenic, and geologic environments, *Science* (80-. ). 349 (2015) aaa6760–aaa6760. <https://doi.org/10.1126/science.aaa6760>.
- [250] P.R. Rios, F. Siciliano Jr, H.R.Z. Sandim, R.L. Plaut, A.F. Padilha, Nucleation and growth during recrystallization, *Mater. Res.* 8 (2005) 225–238. <https://doi.org/10.1590/S1516-14392005000300002>.
- [251] E.J.H. Lee, C. Ribeiro, E. Longo, E.R. Leite, Growth kinetics of tin oxide nanocrystals in colloidal suspensions under hydrothermal conditions, *Chem. Phys.* 328 (2006) 229–235. <https://doi.org/10.1016/j.chemphys.2006.06.032>.
- [252] C. Ribeiro, C. Vila, D.B. Stroppa, V.R. Mastelaro, J. Bettini, E. Longo, E.R. Leite, Anisotropic Growth of Oxide Nanocrystals: Insights into the Rutile TiO<sub>2</sub> Phase, *J. Phys. Chem. C*. 111 (2007) 5871–5875. <https://doi.org/10.1021/jp070051j>.

- [253] M.L. Moreira, J. Andrés, V.R. Mastelaro, J.A. Varela, E. Longo, On the reversed crystal growth of BaZrO<sub>3</sub> decaoctahedron: shape evolution and mechanism, *CrystEngComm*. 13 (2011) 5818. <https://doi.org/10.1039/c1ce05361b>.
- [254] R.L. Penn, J.F. Banfield, Imperfect oriented attachment: Dislocation generation in defect-free nanocrystals, *Science* (80-. ). 281 (1998) 969–971. <https://doi.org/10.1126/science.281.5379.969>.
- [255] A. de la Hoz, Á. Díaz-Ortiz, A. Moreno, Microwaves in organic synthesis. Thermal and non-thermal microwave effects, *Chem. Soc. Rev.* 34 (2005) 164–178. <https://doi.org/10.1039/B411438H>.
- [256] G. Liu, H.G. Yang, J. Pan, Y.Q. Yang, G.Q. (Max) Lu, H.-M. Cheng, Titanium Dioxide Crystals with Tailored Facets, *Chem. Rev.* 114 (2014) 9559–9612. <https://doi.org/10.1021/cr400621z>.
- [257] C. Ribeiro, E.J.H. Lee, E. Longo, E.R. Leite, Oriented Attachment Mechanism in Anisotropic Nanocrystals: A “Polymerization” Approach, *ChemPhysChem*. 7 (2006) 664–670. <https://doi.org/10.1002/cphc.200500508>.
- [258] J. Zhang, F. Huang, Z. Lin, Progress of nanocrystalline growth kinetics based on oriented attachment, *Nanoscale*. 2 (2010) 18–34. <https://doi.org/10.1039/B9NR00047J>.
- [259] S. Arshadi, J. Moghaddam, M. Eskandarian, LaMer diagram approach to study the nucleation and growth of Cu<sub>2</sub>O nanoparticles using supersaturation theory, *Korean J. Chem. Eng.* 31 (2014) 2020–2026. <https://doi.org/10.1007/s11814-014-0130-3>.
- [260] K. Nakata, A. Fujishima, TiO<sub>2</sub> photocatalysis: Design and applications, *J. Photochem. Photobiol. C Photochem. Rev.* 13 (2012) 169–189. <https://doi.org/10.1016/j.jphotochemrev.2012.06.001>.
- [261] W.L. Noorduin, H. Meekes, A.A.C. Bode, W.J.P. van Enkevort, B. Kaptein, R.M. Kellogg, E. Vlieg, Explanation for the Emergence of a Single Chiral Solid State during Attrition-Enhanced Ostwald Ripening: Survival of the Fittest, *Cryst. Growth Des.* 8 (2008) 1675–1681. <https://doi.org/10.1021/cg701211a>.
- [262] B. Ingham, T.H. Lim, C.J. Dotzler, A. Henning, M.F. Toney, R.D. Tilley, How Nanoparticles Coalesce: An in Situ Study of Au Nanoparticle Aggregation and Grain Growth, *Chem. Mater.* 23 (2011) 3312–3317. <https://doi.org/10.1021/cm200354d>.
- [263] P. Grammatikopoulos, M. Sowwan, J. Kioseoglou, Computational Modeling of Nanoparticle Coalescence, *Adv. Theory Simulations*. (2019) 1–26. <https://doi.org/10.1002/adts.201900013>.
- [264] G.C. Kuczynski, Study of the Sintering of Glass, *J. Appl. Phys.* 20 (1949) 1160–1163. <https://doi.org/10.1063/1.1698291>.
- [265] D.N. McCarthy, S.A. Brown, Evolution of neck radius and relaxation of coalescing nanoparticles, *Phys. Rev. B.* 80 (2009) 064107. <https://doi.org/10.1103/PhysRevB.80.064107>.
- [266] N. Lümmer, T. Kraska, Molecular dynamics investigations of the coalescence of iron clusters embedded in an inert-gas heat bath, *Phys. Rev. B.* 71 (2005)



205403. <https://doi.org/10.1103/PhysRevB.71.205403>.

- [267] K.E.J. Lehtinen, M.R. Zachariah, Energy accumulation in nanoparticle collision and coalescence processes, *J. Aerosol Sci.* 33 (2002) 357–368. [https://doi.org/10.1016/S0021-8502\(01\)00177-X](https://doi.org/10.1016/S0021-8502(01)00177-X).
- [268] P. Grammatikopoulos, C. Cassidy, V. Singh, M. Sowwan, Coalescence-induced crystallisation wave in Pd nanoparticles, *Sci. Rep.* 4 (2015) 5779. <https://doi.org/10.1038/srep05779>.
- [269] P. Grammatikopoulos, C. Cassidy, V. Singh, M. Benelmekki, M. Sowwan, Coalescence behaviour of amorphous and crystalline tantalum nanoparticles: a molecular dynamics study, *J. Mater. Sci.* 49 (2014) 3890–3897. <https://doi.org/10.1007/s10853-013-7893-5>.
- [270] Y. Chen, F. Li, T. Li, W. Cao, Shape-controlled hydrothermal synthesis of superhydrophobic and superoleophilic BaMnF<sub>4</sub> micro/nanostructures, *CrystEngComm.* 18 (2016) 3585–3593. <https://doi.org/10.1039/C5CE02502H>.
- [271] E. Zhang, L. Wang, B. Zhang, Y. Xie, G. Wang, Shape-controlled hydrothermal synthesis of CuFe<sub>2</sub>O<sub>4</sub> nanocrystals for enhancing photocatalytic and photoelectrochemical performance, *Mater. Chem. Phys.* 235 (2019) 121633. <https://doi.org/10.1016/j.matchemphys.2019.05.021>.
- [272] F. Wang, J. Wang, X. Zhong, B. Li, J. Liu, D. Wu, D. Mo, D. Guo, S. Yuan, K. Zhang, Y. Zhou, Shape-controlled hydrothermal synthesis of ferroelectric Bi<sub>4</sub>Ti<sub>3</sub>O<sub>12</sub> nanostructures, *CrystEngComm.* 15 (2013) 1397. <https://doi.org/10.1039/c2ce26330k>.
- [273] Y. Cao, P. Hu, D. Jia, Phase- and shape-controlled hydrothermal synthesis of CdS nanoparticles, and oriented attachment growth of its hierarchical architectures, *Appl. Surf. Sci.* 265 (2013) 771–777. <https://doi.org/10.1016/j.apsusc.2012.11.107>.
- [274] P.W. Dunne, C.L. Starkey, M. Gimeno-Fabra, E.H. Lester, The rapid size- and shape-controlled continuous hydrothermal synthesis of metal sulphide nanomaterials, *Nanoscale.* 6 (2014) 2406–2418. <https://doi.org/10.1039/C3NR05749F>.
- [275] H. Zheng, K. Zhu, A. Onda, K. Yanagisawa, Hydrothermal Synthesis of Various Shape-Controlled Europium Hydroxides, *Nanomaterials.* 11 (2021) 529. <https://doi.org/10.3390/nano11020529>.
- [276] H.L. Friedman, Theory of the dielectric constant of solutions, *J. Chem. Phys.* 76 (1982) 1092–1105. <https://doi.org/10.1063/1.443076>.
- [277] C. Burda, X. Chen, R. Narayanan, M.A. El-Sayed, Chemistry and Properties of Nanocrystals of Different Shapes, *Chem. Rev.* 105 (2005) 1025–1102. <https://doi.org/10.1021/cr030063a>.
- [278] A.P. Alivisatos, Perspectives on the Physical Chemistry of Semiconductor Nanocrystals, *J. Phys. Chem.* 100 (1996) 13226–13239. <https://doi.org/10.1021/jp9535506>.
- [279] W. Sun, Y. Pang, J. Li, W. Ao, Particle Coarsening II: Growth Kinetics of Hydrothermal BaTiO<sub>3</sub>, *Chem. Mater.* 19 (2007) 1772–1779.

<https://doi.org/10.1021/cm061741n>.

- [280] S. Kumar, P.D. Sahare, Observation of band gap and surface defects of ZnO nanoparticles synthesized via hydrothermal route at different reaction temperature, *Opt. Commun.* 285 (2012) 5210–5216. <https://doi.org/10.1016/j.optcom.2012.07.125>.
- [281] H. Wang, J.-J. Zhu, J.-M. Zhu, X.-H. Liao, S. Xu, T. Ding, H.-Y. Chen, Preparation of nanocrystalline ceria particles by sonochemical and microwave assisted heating methods, *Phys. Chem. Chem. Phys.* 4 (2002) 3794–3799. <https://doi.org/10.1039/b201394k>.
- [282] A. Ahniyaz, T. Watanabe, M. Yoshimura, Tetragonal Nanocrystals from the Zr<sub>0.5</sub>Ce<sub>0.5</sub>O<sub>2</sub> Solid Solution by Hydrothermal Method, *J. Phys. Chem. B.* 109 (2005) 6136–6139. <https://doi.org/10.1021/jp050047c>.
- [283] I.Z. Dinic, L.T. Mancic, M.E. Rabanal, K. Yamamoto, S. Ohara, S. Tamura, T. Koji, A.M.L.M. Costa, B.A. Marinkovic, O.B. Milosevic, Compositional and structural dependence of up-converting rare earth fluorides obtained through EDTA assisted hydro/solvothermal synthesis, *Adv. Powder Technol.* 28 (2017) 73–82. <https://doi.org/10.1016/j.appt.2016.09.021>.
- [284] Y. Zhang, Z.-R. Tang, X. Fu, Y.-J. Xu, Engineering the Unique 2D Mat of Graphene to Achieve Graphene-TiO<sub>2</sub> Nanocomposite for Photocatalytic Selective Transformation: What Advantage does Graphene Have over Its Forebear Carbon Nanotube?, *ACS Nano.* 5 (2011) 7426–7435. <https://doi.org/10.1021/nn202519j>.
- [285] H. Zhang, X. Lv, Y. Li, Y. Wang, J. Li, P25-Graphene Composite as a High Performance Photocatalyst, *ACS Nano.* 4 (2010) 380–386. <https://doi.org/10.1021/nn901221k>.
- [286] R. Raccichini, A. Varzi, S. Passerini, B. Scrosati, The role of graphene for electrochemical energy storage, *Nat. Mater.* 14 (2015) 271–279. <https://doi.org/10.1038/nmat4170>.
- [287] L. Han, L. Wang, K.-K. Chia, R.E. Cohen, M.F. Rubner, M.C. Boyce, C. Ortiz, Geometrically Controlled Mechanically Responsive Polyelectrolyte Tube Arrays, *Adv. Mater.* 23 (2011) 4667–4673. <https://doi.org/10.1002/adma.201102917>.
- [288] S.C. Warren, E. Thimsen, Plasmonic solar water splitting, *Energy Environ. Sci.* 5 (2012) 5133–5146. <https://doi.org/10.1039/C1EE02875H>.
- [289] I.S. Cho, Z. Chen, A.J. Forman, D.R. Kim, P.M. Rao, T.F. Jaramillo, X. Zheng, Branched TiO<sub>2</sub> Nanorods for Photoelectrochemical Hydrogen Production, *Nano Lett.* 11 (2011) 4978–4984. <https://doi.org/10.1021/nl2029392>.
- [290] J. Giblin, M. Kuno, Nanostructure Absorption: A Comparative Study of Nanowire and Colloidal Quantum Dot Absorption Cross Sections, *J. Phys. Chem. Lett.* 1 (2010) 3340–3348. <https://doi.org/10.1021/jz1013104>.
- [291] X. Huang, Y. Yao, F. Liang, Y. Dai, Concentration-controlled morphology of LiFePO<sub>4</sub> crystals with an exposed (100) facet and their enhanced performance for use in lithium-ion batteries, *J. Alloys Compd.* 743 (2018) 763–772. <https://doi.org/10.1016/j.jallcom.2018.02.048>.

- [292] G. Demazeau, Review. Solvothermal Processes: Definition, Key Factors Governing the Involved Chemical Reactions and New Trends, *Zeitschrift Für Naturforsch. B.* 65 (2010) 999–1006. <https://doi.org/10.1515/znb-2010-0805>.
- [293] K. Kanie, Y. Seino, M. Matsubara, A. Muramatsu, Size-controlled hydrothermal synthesis of monodispersed BaZrO<sub>3</sub> sphere particles by seeding, *Adv. Powder Technol.* 28 (2017) 55–60. <https://doi.org/10.1016/j.appt.2016.07.020>.
- [294] K. Kanie, Y. Seino, M. Matsubara, M. Nakaya, A. Muramatsu, Hydrothermal synthesis of BaZrO<sub>3</sub> fine particles controlled in size and shape and fluorescence behavior by europium doping, *New J. Chem.* 38 (2014) 3548–3555. <https://doi.org/10.1039/C4NJ00443D>.
- [295] T. Kimijima, K. Kanie, M. Nakaya, A. Muramatsu, Hydrothermal synthesis of size- and shape-controlled CaTiO<sub>3</sub> fine particles and their photocatalytic activity, *CrystEngComm.* 16 (2014) 5591–5597. <https://doi.org/10.1039/C4CE00376D>.
- [296] S. Boubenia, A.S. Dahiya, G. Poulin-Vittrant, F. Morini, K. Nadaud, D. Alquier, A facile hydrothermal approach for the density tunable growth of ZnO nanowires and their electrical characterizations, *Sci. Rep.* 7 (2017) 15187. <https://doi.org/10.1038/s41598-017-15447-w>.
- [297] H.Y. Zhao, Y.F. Wang, J.H. Zeng, Hydrothermal Synthesis of Uniform Cuprous Oxide Microcrystals with Controlled Morphology, *Cryst. Growth Des.* 8 (2008) 3731–3734. <https://doi.org/10.1021/cg8003678>.
- [298] P.W. Dunne, A.S. Munn, C.L. Starkey, T.A. Huddle, E.H. Lester, Continuous-flow hydrothermal synthesis for the production of inorganic nanomaterials, *Philos. Trans. R. Soc. A Math. Phys. Eng. Sci.* 373 (2015) 20150015. <https://doi.org/10.1098/rsta.2015.0015>.
- [299] T. Liu, Y. Li, J. Yin, J. Li, H. Wu, Hydrothermal synthesis of uniform urchin-like  $\gamma$ -MnS architectures and their photocatalytic properties, *Phys. E Low-Dimensional Syst. Nanostructures.* 116 (2020) 113711. <https://doi.org/10.1016/j.physe.2019.113711>.
- [300] M.L. Moreira, J. Andrés, J.A. Varela, E. Longo, Synthesis of Fine Micro-sized BaZrO<sub>3</sub> Powders Based on a Decaoctahedron Shape by the Microwave-Assisted Hydrothermal Method, *Cryst. Growth Des.* 9 (2009) 833–839. <https://doi.org/10.1021/cg800433h>.
- [301] A. Gandon, C.C. Nguyen, S. Kaliaguine, T.O. Do, Synthesis of single-phase and controlled monodisperse magnetite Fe<sub>3</sub>O<sub>4</sub> nanoparticles, *Can. J. Chem. Eng.* 99 (2021) 479–488. <https://doi.org/10.1002/cjce.23889>.
- [302] X. Zhang, Z. Quan, J. Yang, P. Yang, H. Lian, J. Lin, Solvothermal synthesis of well-dispersed MF<sub>2</sub> (M = Ca, Sr, Ba) nanocrystals and their optical properties, *Nanotechnology.* 19 (2008) 075603. <https://doi.org/10.1088/0957-4484/19/7/075603>.
- [303] Y. Liu, L. Xia, Y. Lu, S. Dai, M. Takeguchi, H. Hong, Z. Pan, Surfactant-free microwave-assisted hydrothermal synthesis of BaMoO<sub>4</sub> hierarchical self-assemblies and enhanced photoluminescence properties, *J. Colloid Interface Sci.* 381 (2012) 24–29. <https://doi.org/10.1016/j.jcis.2012.05.028>.

- [304] S. Mandizadeh, A. Salehabadi, O. Amiri, M. Salavati-Niasari, Amino acids assisted hydrothermal synthesis of W-type SrFe<sub>18</sub>O<sub>27</sub> nanostructures; a potential hydrodesulfurization catalyst, *Int. J. Hydrogen Energy*. 44 (2019) 15017–15025. <https://doi.org/10.1016/j.ijhydene.2019.04.154>.
- [305] B. Liu, F. Wang, D. Zheng, X. Liu, X. Sun, S. Hou, Y. Xing, Hydrothermal synthesis and magnetic properties of CoS<sub>2</sub> nano-octahedrons, *Mater. Lett.* 65 (2011) 2804–2807. <https://doi.org/10.1016/j.matlet.2011.05.064>.
- [306] X. Lan, J. Zhang, H. Gao, T. Wang, Morphology-controlled hydrothermal synthesis and growth mechanism of microcrystal Cu<sub>2</sub>O, *CrystEngComm*. 13 (2011) 633–636. <https://doi.org/10.1039/C0CE00232A>.
- [307] W. Medina-Ramos, M.A. Mojica, E.D. Cope, R.J. Hart, P. Pollet, C.A. Eckert, C.L. Liotta, Water at elevated temperatures (WET): reactant, catalyst, and solvent in the selective hydrolysis of protecting groups, *Green Chem.* 16 (2014) 2147–2155. <https://doi.org/10.1039/C3GC42569J>.
- [308] H. Ghobarkar, O. Schäf, Y. Massiani, P. Knauth, Hydrothermal Synthesis Under Pressure, in: *Reconstr. Nat. Zeolites*, Springer US, Boston, MA, 2003: pp. 19–33. [https://doi.org/10.1007/978-1-4419-9142-3\\_3](https://doi.org/10.1007/978-1-4419-9142-3_3).
- [309] M.A. Gomes, Á.S. Lima, K.I.B. Eguiluz, G.R. Salazar-Banda, Wet chemical synthesis of rare earth-doped barium titanate nanoparticles, *J. Mater. Sci.* 51 (2016) 4709–4727. <https://doi.org/10.1007/s10853-016-9789-7>.
- [310] S. Chen, Q. Shi, J. Lin, Z. Cai, L. Cao, L. Zhu, Z. Yuan, Growth behavior and influence factors of three-dimensional hierarchical flower-like FeF<sub>3</sub> · 0.33H<sub>2</sub>O, *CrystEngComm*. 22 (2020) 5550–5557. <https://doi.org/10.1039/D0CE00771D>.
- [311] M. Godinho, C. Ribeiro, E. Longo, E.R. Leite, Influence of Microwave Heating on the Growth of Gadolinium-Doped Cerium Oxide Nanorods, *Cryst. Growth Des.* 8 (2008) 384–386. <https://doi.org/10.1021/cg700872b>.
- [312] M. Ghodrati, M. Mousavi-Kamazani, S. Zinatloo-Ajabshir, Zn<sub>3</sub>V<sub>3</sub>O<sub>8</sub> nanostructures: Facile hydrothermal/solvothermal synthesis, characterization, and electrochemical hydrogen storage, *Ceram. Int.* 46 (2020) 28894–28902. <https://doi.org/10.1016/j.ceramint.2020.08.057>.
- [313] J.C. Sczancoski, M.D.R. Bomio, L.S. Cavalcante, M.R. Joya, P.S. Pizani, J.A. Varela, E. Longo, M.S. Li, J.A. Andrés, Morphology and Blue Photoluminescence Emission of PbMoO<sub>4</sub> Processed in Conventional Hydrothermal, *J. Phys. Chem. C*. 113 (2009) 5812–5822. <https://doi.org/10.1021/jp810294q>.
- [314] J.-S. Lee, S.-C. Choi, Solvent effect on synthesis of indium tin oxide nano-powders by a solvothermal process, *J. Eur. Ceram. Soc.* 25 (2005) 3307–3314. <https://doi.org/10.1016/j.jeurceramsoc.2004.08.022>.
- [315] X. Lu, M. Li, S. Hoang, S.L. Suib, P.-X. Gao, Solvent effects on the heterogeneous growth of TiO<sub>2</sub> nanostructure arrays by solvothermal synthesis, *Catal. Today*. 360 (2021) 275–283. <https://doi.org/10.1016/j.cattod.2020.02.044>.
- [316] K. Edalati, A. Shakiba, J. Vahdati-Khaki, S.M. Zebarjad, Low-temperature hydrothermal synthesis of ZnO nanorods: Effects of zinc salt concentration,

- various solvents and alkaline mineralizers, *Mater. Res. Bull.* 74 (2016) 374–379. <https://doi.org/10.1016/j.materresbull.2015.11.001>.
- [317] P. Thuéry, J. Harrowfield, Solvent effects in solvo-hydrothermal synthesis of uranyl ion complexes with 1,3-adamantanediacetate, *CrystEngComm.* 17 (2015) 4006–4018. <https://doi.org/10.1039/c5ce00401b>.
- [318] Y. Liu, Y. Ma, W. Liu, Y. Shang, A. Zhu, P. Tan, X. Xiong, J. Pan, Facet and morphology dependent photocatalytic hydrogen evolution with CdS nanoflowers using a novel mixed solvothermal strategy, *J. Colloid Interface Sci.* 513 (2018) 222–230. <https://doi.org/10.1016/j.jcis.2017.11.030>.
- [319] W. Zhai, J. Lin, Q. Li, K. Zheng, Y. Huang, Y. Yao, X. He, L. Li, C. Yu, C. Liu, Y. Fang, Z. Liu, C. Tang, Solvothermal Synthesis of Ultrathin Cesium Lead Halide Perovskite Nanoplatelets with Tunable Lateral Sizes and Their Reversible Transformation into Cs<sub>4</sub>PbBr<sub>6</sub> Nanocrystals, *Chem. Mater.* 30 (2018) 3714–3721. <https://doi.org/10.1021/acs.chemmater.8b00612>.
- [320] G. Cao, J. Yang, J. Zhu, Y. Li, X. Xi, J. Zheng, Y. Xiong, A solvothermal route to prepare enhanced LiNi<sub>0.88</sub>Co<sub>0.09</sub>Al<sub>0.03</sub>O<sub>2</sub> cathode material taking isopropyl alcohol as solvent, *Ionics (Kiel)*. 26 (2020) 5273–5278. <https://doi.org/10.1007/s11581-020-03701-7>.
- [321] M. Lahav, L. Leiserowitz, The effect of solvent on crystal growth and morphology, *Chem. Eng. Sci.* 56 (2001) 2245–2253. [https://doi.org/10.1016/S0009-2509\(00\)00459-0](https://doi.org/10.1016/S0009-2509(00)00459-0).
- [322] Y. Wang, G. Xu, Z. Ren, X. Wei, W. Weng, P. Du, G. Shen, G. Han, Mineralizer-assisted hydrothermal synthesis and characterization of BiFeO<sub>3</sub> nanoparticles, *J. Am. Ceram. Soc.* 90 (2007) 2615–2617. <https://doi.org/10.1111/j.1551-2916.2007.01735.x>.
- [323] A.S. Barnard, L.A. Curtiss, Prediction of TiO<sub>2</sub> Nanoparticle Phase and Shape Transitions Controlled by Surface Chemistry, *Nano Lett.* 5 (2005) 1261–1266. <https://doi.org/10.1021/nl050355m>.
- [324] R. Lebeda, E. Mendyk, V.A. Tertykh, Effect of medium pH on hydrothermal treatment of silica gels (xerogels) in an autoclave, *Mater. Chem. Phys.* 43 (1996) 53–58. [https://doi.org/10.1016/0254-0584\(95\)01604-S](https://doi.org/10.1016/0254-0584(95)01604-S).
- [325] C. Li, J. Yang, Z. Quan, P. Yang, D. Kong, J. Lin, Different Microstructures of β-NaYF<sub>4</sub> Fabricated by Hydrothermal Process: Effects of pH Values and Fluoride Sources, *Chem. Mater.* 19 (2007) 4933–4942. <https://doi.org/10.1021/cm071668g>.
- [326] T. He, L. Xiang, S. Zhu, Different nanostructures of boehmite fabricated by hydrothermal process: effects of pH and anions, *CrystEngComm.* 11 (2009) 1338. <https://doi.org/10.1039/b900447p>.
- [327] M. Hojamberdiev, G. Zhu, Y. Xu, Template-free synthesis of ZnWO<sub>4</sub> powders via hydrothermal process in a wide pH range, *Mater. Res. Bull.* 45 (2010) 1934–1940. <https://doi.org/10.1016/j.materresbull.2010.08.015>.
- [328] N.-C. Wu, E.-W. Shi, Y.-Q. Zheng, W.-J. Li, Effect of pH of Medium on Hydrothermal Synthesis of Nanocrystalline Cerium(IV) Oxide Powders, *J. Am.*

Ceram. Soc. 85 (2002) 2462–2468. <https://doi.org/10.1111/j.1151-2916.2002.tb00481.x>.

- [329] J. Zhang, K. Huang, L. Yuan, S. Feng, Mineralizer effect on facet-controllable hydrothermal crystallization of perovskite structure  $\text{YbFeO}_3$  crystals, *CrystEngComm*. 20 (2018) 470–476. <https://doi.org/10.1039/C7CE01827D>.
- [330] P.S. Yoo, B.W. Lee, C. Liu, Effects of pH Value, Reaction Time, and Filling Pressure on the Hydrothermal Synthesis of  $\text{ZnFe}_2\text{O}_4$  Nanoparticles, *IEEE Trans. Magn.* 51 (2015) 1–4. <https://doi.org/10.1109/TMAG.2015.2434380>.
- [331] H. Nosrati, R.S. Mamoory, F. Dabir, D.Q. Svend Le, C.E. Bünger, M.C. Perez, M.A. Rodriguez, Effects of hydrothermal pressure on in situ synthesis of 3D graphene- hydroxyapatite nano structured powders, *Ceram. Int.* 45 (2019) 1761–1769. <https://doi.org/10.1016/j.ceramint.2018.10.059>.
- [332] Y. Wang, S. Zhang, K. Wei, N. Zhao, J. Chen, X. Wang, Hydrothermal synthesis of hydroxyapatite nanopowders using cationic surfactant as a template, *Mater. Lett.* 60 (2006) 1484–1487. <https://doi.org/10.1016/j.matlet.2005.11.053>.
- [333] M.-G. Ma, Hierarchically nanostructured hydroxyapatite: hydrothermal synthesis, morphology control, growth mechanism, and biological activity, *Int. J. Nanomedicine*. 7 (2012) 1781. <https://doi.org/10.2147/IJN.S29884>.
- [334] L.Y. Huang, K.W. Xu, J. Lu, A study of the process and kinetics of electrochemical deposition and the hydrothermal synthesis of hydroxyapatite coatings, *J. Mater. Sci. Mater. Med.* 11 (2000) 667–673. <https://doi.org/10.1023/a:1008934522363>.
- [335] Y.X. Gan, A.H. Jayatissa, Z. Yu, X. Chen, M. Li, Hydrothermal Synthesis of Nanomaterials, *J. Nanomater.* 2020 (2020) 1–3. <https://doi.org/10.1155/2020/8917013>.
- [336] N.V. Long, P. Van Viet, L. Van Hieu, C.M. Thi, Y. Yong, M. Nogami, The Controlled Hydrothermal Synthesis and Photocatalytic Characterization of  $\text{TiO}_2$  Nanorods: Effects of Time and Temperature, *Adv. Sci. Eng. Med.* 6 (2014) 214–220. <https://doi.org/10.1166/ asem.2014.1472>.
- [337] H.G. Zhang, Q. Zhu, Surfactant-assisted preparation of fluoride-substituted hydroxyapatite nanorods, *Mater. Lett.* 59 (2005) 3054–3058. <https://doi.org/10.1016/j.matlet.2005.05.019>.
- [338] G.U. Ryu, G.M. Kim, H.R. Khalid, H.K. Lee, The Effects of Temperature on the Hydrothermal Synthesis of Hydroxyapatite-Zeolite Using Blast Furnace Slag, *Materials (Basel)*. 12 (2019) 2131. <https://doi.org/10.3390/ma12132131>.
- [339] F. Ren, Y. Ding, X. Ge, X. Lu, K. Wang, Y. Leng, Growth of one-dimensional single-crystalline hydroxyapatite nanorods, *J. Cryst. Growth*. 349 (2012) 75–82. <https://doi.org/10.1016/j.jcrysgro.2012.04.003>.
- [340] A.F. Gouveia, J.C. Sczancoski, M.M. Ferrer, A.S. Lima, M.R.M.C. Santos, M.S. Li, R.S. Santos, E. Longo, L.S. Cavalcante, Experimental and Theoretical Investigations of Electronic Structure and Photoluminescence Properties of  $\beta\text{-Ag}_2\text{MoO}_4$  Microcrystals, *Inorg. Chem.* 53 (2014) 5589–5599. <https://doi.org/10.1021/ic500335x>.

- [341] J. Khatter, R.P. Chauhan, Effect of temperature on properties of cadmium sulfide nanostructures synthesized by solvothermal method, *J. Mater. Sci. Mater. Electron.* 31 (2020) 2676–2685. <https://doi.org/10.1007/s10854-019-02807-7>.
- [342] X. Jing, T. Liu, D. Wang, J. Liu, L. Meng, Controlled synthesis of water-dispersible and superparamagnetic Fe<sub>3</sub>O<sub>4</sub> nanomaterials by a microwave-assisted solvothermal method: from nanocrystals to nanoclusters, *CrystEngComm*. 19 (2017) 5089–5099. <https://doi.org/10.1039/C7CE01191A>.
- [343] A.C. Mera, C.A. Rodríguez, L. Pizarro-Castillo, M.F. Meléndrez, H. Valdés, Effect of temperature and reaction time during solvothermal synthesis of BiOCl on microspheres formation: implications in the photocatalytic oxidation of gallic acid under simulated solar radiation, *J. Sol-Gel Sci. Technol.* 95 (2020) 146–156. <https://doi.org/10.1007/s10971-020-05312-0>.
- [344] R. Singh, R. Bhateria, Core–shell nanostructures: a simplest two-component system with enhanced properties and multiple applications, *Environ. Geochem. Health.* 1 (2020). <https://doi.org/10.1007/s10653-020-00766-1>.
- [345] F. Caruso, Nanoengineering of Particle Surfaces, *Adv. Mater.* 13 (2001) 11–22. [https://doi.org/10.1002/1521-4095\(200101\)13:1<11::AID-ADMA11>3.0.CO;2-N](https://doi.org/10.1002/1521-4095(200101)13:1<11::AID-ADMA11>3.0.CO;2-N).
- [346] S. Kalele, S.W. Gosavi, J. Urban, S.K. Kulkarni, Nanoshell particles: Synthesis, properties and applications, *Curr. Sci.* 91 (2006) 1038–1052.
- [347] Y. Piao, A. Burns, J. Kim, U. Wiesner, T. Hyeon, Designed Fabrication of Silica-Based Nanostructured Particle Systems for Nanomedicine Applications, *Adv. Funct. Mater.* 18 (2008) 3745–3758. <https://doi.org/10.1002/adfm.200800731>.
- [348] A. Morel, S.I. Nikitenko, K. Gionnet, A. Wattiaux, J. Lai-Kee-Him, C. Labrugere, B. Chevalier, G. Deleris, C. Petibois, A. Brisson, M. Simonoff, Sonochemical Approach to the Synthesis of Fe<sub>3</sub>O<sub>4</sub>@SiO<sub>2</sub> Core–Shell Nanoparticles with Tunable Properties, *ACS Nano.* 2 (2008) 847–856. <https://doi.org/10.1021/nn800091q>.
- [349] R. Harpeness, A. Gedanken, Microwave Synthesis of Core–Shell Gold/Palladium Bimetallic Nanoparticles, *Langmuir.* 20 (2004) 3431–3434. <https://doi.org/10.1021/la035978z>.
- [350] J. Du, J. Qi, D. Wang, Z. Tang, Facile synthesis of Au@TiO<sub>2</sub> core–shell hollow spheres for dye-sensitized solar cells with remarkably improved efficiency, *Energy Environ. Sci.* 5 (2012) 6914. <https://doi.org/10.1039/c2ee21264a>.
- [351] J.T. McKeown, Y. Wu, J.D. Fowlkes, P.D. Rack, G.H. Campbell, Simultaneous in-situ synthesis and characterization of Co@Cu core-shell nanoparticle arrays, *Adv. Mater.* 27 (2015) 1060–1065. <https://doi.org/10.1002/adma.201404374>.
- [352] B. Réti, G.I. Kiss, T. Gyulavári, K. Baan, K. Magyari, K. Hernadi, Carbon sphere templates for TiO<sub>2</sub> hollow structures: Preparation, characterization and photocatalytic activity, *Catal. Today.* 284 (2017) 160–168. <https://doi.org/10.1016/j.cattod.2016.11.038>.
- [353] X. He, F. Wu, M. Zheng, The synthesis of carbon nanoballs and its electrochemical performance, *Diam. Relat. Mater.* 16 (2007) 311–315.

<https://doi.org/10.1016/j.diamond.2006.06.011>.

- [354] J.H. Kim, B. Fang, M. Kim, J.-S. Yu, Hollow spherical carbon with mesoporous shell as a superb anode catalyst support in proton exchange membrane fuel cell, *Catal. Today*. 146 (2009) 25–30. <https://doi.org/10.1016/j.cattod.2009.02.013>.
- [355] J. Liu, N.P. Wickramaratne, S.Z. Qiao, M. Jaroniec, Molecular-based design and emerging applications of nanoporous carbon spheres, *Nat. Mater.* 14 (2015) 763–774. <https://doi.org/10.1038/nmat4317>.
- [356] F. Sauvage, D. Chen, P. Comte, F. Huang, L.-P. Heiniger, Y. Cheng, R.A. Caruso, M. Graetzel, Dye-Sensitized Solar Cells Employing a Single Film of Mesoporous TiO<sub>2</sub> Beads Achieve Power Conversion Efficiencies Over 10%, *ACS Nano*. 4 (2010) 4420–4425. <https://doi.org/10.1021/nn1010396>.
- [357] Y. Ding, L. Zhou, L. Mo, L. Jiang, L. Hu, Z. Li, S. Chen, S. Dai, TiO<sub>2</sub> Microspheres with Controllable Surface Area and Porosity for Enhanced Light Harvesting and Electrolyte Diffusion in Dye-Sensitized Solar Cells, *Adv. Funct. Mater.* 25 (2015) 5946–5953. <https://doi.org/10.1002/adfm.201502224>.
- [358] S. Yin, Y. Goldovsky, M. Herzberg, L. Liu, H. Sun, Y. Zhang, F. Meng, X. Cao, D.D. Sun, H. Chen, A. Kushmaro, X. Chen, Functional Free-Standing Graphene Honeycomb Films, *Adv. Funct. Mater.* 23 (2013) 2972–2978. <https://doi.org/10.1002/adfm.201203491>.
- [359] H. Zou, K. Shang, Synthetic strategies for hollow particles with open holes on their surfaces, *Mater. Chem. Front.* 5 (2021) 3765–3787. <https://doi.org/10.1039/D1QM00217A>.
- [360] X.W. (David) Lou, L.A. Archer, Z. Yang, Hollow Micro-/Nanostructures: Synthesis and Applications, *Adv. Mater.* 20 (2008) 3987–4019. <https://doi.org/10.1002/adma.200800854>.
- [361] Y. Chang, J.J. Teo, H.C. Zeng, Formation of colloidal CuO nanocrystallites and their spherical aggregation and reductive transformation to hollow Cu<sub>2</sub>O nanospheres, *Langmuir*. 21 (2005) 1074–1079. <https://doi.org/10.1021/la0476711>.
- [362] J.J. Teo, Y. Chang, H.C. Zeng, Fabrications of Hollow Nanocubes of Cu<sub>2</sub>O and Cu via Reductive Self-Assembly of CuO Nanocrystals, *Langmuir*. 22 (2006) 7369–7377. <https://doi.org/10.1021/la060439q>.
- [363] G. Liu, G. Hong, J. Wang, X. Dong, Hydrothermal synthesis of spherical and hollow Gd<sub>2</sub>O<sub>3</sub>:Eu<sup>3+</sup> phosphors, *J. Alloys Compd.* 432 (2007) 200–204. <https://doi.org/10.1016/j.jallcom.2006.05.127>.
- [364] B. HU, Z. JING, J. HUANG, J. YUN, Synthesis of hierarchical hollow spherical CdS nanostructures by microwave hydrothermal process, *Trans. Nonferrous Met. Soc. China*. 22 (2012) s89–s94. [https://doi.org/10.1016/S1003-6326\(12\)61689-6](https://doi.org/10.1016/S1003-6326(12)61689-6).
- [365] M. Qin, L. Zhang, H. Wu, Dual-template hydrothermal synthesis of multi-channel porous NiCo<sub>2</sub>O<sub>4</sub> hollow spheres as high-performance electromagnetic wave absorber, *Appl. Surf. Sci.* 515 (2020) 146132. <https://doi.org/10.1016/j.apsusc.2020.146132>.
- [366] S. Das, S. Som, C.-Y. Yang, C.-H. Lu, Optical temperature sensing properties of



- SnO<sub>2</sub>: Eu<sup>3+</sup> microspheres prepared via the microwave assisted solvothermal process, *Mater. Res. Bull.* 97 (2018) 101–108.  
<https://doi.org/10.1016/j.materresbull.2017.08.057>.
- [367] Z. Zhu, Y. Zhang, Y. Zhang, H. Liu, C. Zhu, Y. Wu, PEG-directed microwave-assisted hydrothermal synthesis of spherical  $\alpha$ -Ni(OH)<sub>2</sub> and NiO architectures, *Ceram. Int.* 39 (2013) 2567–2573.  
<https://doi.org/10.1016/j.ceramint.2012.09.017>.
- [368] L. Ma, W.-X. Chen, Y.-F. Zheng, J. Zhao, Z. Xu, Microwave-assisted hydrothermal synthesis and characterizations of PrF<sub>3</sub> hollow nanoparticles, *Mater. Lett.* 61 (2007) 2765–2768. <https://doi.org/10.1016/j.matlet.2006.04.124>.
- [369] H. Ji, X. Miao, L. Wang, B. Qian, G. Yang, Microwave-assisted hydrothermal synthesis of sphere-like C/CuO and CuO nanocrystals and improved performance as anode materials for lithium-ion batteries, *Powder Technol.* 241 (2013) 43–48.  
<https://doi.org/10.1016/j.powtec.2013.02.042>.
- [370] R. Mishra, J. Militky, M. Venkataraman, Nanoporous materials, in: R. Mishra, J. Militky (Eds.), *Nanotechnol. Text.*, Elsevier, 2019: pp. 311–353.  
<https://doi.org/10.1016/B978-0-08-102609-0.00007-9>.
- [371] X.-Y. Yang, L.-H. Chen, Y. Li, J.C. Rooke, C. Sanchez, B.-L. Su, Hierarchically porous materials: synthesis strategies and structure design, *Chem. Soc. Rev.* 46 (2017) 481–558. <https://doi.org/10.1039/C6CS00829A>.
- [372] Y. Yu, W. Zeng, Z. Zhang, Y. Cai, H. Zhang, Hierarchical WO<sub>3</sub>·H<sub>2</sub>O porous microsphere: Hydrothermal synthesis, structure and gas-sensing performance, *Mater. Lett.* 186 (2017) 119–122. <https://doi.org/10.1016/j.matlet.2016.09.106>.
- [373] E. Poonia, S. Duhan, K. Kumar, A. Kumar, S. Jakhar, V.K. Tomer, One pot hydrothermal synthesis of ordered mesoporous SnO<sub>2</sub>/SBA-16 nanocomposites, *J. Porous Mater.* 26 (2019) 553–560. <https://doi.org/10.1007/s10934-018-0651-y>.
- [374] Z. Qing, L. Haixia, L. Huali, L. Yu, Z. Huayong, L. Tianduo, Solvothermal synthesis and photocatalytic properties of NiO ultrathin nanosheets with porous structure, *Appl. Surf. Sci.* 328 (2015) 525–530.  
<https://doi.org/10.1016/j.apsusc.2014.12.077>.
- [375] H. Chen, X. Du, J. Sun, H. Mao, R. Wu, C. Xu, Simple preparation of ZnCo<sub>2</sub>O<sub>4</sub> porous quasi-cubes for high performance asymmetric supercapacitors, *Appl. Surf. Sci.* 515 (2020) 146008. <https://doi.org/10.1016/j.apsusc.2020.146008>.
- [376] H.E. Wang, L.J. Xi, R.G. Ma, Z.G. Lu, C.Y. Chung, I. Bello, J.A. Zapien, Microwave-assisted hydrothermal synthesis of porous SnO<sub>2</sub> nanotubes and their lithium ion storage properties, *J. Solid State Chem.* 190 (2012) 104–110.  
<https://doi.org/10.1016/j.jssc.2012.02.016>.
- [377] L. Nie, K. Deng, S. Yuan, W. Zhang, Q. Tan, Microwave-assisted hydrothermal synthesis of hierarchically porous  $\gamma$ -Al<sub>2</sub>O<sub>3</sub> hollow microspheres with enhanced Cu<sup>2+</sup> adsorption performance, *Mater. Lett.* 132 (2014) 369–372.  
<https://doi.org/10.1016/j.matlet.2014.06.095>.
- [378] G.-J. Ding, Y.-J. Zhu, C. Qi, B.-Q. Lu, J. Wu, F. Chen, Porous microspheres of amorphous calcium phosphate: Block copolymer templated microwave-assisted

- hydrothermal synthesis and application in drug delivery, *J. Colloid Interface Sci.* 443 (2015) 72–79. <https://doi.org/10.1016/j.jcis.2014.12.004>.
- [379] A. Kolmakov, M. Moskovits, CHEMICAL SENSING AND CATALYSIS BY ONE-DIMENSIONAL METAL-OXIDE NANOSTRUCTURES, *Annu. Rev. Mater. Res.* 34 (2004) 151–180. <https://doi.org/10.1146/annurev.matsci.34.040203.112141>.
- [380] C.M. Lieber, One-dimensional nanostructures: Chemistry, physics & applications, *Solid State Commun.* 107 (1998) 607–616. [https://doi.org/10.1016/S0038-1098\(98\)00209-9](https://doi.org/10.1016/S0038-1098(98)00209-9).
- [381] J. Hu, T.W. Odom, C.M. Lieber, Chemistry and Physics in One Dimension: Synthesis and Properties of Nanowires and Nanotubes, *Acc. Chem. Res.* 32 (1999) 435–445. <https://doi.org/10.1021/ar9700365>.
- [382] J. Weber, R. Singhal, S. Zekri, A. Kumar, One-dimensional nanostructures: fabrication, characterisation and applications, *Int. Mater. Rev.* 53 (2008) 235–255. <https://doi.org/10.1179/174328008X348183>.
- [383] C. Koenigsmann, S.S. Wong, One-dimensional noble metal electrocatalysts: a promising structural paradigm for direct methanolfuelcells, *Energy Environ. Sci.* 4 (2011) 1161–1176. <https://doi.org/10.1039/C0EE00197J>.
- [384] Y. Kim, J.G. Kim, Y. Noh, W.B. Kim, An Overview of One-Dimensional Metal Nanostructures for Electrocatalysis, *Catal. Surv. from Asia.* 19 (2015) 88–121. <https://doi.org/10.1007/s10563-015-9187-1>.
- [385] S.V.N.T. Kuchibhatla, A.S. Karakoti, D. Bera, S. Seal, One dimensional nanostructured materials, *Prog. Mater. Sci.* 52 (2007) 699–913. <https://doi.org/10.1016/j.pmatsci.2006.08.001>.
- [386] A.F.V. da Fonseca, R.L. Siqueira, R. Landers, J.L. Ferrari, N.L. Marana, J.R. Sambrano, F. de A. La Porta, M.A. Schiavon, A theoretical and experimental investigation of Eu-doped ZnO nanorods and its application on dye sensitized solar cells, *J. Alloys Compd.* 739 (2018) 939–947. <https://doi.org/10.1016/j.jallcom.2017.12.262>.
- [387] Y. Xia, P. Yang, Y. Sun, Y. Wu, B. Mayers, B. Gates, Y. Yin, F. Kim, H. Yan, One-Dimensional Nanostructures: Synthesis, Characterization, and Applications, *Adv. Mater.* 15 (2003) 353–389. <https://doi.org/10.1002/adma.200390087>.
- [388] Y. Zhu, T. Mei, Y. Wang, Y. Qian, Formation and morphology control of nanoparticles via solution routes in an autoclave, *J. Mater. Chem.* 21 (2011) 11457. <https://doi.org/10.1039/c1jm11079a>.
- [389] Y. Jun, M.F. Casula, J.-H. Sim, S.Y. Kim, J. Cheon, A.P. Alivisatos, Surfactant-Assisted Elimination of a High Energy Facet as a Means of Controlling the Shapes of TiO<sub>2</sub> Nanocrystals, *J. Am. Chem. Soc.* 125 (2003) 15981–15985. <https://doi.org/10.1021/ja0369515>.
- [390] S. Gorai, D. Ganguli, S. Chaudhuri, Synthesis of 1D Cu<sub>2</sub>S with tailored morphology via single and mixed ionic surfactant templates, *Mater. Chem. Phys.* 88 (2004) 383–387. <https://doi.org/10.1016/j.matchemphys.2004.08.004>.
- [391] Y. Gao, Z. Wang, J. Wan, G. Zou, Y. Qian, A facile route to synthesize uniform

- single-crystalline -MnO<sub>2</sub> nanowires, *J. Cryst. Growth*. 279 (2005) 415–419. <https://doi.org/10.1016/j.jcrysgro.2005.02.052>.
- [392] D. Zheng, S. Sun, W. Fan, H. Yu, C. Fan, G. Cao, Z. Yin, X. Song, One-Step Preparation of Single-Crystalline  $\beta$ -MnO<sub>2</sub> Nanotubes, *J. Phys. Chem. B*. 109 (2005) 16439–16443. <https://doi.org/10.1021/jp052370l>.
- [393] P. Zhang, C. Shao, Z. Zhang, M. Zhang, J. Mu, Z. Guo, Y. Sun, Y. Liu, Core/shell nanofibers of TiO<sub>2</sub>@carbon embedded by Ag nanoparticles with enhanced visible photocatalytic activity, *J. Mater. Chem.* 21 (2011) 17746. <https://doi.org/10.1039/c1jm12965a>.
- [394] M. Li, D.-B. Li, J. Pan, J.-C. Lin, G.-H. Li, Selective Synthesis of Vanadium Oxides and Investigation of the Thermochromic Properties of VO<sub>2</sub> by Infrared Spectroscopy, *Eur. J. Inorg. Chem.* 2013 (2013) 1207–1212. <https://doi.org/10.1002/ejic.201201118>.
- [395] N. Moloto, S. Mpelane, L.M. Sikhwivhilu, S. Sinha Ray, Optical and Morphological Properties of ZnO- and TiO<sub>2</sub>-Derived Nanostructures Synthesized via a Microwave-Assisted Hydrothermal Method, *Int. J. Photoenergy*. 2012 (2012) 1–6. <https://doi.org/10.1155/2012/189069>.
- [396] M.N. Nadagouda, R.S. Varma, Microwave-Assisted Shape-Controlled Bulk Synthesis of Ag and Fe Nanorods in Poly(ethylene glycol) Solutions, *Cryst. Growth Des.* 8 (2008) 291–295. <https://doi.org/10.1021/cg070473i>.
- [397] MATRAS-POSTOLEK, Katarzyna, et al, Microwave-assisted synthesis and the surface modification of 1-D dimensional ZnS: Mn nanocrystals for polymer applications., 18th Int. Electron. Conf. Synth. Org. Chem. (2014).
- [398] B. Zhou, J.-J. Zhu, Microwave-assisted synthesis of Sb<sub>2</sub>Se<sub>3</sub> submicron rods, compared with those of Bi<sub>2</sub>Te<sub>3</sub> and Sb<sub>2</sub>Te<sub>3</sub>, *Nanotechnology*. 20 (2009) 085604. <https://doi.org/10.1088/0957-4484/20/8/085604>.
- [399] C. Ashok, K. Venkateswara Rao, Synthesis of Nanostructured Metal Oxide by Microwave-Assisted Method and its Humidity Sensor Application, *Mater. Today Proc.* 4 (2017) 3816–3824. <https://doi.org/10.1016/j.matpr.2017.02.279>.
- [400] Z. Zeng, Z. Yin, X. Huang, H. Li, Q. He, G. Lu, F. Boey, H. Zhang, Single-Layer Semiconducting Nanosheets: High-Yield Preparation and Device Fabrication, *Angew. Chemie Int. Ed.* 50 (2011) 11093–11097. <https://doi.org/10.1002/anie.201106004>.
- [401] K.S. Novoselov, Electric Field Effect in Atomically Thin Carbon Films, *Science* (80-. ). 306 (2004) 666–669. <https://doi.org/10.1126/science.1102896>.
- [402] Z. Yin, H. Li, H. Li, L. Jiang, Y. Shi, Y. Sun, G. Lu, Q. Zhang, X. Chen, H. Zhang, Single-Layer MoS<sub>2</sub> Phototransistors, *ACS Nano*. 6 (2012) 74–80. <https://doi.org/10.1021/nn2024557>.
- [403] A. Splendiani, L. Sun, Y. Zhang, T. Li, J. Kim, C.-Y. Chim, G. Galli, F. Wang, Emerging Photoluminescence in Monolayer MoS<sub>2</sub>, *Nano Lett.* 10 (2010) 1271–1275. <https://doi.org/10.1021/nl903868w>.
- [404] Q. He, Z. Zeng, Z. Yin, H. Li, S. Wu, X. Huang, H. Zhang, Fabrication of Flexible MoS<sub>2</sub> Thin-Film Transistor Arrays for Practical Gas-Sensing

- Applications, *Small*. 8 (2012) 2994–2999.  
<https://doi.org/10.1002/sml.201201224>.
- [405] S. Wu, Z. Zeng, Q. He, Z. Wang, S.J. Wang, Y. Du, Z. Yin, X. Sun, W. Chen, H. Zhang, Electrochemically Reduced Single-Layer MoS<sub>2</sub> Nanosheets: Characterization, Properties, and Sensing Applications, *Small*. 8 (2012) 2264–2270. <https://doi.org/10.1002/sml.201200044>.
- [406] X. Huang, S. Li, Y. Huang, S. Wu, X. Zhou, S. Li, C.L. Gan, F. Boey, C.A. Mirkin, H. Zhang, Synthesis of hexagonal close-packed gold nanostructures, *Nat. Commun.* 2 (2011) 292. <https://doi.org/10.1038/ncomms1291>.
- [407] C. Hu, H. Cheng, Y. Zhao, Y. Hu, Y. Liu, L. Dai, L. Qu, Newly-Designed Complex Ternary Pt/PdCu Nanoboxes Anchored on Three-Dimensional Graphene Framework for Highly Efficient Ethanol Oxidation, *Adv. Mater.* 24 (2012) 5493–5498. <https://doi.org/10.1002/adma.201200498>.
- [408] X. Huang, Z. Zeng, S. Bao, M. Wang, X. Qi, Z. Fan, H. Zhang, Solution-phase epitaxial growth of noble metal nanostructures on dispersible single-layer molybdenum disulfide nanosheets, *Nat. Commun.* 4 (2013) 1444. <https://doi.org/10.1038/ncomms2472>.
- [409] Z. Zeng, C. Tan, X. Huang, S. Bao, H. Zhang, Growth of noble metal nanoparticles on single-layer TiS<sub>2</sub> and TaS<sub>2</sub> nanosheets for hydrogen evolution reaction, *Energy Environ. Sci.* 7 (2014) 797–803. <https://doi.org/10.1039/C3EE42620C>.
- [410] Y. Shi, Y. Wang, J.I. Wong, A.Y.S. Tan, C. Hsu, L. Li, Y. Lu, H.Y. Yang, Self-assembly of hierarchical MoS<sub>x</sub>/CNT nanocomposites (2 < x < 3): towards high performance anode materials for lithium ion batteries, *Sci. Rep.* 3 (2013) 2169. <https://doi.org/10.1038/srep02169>.
- [411] T. Zhu, H. Bin Wu, Y. Wang, R. Xu, X.W.D. Lou, Formation of 1D Hierarchical Structures Composed of Ni<sub>3</sub>S<sub>2</sub> Nanosheets on CNTs Backbone for Supercapacitors and Photocatalytic H<sub>2</sub> Production, *Adv. Energy Mater.* 2 (2012) 1497–1502. <https://doi.org/10.1002/aenm.201200269>.
- [412] W. Guo, F. Zhang, C. Lin, Z.L. Wang, Direct Growth of TiO<sub>2</sub> Nanosheet Arrays on Carbon Fibers for Highly Efficient Photocatalytic Degradation of Methyl Orange, *Adv. Mater.* 24 (2012) 4761–4764. <https://doi.org/10.1002/adma.201201075>.
- [413] L. Zhang, G. Zhang, H. Bin Wu, L. Yu, X.W.D. Lou, Hierarchical Tubular Structures Constructed by Carbon-Coated SnO<sub>2</sub> Nanoplates for Highly Reversible Lithium Storage, *Adv. Mater.* 25 (2013) 2589–2593. <https://doi.org/10.1002/adma.201300105>.
- [414] Z. Yin, Z. Wang, Y. Du, X. Qi, Y. Huang, C. Xue, H. Zhang, Full Solution-Processed Synthesis of All Metal Oxide-Based Tree-like Heterostructures on Fluorine-Doped Tin Oxide for Water Splitting, *Adv. Mater.* 24 (2012) 5374–5378. <https://doi.org/10.1002/adma.201201474>.
- [415] C. Guan, Z. Zeng, X. Li, X. Cao, Y. Fan, X. Xia, G. Pan, H. Zhang, H.J. Fan, Atomic-Layer-Deposition-Assisted Formation of Carbon Nanoflakes on Metal Oxides and Energy Storage Application, *Small*. 10 (2014) 300–307.

<https://doi.org/10.1002/sml.201301009>.

- [416] W. Zhou, X. Cao, Z. Zeng, W. Shi, Y. Zhu, Q. Yan, H. Liu, J. Wang, H. Zhang, One-step synthesis of Ni<sub>3</sub>S<sub>2</sub> nanorod@Ni(OH)<sub>2</sub> nanosheet core-shell nanostructures on a three-dimensional graphene network for high-performance supercapacitors, *Energy Environ. Sci.* 6 (2013) 2216–2221. <https://doi.org/10.1039/C3EE40155C>.
- [417] A.K. Geim, I. V. Grigorieva, Van der Waals heterostructures, *Nature*. 499 (2013) 419–425. <https://doi.org/10.1038/nature12385>.
- [418] K.S. Novoselov, A.H. Castro Neto, Two-dimensional crystals-based heterostructures: materials with tailored properties, *Phys. Scr.* T146 (2012) 014006. <https://doi.org/10.1088/0031-8949/2012/T146/014006>.
- [419] C. Dean, A.F. Young, L. Wang, I. Meric, G.-H. Lee, K. Watanabe, T. Taniguchi, K. Shepard, P. Kim, J. Hone, Graphene based heterostructures, *Solid State Commun.* 152 (2012) 1275–1282. <https://doi.org/10.1016/j.ssc.2012.04.021>.
- [420] R. V. Gorbachev, A.K. Geim, M.I. Katsnelson, K.S. Novoselov, T. Tudorovskiy, I. V. Grigorieva, A.H. MacDonald, S. V. Morozov, K. Watanabe, T. Taniguchi, L.A. Ponomarenko, Strong Coulomb drag and broken symmetry in double-layer graphene, *Nat. Phys.* 8 (2012) 896–901. <https://doi.org/10.1038/nphys2441>.
- [421] S.J. Haigh, A. Gholinia, R. Jalil, S. Romani, L. Britnell, D.C. Elias, K.S. Novoselov, L.A. Ponomarenko, A.K. Geim, R. Gorbachev, Cross-sectional imaging of individual layers and buried interfaces of graphene-based heterostructures and superlattices, *Nat. Mater.* 11 (2012) 764–767. <https://doi.org/10.1038/nmat3386>.
- [422] C. Feng, J. Zhang, Y. He, C. Zhong, W. Hu, L. Liu, Y. Deng, Sub-3 nm Co<sub>3</sub>O<sub>4</sub> Nanofilms with Enhanced Supercapacitor Properties, *ACS Nano*. 9 (2015) 1730–1739. <https://doi.org/10.1021/nm506548d>.
- [423] P.W. Dunne, A.S. Munn, C.L. Starkey, E.H. Lester, The sequential continuous-flow hydrothermal synthesis of molybdenum disulphide, *Chem. Commun.* 51 (2015) 4048–4050. <https://doi.org/10.1039/C4CC10158H>.
- [424] Y. Takahashi, Y. Nakayasu, K. Iwase, H. Kobayashi, I. Honma, Supercritical hydrothermal synthesis of MoS<sub>2</sub> nanosheets with controllable layer number and phase structure, *Dalt. Trans.* 49 (2020) 9377–9384. <https://doi.org/10.1039/D0DT01453B>.
- [425] N. Kumar, D. Mishra, S. Yeob Kim, T. Na, S. Hun Jin, Two dimensional, sponge-like In<sub>2</sub>S<sub>3</sub> nanoflakes aligned on nickel foam via one-pot solvothermal growth and their application toward high performance supercapacitors, *Mater. Lett.* 279 (2020) 128467. <https://doi.org/10.1016/j.matlet.2020.128467>.
- [426] X. Chen, S. Wang, C. Su, Y. Han, C. Zou, M. Zeng, N. Hu, Y. Su, Z. Zhou, Z. Yang, Two-dimensional Cd-doped porous Co<sub>3</sub>O<sub>4</sub> nanosheets for enhanced room-temperature NO<sub>2</sub> sensing performance, *Sensors Actuators B Chem.* 305 (2020) 127393. <https://doi.org/10.1016/j.snb.2019.127393>.
- [427] X. Liu, Y. Wu, H. Wang, Y. Wang, C. Huang, L. Liu, Z. Wang, Two-dimensional β-MoO<sub>3</sub>@C nanosheets as high-performance negative materials

- for supercapacitors with excellent cycling stability, *RSC Adv.* 10 (2020) 17497–17505. <https://doi.org/10.1039/D0RA01258K>.
- [428] S. Zhu, Q. Liang, Y. Xu, H. Fu, X. Xiao, Facile Solvothermal Synthesis of Black Phosphorus Nanosheets from Red Phosphorus for Efficient Photocatalytic Hydrogen Evolution, *Eur. J. Inorg. Chem.* 2020 (2020) 773–779. <https://doi.org/10.1002/ejic.202000048>.
- [429] Q.-Y. Tang, M.-J. Yang, S.-Y. Yang, Y.-H. Xu, Enhanced photocatalytic degradation of glyphosate over 2D CoS/BiOBr heterojunctions under visible light irradiation, *J. Hazard. Mater.* 407 (2021) 124798. <https://doi.org/10.1016/j.jhazmat.2020.124798>.
- [430] C. Pan, Z. Liu, M. Huang, 2D iron-doped nickel MOF nanosheets grown on nickel foam for highly efficient oxygen evolution reaction, *Appl. Surf. Sci.* 529 (2020) 147201. <https://doi.org/10.1016/j.apsusc.2020.147201>.
- [431] Y. Su, J. Wang, S. Li, J. Zhu, W. Liu, Z. Zhang, Self-templated microwave-assisted hydrothermal synthesis of two-dimensional holey hydroxyapatite nanosheets for efficient heavy metal removal, *Environ. Sci. Pollut. Res.* 26 (2019) 30076–30086. <https://doi.org/10.1007/s11356-019-06160-4>.
- [432] L. Man, J. Zhang, J. Wang, H. Xu, B. Cao, Microwave-assisted hydrothermal synthesis and gas sensitivity of nanostructured SnO<sub>2</sub>, *Particuology.* 11 (2013) 242–248. <https://doi.org/10.1016/j.partic.2012.01.005>.
- [433] X. Jiang, Y. Song, M. Dou, J. Ji, F. Wang, Selective growth of vertically aligned two-dimensional MoS<sub>2</sub>/WS<sub>2</sub> nanosheets with decoration of Bi<sub>2</sub>S<sub>3</sub> nanorods by microwave-assisted hydrothermal synthesis: Enhanced photo- and electrochemical performance for hydrogen evolution reaction, *Int. J. Hydrogen Energy.* 43 (2018) 21290–21298. <https://doi.org/10.1016/j.ijhydene.2018.09.160>.
- [434] Y. Lv, S. Duan, R. Wang, Structure design, controllable synthesis, and application of metal-semiconductor heterostructure nanoparticles, *Prog. Nat. Sci. Mater. Int.* 30 (2020) 1–12. <https://doi.org/10.1016/j.pnsc.2019.12.005>.
- [435] Ç.K. Söz, S. Trosien, M. Biesalski, Janus Interface Materials: A Critical Review and Comparative Study, *ACS Mater. Lett.* 2 (2020) 336–357. <https://doi.org/10.1021/acsmaterialslett.9b00489>.
- [436] F. V. Gutierrez, A. De Falco, E. Yokoyama, L.A.F. Mendoza, C. Luz-Lima, G. Perez, R.P. Loreto, W.E. Pottker, F.A. La Porta, G. Solorzano, S. Arsalani, O. Baffa, J.F.D.F. Araujo, Magnetic Characterization by Scanning Microscopy of Functionalized Iron Oxide Nanoparticles, *Nanomaterials.* 11 (2021) 2197. <https://doi.org/10.3390/nano11092197>.
- [437] M. Kurian, S. Thankachan, Structural diversity and applications of spinel ferrite core - Shell nanostructures- A review, *Open Ceram.* 8 (2021) 100179. <https://doi.org/10.1016/j.oceram.2021.100179>.
- [438] X. Sun, J. Han, R. Guo, A Mini Review on Yolk-Shell Structured Nanocatalysts, *Front. Chem.* 8 (2020). <https://doi.org/10.3389/fchem.2020.606044>.
- [439] Z. Li, M. Li, Z. Bian, Y. Kathiraser, S. Kawi, Design of highly stable and selective core/yolk-shell nanocatalysts—A review, *Appl. Catal. B Environ.* 188

(2016) 324–341. <https://doi.org/10.1016/j.apcatb.2016.01.067>.

- [440] L.-S. Lin, J. Song, H.-H. Yang, X. Chen, Yolk-Shell Nanostructures: Design, Synthesis, and Biomedical Applications, *Adv. Mater.* 30 (2018) 1704639. <https://doi.org/10.1002/adma.201704639>.
- [441] C. Marschelke, A. Fery, A. Synytska, Janus particles: from concepts to environmentally friendly materials and sustainable applications, *Colloid Polym. Sci.* 298 (2020) 841–865. <https://doi.org/10.1007/s00396-020-04601-y>.
- [442] W.-J. Yin, H.-J. Tan, P.-J. Ding, B. Wen, X.-B. Li, G. Teobaldi, L.-M. Liu, Recent advances in low-dimensional Janus materials: theoretical and simulation perspectives, *Mater. Adv.* 2 (2021) 7543–7558. <https://doi.org/10.1039/D1MA00660F>.
- [443] J. Andrés, L. Gracia, P. Gonzalez-Navarrete, V.M. Longo, W. Avansi, D.P. Volanti, M.M. Ferrer, P.S. Lemos, F.A. La Porta, A.C. Hernandez, E. Longo, Structural and electronic analysis of the atomic scale nucleation of Ag on  $\alpha$ -Ag<sub>2</sub>WO<sub>4</sub> induced by electron irradiation, *Sci. Rep.* 4 (2015) 5391. <https://doi.org/10.1038/srep05391>.
- [444] M.T. Fabbro, C. Saliby, L.R. Rios, F.A. La Porta, L. Gracia, M.S. Li, J. Andrés, L.P.S. Santos, E. Longo, Identifying and rationalizing the morphological, structural, and optical properties of  $\beta$ -Ag<sub>2</sub>MoO<sub>4</sub> microcrystals, and the formation process of Ag nanoparticles on their surfaces: combining experimental data and first-principles calculations, *Sci. Technol. Adv. Mater.* 16 (2015) 065002. <https://doi.org/10.1088/1468-6996/16/6/065002>.
- [445] L.H. Oliveira, M.A. Ramírez, M.A. Ponce, L.A. Ramajo, A.R. Albuquerque, J.R. Sambrano, E. Longo, M.S. Castro, F.A. La Porta, Optical and gas-sensing properties, and electronic structure of the mixed-phase CaCu<sub>3</sub>Ti<sub>4</sub>O<sub>12</sub>/CaTiO<sub>3</sub> composites, *Mater. Res. Bull.* 93 (2017) 47–55. <https://doi.org/10.1016/j.materresbull.2017.04.037>.
- [446] K.W. Shah, G.F. Huseien, H.W. Kua, A State-of-the-Art Review on Core–Shell Pigments Nanostructure Preparation and Test Methods, *Micro.* 1 (2021) 55–85. <https://doi.org/10.3390/micro1010006>.
- [447] A. Spoială, C.-I. Ilie, L.N. Crăciun, D. Ficai, A. Ficai, E. Andronescu, Magnetite-Silica Core/Shell Nanostructures: From Surface Functionalization towards Biomedical Applications—A Review, *Appl. Sci.* 11 (2021) 11075. <https://doi.org/10.3390/app112211075>.
- [448] S. Mishra, T.G. Lohr, C.A. Pignedoli, J. Liu, R. Berger, J.I. Urgel, K. Müllen, X. Feng, P. Ruffieux, R. Fasel, Tailoring Bond Topologies in Open-Shell Graphene Nanostructures, *ACS Nano.* 12 (2018) 11917–11927. <https://doi.org/10.1021/acsnano.8b07225>.
- [449] L. Chen, M. Wu, D. Wang, L. Zhou, N. Yu, P. Zhang, J. Huang, X. Liu, G. Qiu, Urchin-like m-LaVO<sub>4</sub> and m-LaVO<sub>4</sub>/Ag microspheres: Synthesis and characterization, *Mater. Charact.* 98 (2014) 162–167. <https://doi.org/10.1016/j.matchar.2014.10.021>.
- [450] J. He, X. Liu, Y. Deng, Y. Peng, L. Deng, H. Luo, C. Cheng, S. Yan, Improved magnetic loss and impedance matching of the FeNi-decorated Ti<sub>3</sub>C<sub>2</sub>T MXene

- composite toward the broadband microwave absorption performance, *J. Alloys Compd.* 862 (2021) 158684. <https://doi.org/10.1016/j.jallcom.2021.158684>.
- [451] W. Chen, R.-Q. Yan, G.-H. Chen, M.-Y. Chen, G.-B. Huang, X.-H. Liu, Hydrothermal route to synthesize helical CdS@ZnIn<sub>2</sub>S<sub>4</sub> core-shell heterostructures with enhanced photocatalytic hydrogenation activity, *Ceram. Int.* 45 (2019) 1803–1811. <https://doi.org/10.1016/j.ceramint.2018.10.067>.
- [452] L. Sun, J. Sun, N. Han, D. Liao, S. Bai, X. Yang, R. Luo, D. Li, A. Chen, rGO decorated W doped BiVO<sub>4</sub> novel material for sensing detection of trimethylamine, *Sensors Actuators B Chem.* 298 (2019) 126749. <https://doi.org/10.1016/j.snb.2019.126749>.
- [453] D. Zhang, Y. Sun, C. Jiang, Y. Zhang, Room temperature hydrogen gas sensor based on palladium decorated tin oxide/molybdenum disulfide ternary hybrid via hydrothermal route, *Sensors Actuators B Chem.* 242 (2017) 15–24. <https://doi.org/10.1016/j.snb.2016.11.005>.
- [454] S.B.S. Gusmão, A. Ghosh, T.M.F. Marques, O.P. Ferreira, A.O. Lobo, J.A.O. Osajima, C. Luz-Lima, R.R.M. Sousa, J.M.E. Matos, B.C. Viana, One-Pot Synthesis of Titanate Nanotubes Decorated with Anatase Nanoparticles Using a Microwave-Assisted Hydrothermal Reaction, *J. Nanomater.* 2019 (2019) 1–10. <https://doi.org/10.1155/2019/4825432>.
- [455] U. Rajaji, M. Govindasamy, S.-M. Chen, T.-W. Chen, X. Liu, S. Chinnapaiyan, Microwave-assisted synthesis of Bi<sub>2</sub>WO<sub>6</sub> flowers decorated graphene nanoribbon composite for electrocatalytic sensing of hazardous dihydroxybenzene isomers, *Compos. Part B Eng.* 152 (2018) 220–230. <https://doi.org/10.1016/j.compositesb.2018.07.003>.
- [456] H. Liu, H. Liu, J. Yang, H. Zhai, X. Liu, H. Jia, Microwave-assisted one-pot synthesis of Ag decorated flower-like ZnO composites photocatalysts for dye degradation and NO removal, *Ceram. Int.* 45 (2019) 20133–20140. <https://doi.org/10.1016/j.ceramint.2019.06.279>.
- [457] W. Alghazzawi, E. Danish, H. Alnahdi, M.A. Salam, Rapid microwave-assisted hydrothermal green synthesis of rGO/NiO nanocomposite for glucose detection in diabetes, *Synth. Met.* 267 (2020) 116401. <https://doi.org/10.1016/j.synthmet.2020.116401>.
- [458] A. Salvatore, C. Montis, D. Berti, P. Baglioni, Multifunctional Magnetoliposomes for Sequential Controlled Release, *ACS Nano.* 10 (2016) 7749–7760. <https://doi.org/10.1021/acsnano.6b03194>.
- [459] M.R. Jones, K.D. Osberg, R.J. Macfarlane, M.R. Langille, C.A. Mirkin, Templated Techniques for the Synthesis and Assembly of Plasmonic Nanostructures, *Chem. Rev.* 111 (2011) 3736–3827. <https://doi.org/10.1021/cr1004452>.
- [460] R. Purbia, S. Paria, Yolk/shell nanoparticles: classifications, synthesis, properties, and applications, *Nanoscale.* 7 (2015) 19789–19873. <https://doi.org/10.1039/C5NR04729C>.
- [461] H. Nishimura, K. Enomoto, Y.-J. Pu, D. Kim, Hydrothermal synthesis of water-soluble Mn- and Cu-doped CdSe quantum dots with multi-shell structures and



- their photoluminescence properties, *RSC Adv.* 12 (2022) 6255–6264.  
<https://doi.org/10.1039/D1RA08491G>.
- [462] B. Wang, Q. Yu, S. Zhang, T. Wang, P. Sun, X. Chuai, G. Lu, Gas sensing with yolk-shell LaFeO<sub>3</sub> microspheres prepared by facile hydrothermal synthesis, *Sensors Actuators B Chem.* 258 (2018) 1215–1222.  
<https://doi.org/10.1016/j.snb.2017.12.018>.
- [463] W. Li, Y. Deng, Z. Wu, X. Qian, J. Yang, Y. Wang, D. Gu, F. Zhang, B. Tu, D. Zhao, Hydrothermal Etching Assisted Crystallization: A Facile Route to Functional Yolk-Shell Titanate Microspheres with Ultrathin Nanosheets-Assembled Double Shells, *J. Am. Chem. Soc.* 133 (2011) 15830–15833.  
<https://doi.org/10.1021/ja2055287>.
- [464] S. Guo, S. Dong, E. Wang, A General Route to Construct Diverse Multifunctional Fe<sub>3</sub>O<sub>4</sub>/Metal Hybrid Nanostructures, *Chem. - A Eur. J.* 15 (2009) 2416–2424. <https://doi.org/10.1002/chem.200801942>.
- [465] Wang, J. Luo, Q. Fan, M. Suzuki, I.S. Suzuki, M.H. Engelhard, Y. Lin, N. Kim, J.Q. Wang, C.-J. Zhong, Monodispersed Core-Shell Fe<sub>3</sub>O<sub>4</sub>@Au Nanoparticles, *J. Phys. Chem. B.* 109 (2005) 21593–21601.  
<https://doi.org/10.1021/jp0543429>.
- [466] A. Goyal, A. Kumar, P.M. Ajayan, Metal salt induced synthesis of hybrid metal core-siloxane shell nanoparticles and siloxane nanowires, *Chem. Commun.* 46 (2010) 964. <https://doi.org/10.1039/b919750h>.
- [467] X. Huang, H. Wu, S. Pu, W. Zhang, X. Liao, B. Shi, One-step room-temperature synthesis of Au@Pd core-shell nanoparticles with tunable structure using plant tannin as reductant and stabilizer, *Green Chem.* 13 (2011) 950.  
<https://doi.org/10.1039/c0gc00724b>.
- [468] W. Wagner, A. Pruß, The IAPWS Formulation 1995 for the Thermodynamic Properties of Ordinary Water Substance for General and Scientific Use, *J. Phys. Chem. Ref. Data.* 31 (2002) 387–535. <https://doi.org/10.1063/1.1461829>.
- [469] M. Uematsu, E.U. Frank, Static Dielectric Constant of Water and Steam, *J. Phys. Chem. Ref. Data.* 9 (1980) 1291–1306. <https://doi.org/10.1063/1.555632>.
- [470] L. Zhang, W. Lu, L. Yan, Y. Feng, X. Bao, J. Ni, X. Shang, Y. Lv, Hydrothermal synthesis and characterization of core/shell ALOOH microspheres, *Microporous Mesoporous Mater.* 119 (2009) 208–216.  
<https://doi.org/10.1016/j.micromeso.2008.10.017>.
- [471] N. Li, Y. Li, W. Li, S. Ji, P. Jin, One-Step Hydrothermal Synthesis of TiO<sub>2</sub>@MoO<sub>3</sub> Core-Shell Nanomaterial: Microstructure, Growth Mechanism, and Improved Photochromic Property, *J. Phys. Chem. C.* 120 (2016) 3341–3349.  
<https://doi.org/10.1021/acs.jpcc.5b10752>.
- [472] X. Zhang, Z. Zhang, S. Sun, Y. Wu, Q. Sun, X. Liu, A facile one-step hydrothermal approach to synthesize hierarchical core-shell NiFe<sub>2</sub>O<sub>4</sub>@NiFe<sub>2</sub>O<sub>4</sub> nanosheet arrays on Ni foam with large specific capacitance for supercapacitors, *RSC Adv.* 8 (2018) 15222–15228.  
<https://doi.org/10.1039/C8RA02559B>.

- [473] Y. Li, S. Wang, J. Wu, J. Ma, L. Cui, H. Lu, Z. Sheng, One-step hydrothermal synthesis of hybrid core-shell Co<sub>3</sub>O<sub>4</sub>@SnO<sub>2</sub>-SnO for supercapacitor electrodes, *Ceram. Int.* 46 (2020) 15793–15800. <https://doi.org/10.1016/j.ceramint.2020.03.126>.
- [474] R. Buonsanti, V. Grillo, E. Carlino, C. Giannini, M.L. Curri, C. Innocenti, C. Sangregorio, K. Achterhold, F.G. Parak, A. Agostiano, P.D. Cozzoli, Seeded Growth of Asymmetric Binary Nanocrystals Made of a Semiconductor TiO<sub>2</sub> Rodlike Section and a Magnetic  $\gamma$ -Fe<sub>2</sub>O<sub>3</sub> Spherical Domain, *J. Am. Chem. Soc.* 128 (2006) 16953–16970. <https://doi.org/10.1021/ja066557h>.
- [475] J. Yang, H.I. Elim, Q. Zhang, J.Y. Lee, W. Ji, Rational Synthesis, Self-Assembly, and Optical Properties of PbS–Au Heterogeneous Nanostructures via Preferential Deposition, *J. Am. Chem. Soc.* 128 (2006) 11921–11926. <https://doi.org/10.1021/ja062494r>.
- [476] D. V. Talapin, H. Yu, E. V. Shevchenko, A. Lobo, C.B. Murray, Synthesis of Colloidal PbSe/PbS Core–Shell Nanowires and PbS/Au Nanowire–Nanocrystal Heterostructures, *J. Phys. Chem. C.* 111 (2007) 14049–14054. <https://doi.org/10.1021/jp074319i>.
- [477] S.R. Nalluri, R. Nagarjuna, D. Patra, R. Ganesan, G. Balaji, Large Scale Solid-state Synthesis of Catalytically Active Fe<sub>3</sub>O<sub>4</sub>@M (M = Au, Ag and Au-Ag alloy) Core-shell Nanostructures, *Sci. Rep.* 9 (2019) 6603. <https://doi.org/10.1038/s41598-019-43116-7>.
- [478] F. Patolsky, Y. Weizmann, E. Katz, I. Willner, Magnetically Amplified DNA Assays (MADA): Sensing of Viral DNA and Single-Base Mismatches by Using Nucleic Acid Modified Magnetic Particles, *Angew. Chemie Int. Ed.* 42 (2003) 2372–2376. <https://doi.org/10.1002/anie.200250379>.
- [479] B.J. Kim, T. Park, H.C. Moon, S.-Y. Park, D. Hong, E.H. Ko, J.Y. Kim, J.W. Hong, S.W. Han, Y.-G. Kim, I.S. Choi, Cytoprotective Alginate/Polydopamine Core/Shell Microcapsules in Microbial Encapsulation, *Angew. Chemie Int. Ed.* 53 (2014) 14443–14446. <https://doi.org/10.1002/anie.201408454>.
- [480] T. Ozel, G.R. Bourret, A.L. Schmucker, K.A. Brown, C.A. Mirkin, Hybrid Semiconductor Core-Shell Nanowires with Tunable Plasmonic Nanoantennas, *Adv. Mater.* 25 (2013) 4515–4520. <https://doi.org/10.1002/adma.201301367>.
- [481] Z. Shan, D. Clayton, S. Pan, P.S. Archana, A. Gupta, Visible Light Driven Photoelectrochemical Properties of Ti@TiO<sub>2</sub> Nanowire Electrodes Sensitized with Core–Shell Ag@Ag<sub>2</sub>S Nanoparticles, *J. Phys. Chem. B.* 118 (2014) 14037–14046. <https://doi.org/10.1021/jp504346k>.
- [482] R. Ghosh Chaudhuri, S. Paria, Core/Shell Nanoparticles: Classes, Properties, Synthesis Mechanisms, Characterization, and Applications, *Chem. Rev.* 112 (2012) 2373–2433. <https://doi.org/10.1021/cr100449n>.
- [483] M.B. Gawande, A. Goswami, T. Asefa, H. Guo, A. V. Biradar, D.-L. Peng, R. Zboril, R.S. Varma, Core–shell nanoparticles: synthesis and applications in catalysis and electrocatalysis, *Chem. Soc. Rev.* 44 (2015) 7540–7590. <https://doi.org/10.1039/C5CS00343A>.
- [484] R. Liu, R.D. Priestley, Rational design and fabrication of core–shell nanoparticles

- through a one-step/pot strategy, *J. Mater. Chem. A*. 4 (2016) 6680–6692.  
<https://doi.org/10.1039/C5TA09607C>.
- [485] W. Shen, X. Huo, M. Zhang, M. Guo, Synthesis of oriented core/shell hexagonal tungsten oxide/amorphous titanium dioxide nanorod arrays and its electrochromic-pseudocapacitive properties, *Appl. Surf. Sci.* 515 (2020) 146034.  
<https://doi.org/10.1016/j.apsusc.2020.146034>.
- [486] Z. Li, E. Yang, X. Qi, R. Xie, T. Jing, S. Qin, C. Deng, W. Zhong, Outstanding comprehensive performance versus facile synthesis: Constructing core and shell-interchangeable nanocomposites as microwave absorber, *J. Colloid Interface Sci.* 565 (2020) 227–238. <https://doi.org/10.1016/j.jcis.2020.01.002>.
- [487] T. Jiang, X. Wang, J. Zhou, D. Chen, Z. Zhao, Hydrothermal synthesis of Ag@MSiO<sub>2</sub>@Ag three core-shell nanoparticles and their sensitive and stable SERS properties, *Nanoscale*. 8 (2016) 4908–4914.  
<https://doi.org/10.1039/C6NR00006A>.
- [488] M. Dai, X. Jia, H. Liu, Y. Tong, D. Zhao, X. Wu, B. Wang, Enhanced electrochemical performances of ZnCo<sub>2</sub>O<sub>4</sub>@CoMoO<sub>4</sub> core-shell structures with long cycling stabilities, *Dalt. Trans.* 49 (2020) 6242–6248.  
<https://doi.org/10.1039/D0DT01211D>.
- [489] E.A. Bakr, M.N. El-Nahass, W.M. Hamada, T.A. Fayed, Facile synthesis of superparamagnetic Fe<sub>3</sub>O<sub>4</sub>@noble metal core-shell nanoparticles by thermal decomposition and hydrothermal methods: comparative study and catalytic applications, *RSC Adv.* 11 (2021) 781–797.  
<https://doi.org/10.1039/D0RA08230A>.
- [490] Y.-S. Kim, P. Rai, Y.-T. Yu, Microwave assisted hydrothermal synthesis of Au@TiO<sub>2</sub> core-shell nanoparticles for high temperature CO sensing applications, *Sensors Actuators B Chem.* 186 (2013) 633–639.  
<https://doi.org/10.1016/j.snb.2013.06.038>.
- [491] T. Yanagimoto, Y.-T. Yu, K. Kaneko, Microstructure and CO gas sensing property of Au/SnO<sub>2</sub> core-shell structure nanoparticles synthesized by precipitation method and microwave-assisted hydrothermal synthesis method, *Sensors Actuators B Chem.* 166–167 (2012) 31–35.  
<https://doi.org/10.1016/j.snb.2011.11.047>.
- [492] S. Soltani, N. Khanian, T. Shean Yaw Choong, N. Asim, Y. Zhao, Microwave-assisted hydrothermal synthesis of sulfonated TiO<sub>2</sub>-GO core-shell solid spheres as heterogeneous esterification mesoporous catalyst for biodiesel production, *Energy Convers. Manag.* 238 (2021) 114165.  
<https://doi.org/10.1016/j.enconman.2021.114165>.
- [493] C. Jin, Y. Lu, G. Tong, R. Che, H. Xu, Excellent microwave absorbing properties of ZnO/ZnFe<sub>2</sub>O<sub>4</sub>/Fe core-shell microrods prepared by a rapid microwave-assisted hydrothermal-chemical vapor decomposition method, *Appl. Surf. Sci.* 531 (2020) 147353. <https://doi.org/10.1016/j.apsusc.2020.147353>.
- [494] Y. Sun, X. Du, J. Zhang, N. Huang, L. Yang, X. Sun, Microwave-assisted preparation and improvement mechanism of carbon nanotube@NiMn<sub>2</sub>O<sub>4</sub> core-shell nanocomposite for high performance asymmetric supercapacitors, *J. Power*

Sources. 473 (2020) 228609. <https://doi.org/10.1016/j.jpowsour.2020.228609>.

- [495] X. Wang, H. Fan, P. Ren, M. Li, Homogeneous SnO<sub>2</sub> core-shell microspheres: Microwave-assisted hydrothermal synthesis, morphology control and photocatalytic properties, *Mater. Res. Bull.* 50 (2014) 191–196. <https://doi.org/10.1016/j.materresbull.2013.10.036>.
- [496] Z. Teng, S. Wang, X. Su, G. Chen, Y. Liu, Z. Luo, W. Luo, Y. Tang, H. Ju, D. Zhao, G. Lu, Facile Synthesis of Yolk-Shell Structured Inorganic-Organic Hybrid Spheres with Ordered Radial Mesochannels, *Adv. Mater.* 26 (2014) 3741–3747. <https://doi.org/10.1002/adma.201400136>.
- [497] S. Wu, J. Dzubiella, J. Kaiser, M. Drechsler, X. Guo, M. Ballauff, Y. Lu, Thermosensitive Au-PNIPAA Yolk-Shell Nanoparticles with Tunable Selectivity for Catalysis, *Angew. Chemie Int. Ed.* 51 (2012) 2229–2233. <https://doi.org/10.1002/anie.201106515>.
- [498] C.-H. Kuo, Y. Tang, L.-Y. Chou, B.T. Sneed, C.N. Brodsky, Z. Zhao, C.-K. Tsung, Yolk-Shell Nanocrystal@ZIF-8 Nanostructures for Gas-Phase Heterogeneous Catalysis with Selectivity Control, *J. Am. Chem. Soc.* 134 (2012) 14345–14348. <https://doi.org/10.1021/ja306869j>.
- [499] A.G.M. da Silva, T.S. Rodrigues, V.G. Correia, T. V. Alves, R.S. Alves, R.A. Ando, F.R. Ornellas, J. Wang, L.H. Andrade, P.H.C. Camargo, Plasmonic Nanorattles as Next-Generation Catalysts for Surface Plasmon Resonance-Mediated Oxidations Promoted by Activated Oxygen, *Angew. Chemie Int. Ed.* 55 (2016) 7111–7115. <https://doi.org/10.1002/anie.201601740>.
- [500] J. Lee, J.C. Park, H. Song, A Nanoreactor Framework of a Au@SiO<sub>2</sub> Yolk/Shell Structure for Catalytic Reduction of p-Nitrophenol, *Adv. Mater.* 20 (2008) 1523–1528. <https://doi.org/10.1002/adma.200702338>.
- [501] L. Tan, D. Chen, H. Liu, F. Tang, A Silica Nanorattle with a Mesoporous Shell: An Ideal Nanoreactor for the Preparation of Tunable Gold Cores, *Adv. Mater.* 22 (2010) 4885–4889. <https://doi.org/10.1002/adma.201002277>.
- [502] Y. Yang, X. Liu, X. Li, J. Zhao, S. Bai, J. Liu, Q. Yang, A Yolk-Shell Nanoreactor with a Basic Core and an Acidic Shell for Cascade Reactions, *Angew. Chemie Int. Ed.* 51 (2012) 9164–9168. <https://doi.org/10.1002/anie.201204829>.
- [503] S. Li, J. Niu, Y.C. Zhao, K.P. So, C. Wang, C.A. Wang, J. Li, High-rate aluminium yolk-shell nanoparticle anode for Li-ion battery with long cycle life and ultrahigh capacity, *Nat. Commun.* 6 (2015) 7872. <https://doi.org/10.1038/ncomms8872>.
- [504] Z. Wei Seh, W. Li, J.J. Cha, G. Zheng, Y. Yang, M.T. McDowell, P.-C. Hsu, Y. Cui, Sulphur-TiO<sub>2</sub> yolk-shell nanoarchitecture with internal void space for long-cycle lithium-sulphur batteries, *Nat. Commun.* 4 (2013) 1331. <https://doi.org/10.1038/ncomms2327>.
- [505] W. Zhou, Y. Yu, H. Chen, F.J. DiSalvo, H.D. Abruña, Yolk-Shell Structure of Polyaniline-Coated Sulfur for Lithium-Sulfur Batteries, *J. Am. Chem. Soc.* 135 (2013) 16736–16743. <https://doi.org/10.1021/ja409508q>.

- [506] Y.J. Hong, M.Y. Son, Y.C. Kang, One-Pot Facile Synthesis of Double-Shelled SnO<sub>2</sub> Yolk-Shell-Structured Powders by Continuous Process as Anode Materials for Li-ion Batteries, *Adv. Mater.* 25 (2013) 2279–2283. <https://doi.org/10.1002/adma.201204506>.
- [507] J. Liu, L. Yu, C. Wu, Y. Wen, K. Yin, F.-K. Chiang, R. Hu, J. Liu, L. Sun, L. Gu, J. Maier, Y. Yu, M. Zhu, New Nanoconfined Galvanic Replacement Synthesis of Hollow Sb@C Yolk-Shell Spheres Constituting a Stable Anode for High-Rate Li/Na-Ion Batteries, *Nano Lett.* 17 (2017) 2034–2042. <https://doi.org/10.1021/acs.nanolett.7b00083>.
- [508] J. Liu, J. Bu, W. Bu, S. Zhang, L. Pan, W. Fan, F. Chen, L. Zhou, W. Peng, K. Zhao, J. Du, J. Shi, Real-Time In Vivo Quantitative Monitoring of Drug Release by Dual-Mode Magnetic Resonance and Upconverted Luminescence Imaging, *Angew. Chemie Int. Ed.* 53 (2014) 4551–4555. <https://doi.org/10.1002/anie.201400900>.
- [509] J. Gao, G. Liang, B. Zhang, Y. Kuang, X. Zhang, B. Xu, FePt@CoS<sub>2</sub> Yolk-Shell Nanocrystals as a Potent Agent to Kill HeLa Cells, *J. Am. Chem. Soc.* 129 (2007) 1428–1433. <https://doi.org/10.1021/ja067785e>.
- [510] J. Liu, Y. Liu, W. Bu, J. Bu, Y. Sun, J. Du, J. Shi, Ultrasensitive Nanosensors Based on Upconversion Nanoparticles for Selective Hypoxia Imaging in Vivo upon Near-Infrared Excitation, *J. Am. Chem. Soc.* 136 (2014) 9701–9709. <https://doi.org/10.1021/ja5042989>.
- [511] H. Liu, T. Liu, X. Wu, L. Li, L. Tan, D. Chen, F. Tang, Targeting Gold Nanoshells on Silica Nanorattles: a Drug Cocktail to Fight Breast Tumors via a Single Irradiation with Near-Infrared Laser Light, *Adv. Mater.* 24 (2012) 755–761. <https://doi.org/10.1002/adma.201103343>.
- [512] M.-F. Tsai, S.-H.G. Chang, F.-Y. Cheng, V. Shanmugam, Y.-S. Cheng, C.-H. Su, C.-S. Yeh, Au Nanorod Design as Light-Absorber in the First and Second Biological Near-Infrared Windows for in Vivo Photothermal Therapy, *ACS Nano.* 7 (2013) 5330–5342. <https://doi.org/10.1021/nn401187c>.
- [513] L.-S. Lin, X. Yang, Z. Zhou, Z. Yang, O. Jacobson, Y. Liu, A. Yang, G. Niu, J. Song, H.-H. Yang, X. Chen, Yolk-Shell Nanostructure: An Ideal Architecture to Achieve Harmonious Integration of Magnetic-Plasmonic Hybrid Theranostic Platform, *Adv. Mater.* 29 (2017) 1606681. <https://doi.org/10.1002/adma.201606681>.
- [514] Q. Zhang, H. Bai, Q. Zhang, Q. Ma, Y. Li, C. Wan, G. Xi, MoS<sub>2</sub> yolk-shell microspheres with a hierarchical porous structure for efficient hydrogen evolution, *Nano Res.* 9 (2016) 3038–3047. <https://doi.org/10.1007/s12274-016-1186-7>.
- [515] J. Liu, J. Xu, R. Che, H. Chen, M. Liu, Z. Liu, Hierarchical Fe<sub>3</sub>O<sub>4</sub>@TiO<sub>2</sub> yolk-shell microspheres with enhanced microwave-absorption properties, *Chem. - A Eur. J.* 19 (2013) 6746–6752. <https://doi.org/10.1002/chem.201203557>.
- [516] J. Chen, K. Yang, J. Wang, Q. Zhang, B. Zhang, Peanut-like yolk/core-shell MnO/C microspheres for improved lithium storage and the formation mechanism of MnCO<sub>3</sub> precursors, *J. Alloys Compd.* 849 (2020) 156637.

<https://doi.org/10.1016/j.jallcom.2020.156637>.

- [517] H. Liu, J. Chang, CeVO<sub>4</sub> yolk-shell microspheres constructed by nanosheets with enhanced lithium storage performances, *J. Alloys Compd.* 849 (2020) 156682. <https://doi.org/10.1016/j.jallcom.2020.156682>.
- [518] Q.-Q. Xu, W. Huo, S.-S. Li, J.-H. Fang, L. Li, B.-Y. Zhang, F. Zhang, Y.-X. Zhang, S.-W. Li, Crystal phase determined Fe active sites on Fe<sub>2</sub>O<sub>3</sub> ( $\gamma$ - and  $\alpha$ -Fe<sub>2</sub>O<sub>3</sub>) yolk-shell microspheres and their phase dependent electrocatalytic oxygen evolution reaction, *Appl. Surf. Sci.* 533 (2020) 147368. <https://doi.org/10.1016/j.apsusc.2020.147368>.
- [519] X. Huang, Z. Nan, Formation of octahedron-shaped ZnFe<sub>2</sub>O<sub>4</sub>/SiO<sub>2</sub> with yolk-shell structure, *J. Phys. Chem. Solids.* 141 (2020) 109410. <https://doi.org/10.1016/j.jpcs.2020.109410>.
- [520] X. Shi, C. Wang, Y. Ma, H. Liu, S. Wu, Q. Shao, Z. He, L. Guo, T. Ding, Z. Guo, Template-free microwave-assisted synthesis of FeTi coordination complex yolk-shell microspheres for superior catalytic removal of arsenic and chemical degradation of methylene blue from polluted water, *Powder Technol.* 356 (2019) 726–734. <https://doi.org/10.1016/j.powtec.2019.09.002>.
- [521] Y. Su, D. Ao, H. Liu, Y. Wang, MOF-derived yolk-shell CdS microcubes with enhanced visible-light photocatalytic activity and stability for hydrogen evolution, *J. Mater. Chem. A.* 5 (2017) 8680–8689. <https://doi.org/10.1039/C7TA00855D>.
- [522] W. Guo, W. Sun, L.-P. Lv, S. Kong, Y. Wang, Microwave-Assisted Morphology Evolution of Fe-Based Metal–Organic Frameworks and Their Derived Fe<sub>2</sub>O<sub>3</sub> Nanostructures for Li-Ion Storage, *ACS Nano.* 11 (2017) 4198–4205. <https://doi.org/10.1021/acsnano.7b01152>.
- [523] G.-J. Ding, Y.-J. Zhu, C. Qi, T.-W. Sun, J. Wu, F. Chen, Yolk-Shell Porous Microspheres of Calcium Phosphate Prepared by Using Calcium  $\langle \text{L} \rangle$ -Lactate and Adenosine 5'-Triphosphate Disodium Salt: Application in Protein/Drug Delivery, *Chem. - A Eur. J.* 21 (2015) 9868–9876. <https://doi.org/10.1002/chem.201406547>.
- [524] H. Yu, M. Chen, P.M. Rice, S.X. Wang, R.L. White, S. Sun, Dumbbell-like Bifunctional Au–Fe<sub>3</sub>O<sub>4</sub> Nanoparticles, *Nano Lett.* 5 (2005) 379–382. <https://doi.org/10.1021/nl047955q>.
- [525] C. Wang, C. Xu, H. Zeng, S. Sun, Recent progress in syntheses and applications of dumbbell-like nanoparticles, *Adv. Mater.* 21 (2009) 3045–3052. <https://doi.org/10.1002/adma.200900320>.
- [526] T. Yang, L. Wei, L. Jing, J. Liang, X. Zhang, M. Tang, M.J. Monteiro, Y.I. Chen, Y. Wang, S. Gu, D. Zhao, H. Yang, J. Liu, G.Q.M. Lu, Dumbbell-Shaped Bi-component Mesoporous Janus Solid Nanoparticles for Biphasic Interface Catalysis, *Angew. Chemie Int. Ed.* 56 (2017) 8459–8463. <https://doi.org/10.1002/anie.201701640>.
- [527] C. Xu, J. Xie, D. Ho, C. Wang, N. Kohler, E.G. Walsh, J.R. Morgan, Y.E. Chin, S. Sun, Au–Fe<sub>3</sub>O<sub>4</sub> Dumbbell Nanoparticles as Dual-Functional Probes, *Angew. Chemie Int. Ed.* 47 (2008) 173–176. <https://doi.org/10.1002/anie.200704392>.

- [528] C. Kang, A. Honciuc, Influence of Geometries on the Assembly of Snowman-Shaped Janus Nanoparticles, *ACS Nano*. 12 (2018) 3741–3750. <https://doi.org/10.1021/acsnano.8b00960>.
- [529] X. Wang, X. Feng, G. Ma, L. Yao, M. Ge, Amphiphilic Janus Particles Generated via a Combination of Diffusion-Induced Phase Separation and Magnetically Driven Dewetting and Their Synergistic Self-Assembly, *Adv. Mater.* 28 (2016) 3131–3137. <https://doi.org/10.1002/adma.201506358>.
- [530] Y. Liu, J. Hu, X. Yu, X. Xu, Y. Gao, H. Li, F. Liang, Preparation of Janus-type catalysts performance at emulsion interface and their Beijing National Laboratory for Molecular Sciences, *Zhongguancun North First, J. Colloid Interface Sci.* (2016). <https://doi.org/10.1016/j.jcis.2016.11.053>.
- [531] Q. Zhang, L. Zhang, S. Li, X. Chen, M. Zhang, T. Wang, L. Li, C. Wang, Designed Synthesis of Au/Fe<sub>3</sub>O<sub>4</sub>@C Janus Nanoparticles for Dual-Modal Imaging and Actively Targeted Chemo-Photothermal Synergistic Therapy of Cancer Cells, *Chem. - A Eur. J.* 23 (2017) 17242–17248. <https://doi.org/10.1002/chem.201703498>.
- [532] I. Schick, S. Lorenz, D. Gehrig, A.-M. Schilmann, H. Bauer, M. Panthöfer, K. Fischer, D. Strand, F. Laquai, W. Tremel, Multifunctional Two-Photon Active Silica-Coated Au@MnO Janus Particles for Selective Dual Functionalization and Imaging, *J. Am. Chem. Soc.* 136 (2014) 2473–2483. <https://doi.org/10.1021/ja410787u>.
- [533] X. Fu, J. Liu, H. Yang, J. Sun, X. Li, X. Zhang, Y. Jia, Arrays of Au–TiO<sub>2</sub> Janus-like nanoparticles fabricated by block copolymer templates and their photocatalytic activity in the degradation of methylene blue, *Mater. Chem. Phys.* 130 (2011) 334–339. <https://doi.org/10.1016/j.matchemphys.2011.06.054>.
- [534] R. Zhao, X. Yu, D. Sun, L. Huang, F. Liang, Z. Liu, Functional Janus Particles Modified with Ionic Liquids for Dye Degradation, *ACS Appl. Nano Mater.* 2 (2019) 2127–2132. <https://doi.org/10.1021/acsanm.9b00090>.
- [535] F. Mou, C. Chen, J. Guan, D.-R. Chen, H. Jing, Oppositely charged twin-head electrospray: a general strategy for building Janus particles with controlled structures, *Nanoscale*. 5 (2013) 2055. <https://doi.org/10.1039/c2nr33523a>.
- [536] A. Kirillova, C. Marschelke, J. Friedrichs, C. Werner, A. Synytska, Hybrid Hairy Janus Particles as Building Blocks for Antibiofouling Surfaces, *ACS Appl. Mater. Interfaces*. 8 (2016) 32591–32603. <https://doi.org/10.1021/acsami.6b10588>.
- [537] A. Kirillova, G. Stoychev, L. Ionov, K.-J. Eichhorn, M. Malanin, A. Synytska, Platelet Janus Particles with Hairy Polymer Shells for Multifunctional Materials, *ACS Appl. Mater. Interfaces*. 6 (2014) 13106–13114. <https://doi.org/10.1021/am502973y>.
- [538] J.R. Link, M.J. Sailor, Smart dust: Self-assembling, self-orienting photonic crystals of porous Si, *Proc. Natl. Acad. Sci.* 100 (2003) 10607–10610. <https://doi.org/10.1073/pnas.1233824100>.
- [539] J. Yan, K. Chaudhary, S. Chul Bae, J.A. Lewis, S. Granick, Colloidal ribbons and rings from Janus magnetic rods, *Nat. Commun.* 4 (2013) 1516.

<https://doi.org/10.1038/ncomms2520>.

- [540] B. Zhao, H. Zhou, C. Liu, Y. Long, G. Yang, C.-H. Tung, K. Song, Fabrication and directed assembly of magnetic Janus rods, *New J. Chem.* 40 (2016) 6541–6545. <https://doi.org/10.1039/C6NJ00825A>.
- [541] X. Lv, Z. Xiao, C. Zhou, Y. Wang, S. Duan, J. Chen, W. Duan, X. Ma, W. Wang, Tadpole-Shaped Catalytic Janus Microrotors Enabled by Facile and Controllable Growth of Silver Nanotails, *Adv. Funct. Mater.* 30 (2020) 2004858. <https://doi.org/10.1002/adfm.202004858>.
- [542] N. Ali, B. Zhang, H. Zhang, W. Zaman, W. Li, Q. Zhang, Key synthesis of magnetic Janus nanoparticles using a modified facile method, *Particuology*. 17 (2014) 59–65. <https://doi.org/10.1016/j.partic.2014.02.001>.
- [543] Y. Li, S. Yang, X. Lu, W. Duan, T. Moriga, Synthesis and evaluation of the SERS effect of Fe<sub>3</sub>O<sub>4</sub>-Ag Janus composite materials for separable, highly sensitive substrates, *RSC Adv.* 9 (2019) 2877–2884. <https://doi.org/10.1039/C8RA09569H>.
- [544] J. Song, B. Wu, Z. Zhou, G. Zhu, Y. Liu, Z. Yang, L. Lin, G. Yu, F. Zhang, G. Zhang, H. Duan, G.D. Stucky, X. Chen, Double-Layered Plasmonic-Magnetic Vesicles by Self-Assembly of Janus Amphiphilic Gold-Iron(II,III) Oxide Nanoparticles, *Angew. Chemie.* 129 (2017) 8222–8226. <https://doi.org/10.1002/ange.201702572>.
- [545] M. Lattuada, T.A. Hatton, Synthesis, properties and applications of Janus nanoparticles, *Nano Today*. 6 (2011) 286–308. <https://doi.org/10.1016/j.nantod.2011.04.008>.
- [546] E. Poggi, J.-F. Gohy, Janus particles: from synthesis to application, *Colloid Polym. Sci.* 295 (2017) 2083–2108. <https://doi.org/10.1007/s00396-017-4192-8>.
- [547] A. Perro, S. Reculosa, S. Ravaine, E. Bourgeat-Lami, E. Duguet, Design and synthesis of Janus micro- and nanoparticles, *J. Mater. Chem.* 15 (2005) 3745. <https://doi.org/10.1039/b505099e>.
- [548] N. Mertzsch, Hydrothermal processes in industry, *ChemTexts*. 6 (2020) 21. <https://doi.org/10.1007/s40828-020-00116-9>.
- [549] P. Raccuglia, K.C. Elbert, P.D.F. Adler, C. Falk, M.B. Wenny, A. Mollo, M. Zeller, S.A. Friedler, J. Schrier, A.J. Norquist, Machine-learning-assisted materials discovery using failed experiments, *Nature*. 533 (2016) 73–76. <https://doi.org/10.1038/nature17439>.